Dynamical Structures and Precipitation Distributions of Transitioning Tropical Cyclones in Eastern Canada, 1979-2004

Shawn M. Milrad

Department of Atmospheric and Oceanic Sciences

McGill University

Montreal, Quebec, Canada

January, 2006

A thesis submitted to McGill University in partial fulfillment of the requirements of the degree of Master of Science.

Your file Votre référence
ISBN: 978-0-494-24742-6
Our file Notre référence
ISBN: 978-0-494-24742-6

Abstract

From 1979-2004, 32 storms originally tropical in nature (as classified by the National Hurricane Center) have affected Eastern Canada to various degrees during or after extratropical transition (ET). This study examines the dynamical structure of these 32 cases from quasi-geostrophic (QG) and potential vorticity (PV) perspectives, primarily utilizing the National Centers for Environmental Prediction (NCEP) North American Regional Reanalysis (NARR). A composite diagnosis is performed using the Sutcliffe/Trenberth (advection of mid-tropospheric vorticity by the thermal wind), the storms were partitioned into two groups, "intensifying" and "decaying", based upon the QG forcing for ascent. Composite synoptic structures, from both QG and potential vorticity (PV) views, will be presented for both partitioned groups of storms. In addition, precipitation distributions are analyzed using the 3-hour accumulated precipitation field in the NARR.

Résumé

De 1979 à 2004, 32 tempêtes, de nature tropicale à l'origine (tel que défini par le National Hurricane Center), ont affecté à différents degrés l'est du Canada pendant ou après leur transition extra-tropicale. Cette étude examine la structure dynamique de ces 32 cas des points de vues quasi-géostrophique et vorticité potentielle, principalement à partir des données du NCEP North American Regional Reanalysis (NARR). Un diagnostique composite est éffectué à partir de l'approximation de Sutcliffe et Trenberth (advection de vorticité du milieu de la troposphère par le vent thermique) et les tempêtes sont divisées en deux groupes; <<augmentant en intensité>> et <<diminuant en intensité>>, selon le forçage QG pour l'ascension. Un composite des structures synoptiques sera présenté pour chacun des groupes de tempêtes, d'une part du point de vue QG et de l'autre du point de vue de la vorticité potentielle. De plus, la distribution de précipitation pour chacun des cas de l'étude est analysée à partir des champs d'accumulation de précipitation sur 3 heures de NARR.

Acknowledgements

This section is a case of too many people to thank, and too little space to do so in. First and foremost, I would like to acknowledge my thesis advisor, Dr. John Gyakum for his advice and guidance along the way, as well as his interest in extratropical transition, which originally inspired me to get involved in this project. Secondly, the Natural Sciences and Engineering Research Council of Canada and the Canadian Foundation for Climate and Atmospheric Sciences each warrant a mention, since without their generous grants, this research would not be possible. In addition, thanks to Environment Canada and in particular Gérard Morin at the Atlantic Canada Climate Centre, for providing me with numerous radar images contained in this thesis. Very special thanks goes to Dr. Eyad Atallah, for all his efforts and countless hours he spent providing me with anything and everything I needed or did not know how to do for this study. The translation of the abstract was completed by Blaise Gauvin-St.Denis. Also, much appreciation to the people at NCEP who manage the North American Regional Reanalysis, for without their hard work in running the dataset, this study would not be possible. Additional thanks go to Erin Roberts, Andrew Way and Jennifer Lilly, for many delicious Montreal lunches, and to etrain, my trusty linux machine. Finally, to Clare Salustro for her LaTeX know-how and support, and for keeping me somewhat sane throughout all of this.

Contents

List of Tables

List of Figures

Chapter 1

Introduction

1.1. Motivation

Tropical cyclones pose an annual threat to land masses in the western North Atlantic Basin. However, forecasters often overlook the potential danger presented by tropical cyclones that transition into extratropical cyclones at higher latitudes. Occurring mainly during the late summer and early autumn, these storms can have a large impact on the weather of Eastern Canada, especially in terms of extreme rainfall events. Operational forecasters in the region face a major challenge (Fogarty 2002) in predicting extratropical transitions of tropical cyclones (ET) in Eastern Canada, which occur 1-2 times per year on average (Hart and Evans 2001).

Prior to the 1990's, there were relatively few published studies on ET. However, one particularly prominent major flooding event in the Northeast U.S. and Eastern Canada, as a result of the ET of Hurricane Hazel in 1954 (Palmén 1958; Anthes 1990; Weese 2003; Gyakum 2003), helped to inspire in-depth studies of ET. During the past decade, studies on ET have gradually become more numerous. Research has mostly been limited to clusters of case studies, focused either on the western North Pacific Basin (Matano and Sekioka 1971a,b; Harr et al. 2000; Harr and Elsberry 2000; Klein et al. 2000; Ritchie and Elsberry 2003; Elsberry 2002; Klein et al. 2002), western Europe (Thorncroft and Jones 2000; Browning et al. 1998; Agusti-Panareda et al. 2004; Browning et al. 2000), or the United States (DiMego and Bosart 1982a,b; Atallah and Bosart 2003; Bosart and Dean 1991; Colle 2003; Carr and Bosart 1978; Srock et al. 2004a,b; Dickinson et al. 2004). Jones et al. (2003) produced a summary of the ET process, past research, and future prospects, while Hart and Evans (2001) were the first to publish a somewhat complete (1899-1996) ET climatology in the Atlantic Basin. Furthermore, Evans and Hart (2003); Muir-Wood et al. (2004) and, to some

extent Hart (2003), attempted to objectively define a phase space classification for cyclones undergoing ET in the Atlantic Basin. However, while research on ET has generally increased in the past 5-10 years, studies on the impact of ET in Canada are few; those completed primarily focusing on single case studies such as the disputed ET of Earl in 1998 (McTaggart-Cowan et al. 2001, 2003; Ma et al. 2003; McTaggart-Cowan et al. 2004a; Elsberry 2004; McTaggart-Cowan et al. 2004b) and Michael in 2000 (Fogarty 2000; Abraham et al. 2002). Since tropical cyclones that are undergoing or have undergone ET can rapidly intensify into dangerous extra-tropical cyclones before impacting Eastern Canada, a more inclusive, recent, and higher resolution study focusing on Canada is necessary.

When a tropical cyclone affects a populated land area, the media tends to concentrate on the high winds and potential wind damage while giving only secondary consideration to the threat posed by heavy precipitation. In numerous cases (e.g. Floyd 1999) (Atallah and Bosart 2003), however, it is the heavy flooding resulting from these storms and not the high winds, which causes the most significant and costly damage. While transitioning storms can develop into strong extratropical cyclones with gale or even minimal hurricane force winds, rarely do they achieve the same intensity as a strong tropical cyclone (Hart and Evans 2001). Therefore, precipitation, not wind, is often the primary concern of the ET forecaster. While Fogarty and Gyakum (2005) and Gyakum (2003) produced dynamic analyses of ET in Eastern Canada through 1996, no study has yet attempted to objectively analyze the precipitation associated with transitioning cyclones in Eastern Canada in similar fashion to what the study of Atallah and Bosart (2004) did for the United States, despite the significant number of flooding events resulting from transitioning cyclones in the last 3 decades. The hope is that the 26-year climatology of transitioning or transitioned storms affecting Eastern Canada contained in this study will serve as an aid to the Canadian (particularly in the Atlantic provinces) forecaster in predicting precipitation amounts and distributions as a result of these dangerous annual events.

1.2. Objectives

McTaggart-Cowan et al. (2004b) recently stated that "the problem of understanding extratropical transition (ET) is, by definition, complicated by the interplay of tropical and extratropical structures and forcings....As both a forecasting and a diagnostic tool, it is often convenient to sort features involved in the ET process into the mutually exclusive categories of either "tropical" or "extratropical." Such a sim-

plification is useful to the extent that it allows us to define a common framework under which to discuss these events; however, it can lead to an incorrect conclusion that these features exist in isolation of each other and of their life cycles." Therefore, it is not a priority of this study to define the exact phase each storm is in during the period of study. Instead, the main goal of this research is to examine the threat posed to Canada by storms that undergo ET at some point in their life cycles.

Eastern Canada, because of its latitude, is often situated near the region of transition. The region can vary based on several variables (season, sea surface temperature, track, synoptic situation, etc.). Thus, it would be difficult to categorize most of the storms in this study as having undergone transition or not, as Darr (2002) did in his study on western Atlantic ET. Alternatively, because of our interest in a particular geographical region, each storm is examined without any labels and/or categorizations (i.e. "tropical" or "extratropical"), that could hinder analysis. The word "transitioning" in the title is used in a very broad sense, and should indicate that storms ranging from purely tropical (e.g. Hurricane Juan (2003)) to purely extratropical (e.g. former Hurricane Earl (1998)) during their period of impact to Canada are included, provided they have been designated as a named tropical cyclone at some point in their life cycle.

This study examines thirty-two storms that have affected Eastern Canada from 1979-2004. Both dynamically-based and thermodynamically-based fields are examined, including sea-level pressure, mid-tropospheric vorticity, moisture convergence and upper-tropospheric potential vorticity. For the remainder of this section, the specific objectives of this study are spelled out.

Recently, Atallah and Bosart (2004) sought an evaluation of precipitation distributions associated with landfalling, and later, transitioning tropical cyclones. Meanwhile, Darr (2002) chose a set of tropical cyclones in the western North Atlantic Basin and classified them as storms that underwent either a strong transition or no transition at all during their life cycles. A goal here is to combine the dynamical approach of Darr (2002) and the precipitation focus of Atallah and Bosart (2003, 2004), while utilizing a much higher resolution dataset (NCEP North American Regional Reanalysis (Mesinger et al. 2004)), to help resolve features not previously examined using lower-resolution analyses.

The dynamical analysis approach allows the objective definition of synoptic patterns in which one might expect a particular storm to intensify or decay when it threatens Eastern Canada. Our methodology is centered upon a dynamically-based partitioning of the storms, which in turn is used to objectively categorize different

types of precipitation distributions. Therefore, an initial dynamical partition will assist in precipitation forecasting for a particular storm class, in contrast to Atallah and Bosart (2004), who began with a precipitation analysis and used it to perform a dynamical analysis.

Finally, advantages and disadvantages of using the NARR for this synoptic study will be outlined. This study provides a unique opportunity to evaluate the NARR with respect to both tropical and extratropical cyclones, as well as for heavy precipitation events. Originally developed to serve the hydrological community (Mesinger et al. 2004), synoptic studies using the NARR are currently few and far between. Thus, an evaluation of the good and not-so-good aspects of this overall promising dataset is integral to any future usage of it in the synoptic research community.

1.3. Data

The pursuit of a higher horizontal resolution study than allowed by the 2.5 degree grid in the NCEP/NCAR global reanalysis (Kalnay et al. 1996), led to the use of the NCEP North American Regional Reanalysis (NARR), with a 32 km horizontal resolution (Mesinger et al. 2004). This choice is important from a timeline standpoint since the NARR extends only from 1979 to the present. Thus, the storm selection process is limited to the past 26 years (1979-2004). Storms were chosen from the National Hurricane Center (NHC) best track archive dataset, available online at http://www.nhc.noaa.gov. Thirty-two storms are found to have affected the Canadian mainland from 1979-2004, as listed in Table 1.1. "Affected" is defined as the NHC best track of the storm touching some part of Canada during the storm's life cycle.

The tracks of all 32 cases (1979-2004) can be found in Figure 1.1. The map was created using the National Oceanic and Atmospheric Agency's (NOAA) Coastal Service Center tropical cyclone track page, available at http://hurricane.csc.noaa.gov/hurricanes.

Figure 1.1 shows that the overwhelming majority of storm cases affected the Atlantic provinces of Canada. While the most famous case of ET in Canada (Hazel, 1954) caused enormous flooding damage in Southern Ontario (McTaggart-Cowan et al. 2001), the Maritime region consistently faces the largest threat from these storms. Additionally, cases of ET that affect the Maritimes may pose a significant wind damage threat, in addition to extreme precipitation possibilities.

Both the NCEP/NCAR Global Reanalysis (Kalnay et al. 1996) and the NCEP North American Regional Reanalysis (NARR) (Mesinger et al. 2004) are utilized in

Year	Storm Name
1979	David, Frederic
1985	Gloria
1988	Alberto, Chris
1989	Dean, Hugo
1990	Bertha, Lili
1991	Bob, Unnamed
1995	Allison, Barry, Luis, Opal
1996	Bertha, Fran, Hortense, Josephine
1998	Earl
1999	Dennis, Floyd
2000	Gordon, Leslie, Michael
2001	Erin, Karen
2002	Arthur, Gustav
2003	Isabel, Juan
2004	Frances

Table 1.1: All 32 storms by year.

this study. However, the NARR, with a 32 km horizontal resolution (as opposed to a 2.5 degree horizontal grid in the Global Reanalysis), higher temporal resolution (3 hr vs. 6 hr), and the availability of a 3-hourly accumulated precipitation field, is chosen as the primary dataset for analysis. The NCEP global reanalysis serves as both a quality control and comparison tool for the NARR in this study. Mesinger et al. (2004) state that "the NARR was developed as a major improvement upon the earlier NCEP/NCAR Global Reanalysis, in both resolution and accuracy." Thus, it is important to gauge the accuracy of this claim, with respect to transitioning tropical cyclones in the western North Atlantic.

Unlike the NCEP Global Reanalysis, which initializes in 1948, the NARR initializes in 1979. While this may be seen as a disadvantage (in terms of eliminating earlier cases), the advantages of using the NARR far outweigh this concern. The NARR utilizes the ETA regional model (Mesinger et al. 1990), a model that incorporates many improvements in the modelling field that were made after the Global Reanalysis came online (Mesinger et al. 2004). In addition, the NARR contains a 3-hourly precipitation field, using an assimilation scheme which combines both model and observed precipitation data to deliver a rather accurate product (Mesinger et al. 2004). The availability of a precipitation field is a major reason for choosing the NARR for this study. While some such as Atallah and Bosart (2003) have made good use of the NCEP Unified Precipitation Dataset (UPD) in studies of ET, the UPD is limited to

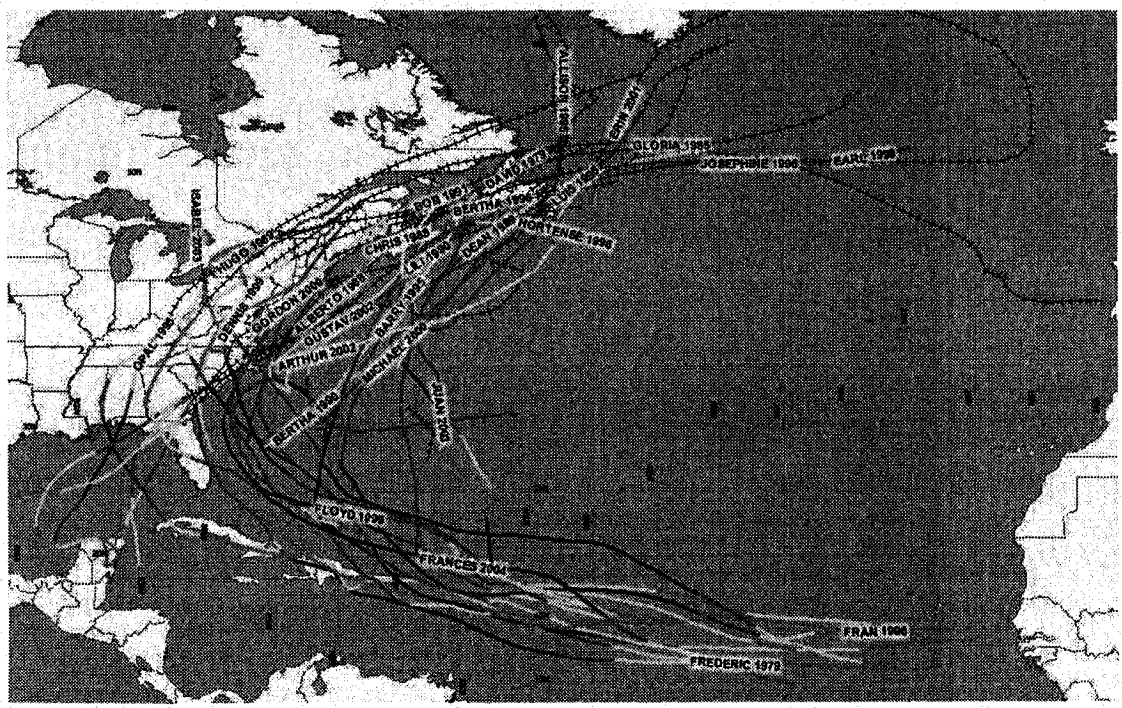

Figure 1.1: All 32 storm tracks.

the contiguous United States. Therefore, the assimilation of precipitation over Canada and the western North Atlantic Ocean via the NARR is an important motivation in choosing a dataset.

Canadian radar data are supplied by Environment Canada. The overwhelming majority of calculations and analyses in this study are performed and displayed using the General Meteorological Package version 5.7.4 (Koch et al. 1983), a commonly used data manipulation and visualization software package in synoptic analyses.

Chapter 2

The Extratropical Transition of Tropical Cyclones

2.1. Definition and climatology

2.1a. Definition of ET

The United States National Hurricane Center (NHC) defines a transitioning tropical cyclone as one that "transitions from tropical to extratropical at some point in its lifetime (Evans and Hart 2003)". However, as Evans and Hart (2003) point out, "no universally accepted definition of extratropical transition of tropical cyclones (ET) presently exits." Jones et al. (2003) agree with this lack of a single definition and also note that different forecast centers around the globe have different methodologies for determining whether or not a storm is undergoing ET. In Canada, for example, in addition to an ET system being called by its former tropical name (as is the case in most countries), it is referred to as a "post tropical cyclone" so that the general public does not take lightly the threat posed by the storm (Jones et al. 2003). Despite the lack of an official definition, Jones et al. (2003) summarize a few indicators one may look for in order to identify a storm undergoing ET:

- Appearance of a comma-shaped cloud pattern, frontal structure, or the opening of the low level center of the storm as viewed using satellite imagery.
- Increase in the radius of gale force winds.
- Asymmetries in the wind and precipitation fields.
- A decrease in sea surface temperatures (SSTs) beneath the tropical cyclone.

It is unwise to attempt to explicitly and definitively define ET in an overly concise fashion. Instead, it is more important to contribute in ways that make it easier for the forecaster to have a good understanding of what to look for and how to handle storms that undergo ET.

2.1b. ET climatology

The extratropical transition of tropical cyclones is a global phenomenon that occurs in almost every ocean Basin that has a tropical cyclone season (Jones et al. 2003). According to Evans and Hart (2003), the percentages of tropical cyclones that undergo ET on average in each Basin are:

- Atlantic Basin (1979-1993): 46% (Hart and Evans 2001)
- Western North Pacific Basin (1979-1993): 27% (Klein et al. 2000)
- East Indian Ocean/Western Australia Basin (1964-1990): 10% (Foley and Hanstrum 1994)

Furthermore, Jones et al. (2003) point out that, while the largest percentage of tropical cyclones that undergo ET can be found in the Atlantic Basin, the largest number of ET events occur in the western North Pacific Basin because of its larger number of tropical cyclones. The significantly higher percentage of ET in the Atlantic has much to do with the synoptic conditions often found there, particularly a strong subtropical ridge that is often not seen in the western North Pacific.

Hart and Evans (2001) show that 50% of landfalling tropical cyclones in the Western Atlantic are storms that have undergone or are undergoing extratropical transition. During the Hart and Evans (2001) climatology period, 46% of Atlantic tropical cyclones underwent ET at some point. Moreover, of the 61 transitioning tropical cyclones during the period of the Hart and Evans (2001) climatology (1979-1993), 51% underwent post-transition intensification, the synoptic conditions of which will be described later in this study. In addition, Hart and Evans (2001) found a latitudinal dependence whereby 60% of tropical cyclones that underwent post-ET intensification had their point of origin south of 20 degrees North. In contrast, 90% of tropical cyclones that weakened post-ET originated north of 20 degrees N. This suggests that baroclinic characteristics in the initial tropical vortex may not be conducive to a strong ET later in the storm's lifetime.

An integral part of the Hart and Evans (2001) Atlantic climatology is the seasonal dependence of ET occurrence. As shown in Fig. 2.1, the probability of a storm

undergoing ET in the Basin increases as the tropical cyclone season progresses, i.e. during October. In addition, their findings indicate that ET typically occurs at lower latitudes at the beginning and the end of the season and higher latitudes during peak season (late August/September). This is primarily due to the delayed warming of the Atlantic ocean, which allows tropical systems to survive as purely tropical entities at higher latitudes during September (Hart and Evans 2001); however, the trend is mitigated as the climatologically preferred region for baroclinic development moves southward later in the season. Figure 2.2 below displays ET by month from the Hart and Evans (2001) climatology along with a bar chart of the latitudinal variation of ET by month. Figure 2.2 also shows that ET can occur at a much wider range of latitudes in September and October; when combined with peak hurricane season occurring in mid-September, this can pose a dangerous threat to Eastern Canada given the appropriate synoptic conditions.

In conclusion, while the Hart and Evans (2001) paper (and to lesser extent, similar research in other basins) provides an extensive overview of annual ET patterns in the Atlantic Basin, it is important to expand upon this study and create an analysis of synoptic patterns related to ET events that affect eastern Canada. Moreover, an analysis of a sufficient number of cases over a significant time period using a high resolution dataset will produce a climatology unique to Eastern Canada that will further aid forecasters of ET.

2.2. Synoptic overview of ET

Extratropical transition (ET) is a complex phenomenon that entails a high degree of forecasting uncertainty (Jones et al. 2003). The complexity of ET derives partially from the fact that the process itself is essentially the merging of two systems (a tropical cyclone and a mid-latitude trough) that individually are on two separate length scales (i.e. a tropical cyclone is at the high end of the mesoscale and a mid-latitude trough/ridge couplet is at the high end of the synoptic scale). As ET research has become more commonplace over the past decade, numerous patterns within trough-tropical cyclone interactions have been discovered. It is crucial, therefore, to understand how one can apply quasi-geostrophic theory to these events before proceeding with any new research.

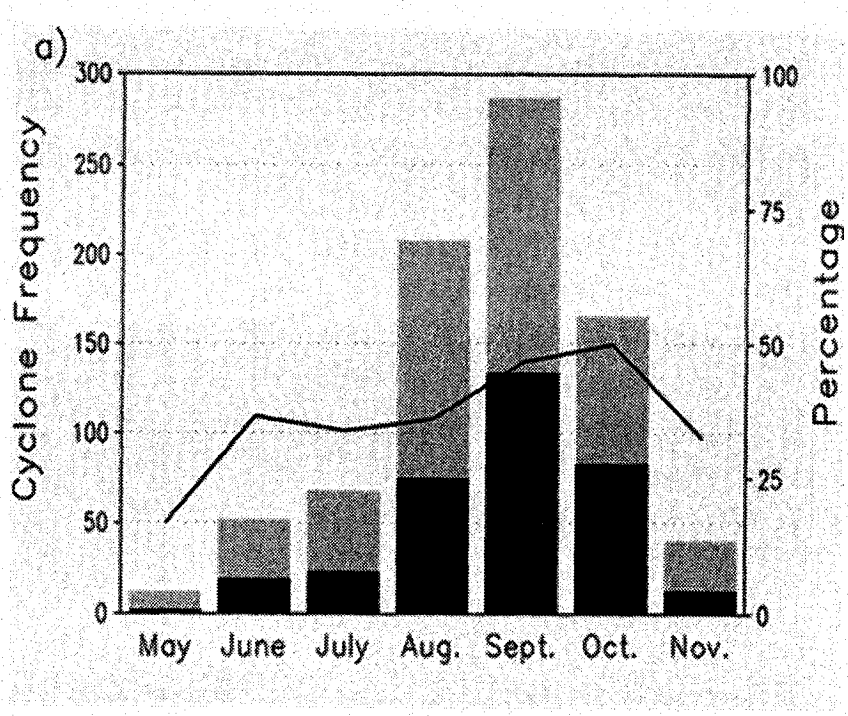

Figure 2.1: From Hart and Evans (2001): Storms undergoing ET in the dark shading compared with all Atlantic tropical cyclones (lighter shading, with the solid line indicating the percentage of Atlantic tropical cyclones that transitioned, by month).

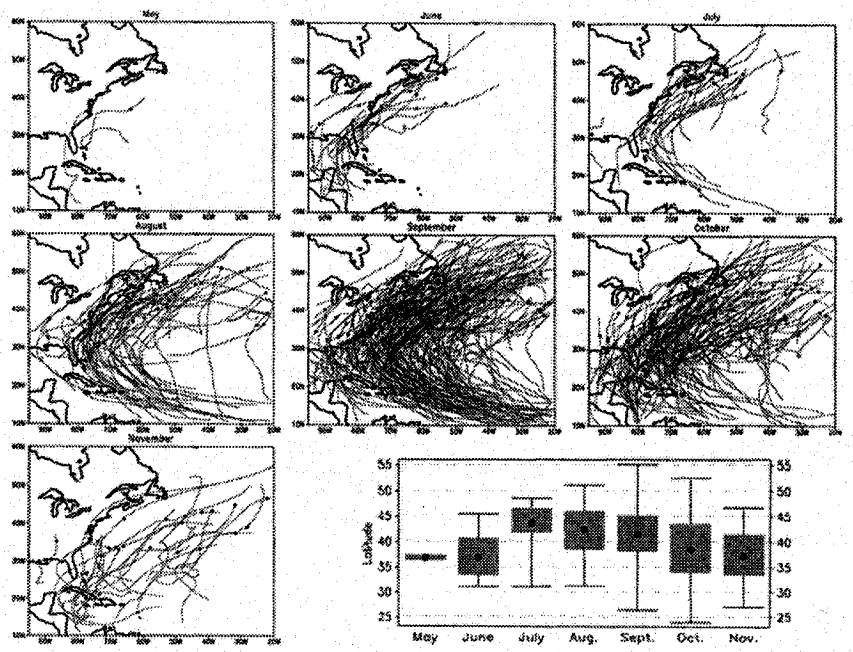

Figure 2.2: From Hart and Evans (2001): Tracks of storms that underwent ET by month and bar chart showing latitudinal variation of ET by month where circles represent mean transition location and shaded bars represent the middle 50% of transition locations.

2.2a. The tropical cyclone-trough interaction and ET classifications

The study of ET essentially began after the transition of Hurricane Hazel in 1954, which caused severe flooding in the northeastern United States and southern Ontario. Both Matano (1958) and Hughes et al. (1955) examined the synoptic situation during the ET of Hazel. Similarily, Richter and DiLoreto (1956) analyzed the 1956 ET of Hurricane Flossy (at that time it was referred to as a "transformation"), aptly noting that "it was difficult to determine exactly when the hurricane began to acquire extratropical distinction." These early studies all noticed the interaction of the respective tropical cyclones with a 500 hPa (or mid-tropospheric) trough, but it was not until the work of Matano and Sekioka (1971a,b) that an attempt was made at objectively classifying ET types into two different groups based upon associated synoptic conditions.

Specifically, Matano and Sekioka (1971a,b) studied the transitions of several typhoons in the Pacific Basin and Hurricane Hazel (Matano 1958) in the Atlantic Basin to define two categories for systems undergoing ET: the "complex" system and the "compound" system. The "complex" system is defined as occurring when the tropical cyclone induces an extratropical cyclone ahead of the 500 hPa trough (often on a pre-existing front), which subsequently merges with and absorbs the original tropical vortex. While Matano (1958) found Hurricane Hazel to be a good example of a "complex" system, Matano and Sekioka (1971a) use Typhoon Cora (1969) as an example of a "compound" system, in which a pre-existing extratropical low (typically just ahead of a 500 hPa trough) absorbs the tropical cyclone and becomes its successor cyclone. Matano and Sekioka (1971a,b) make an admirable first attempt at a classification of ET, especially in distinguishing cases where there is the potential of a pre-existing extratropical cyclone ("compound") from those where there is not ("complex"). Later studies have deemed their scheme to be too simplistic and exclusive (Klein et al. 2000; Jones et al. 2003).

In particular, Klein et al. (2000) studied thirty cases of ET in the Western Pacific Basin and defined an ET classification from a dynamical standpoint, wherein there are two distinct stages: transformation and re-intensification. The transformation stage consists of a warm-core, mostly symmetric tropical cyclone vortex becoming a typically cold-core, baroclinic, extratropical cyclone following an interaction between the tropical vortex and a mid-tropospheric trough. Klein et al. (2000) found that the best way to observe the transformation stage of ET is to examine a time series of infared (IR) satellite images that display the storm evolving from a mostly symmetric tropical system to a mostly asymmetric extratropical system. Thus, Klein et al.

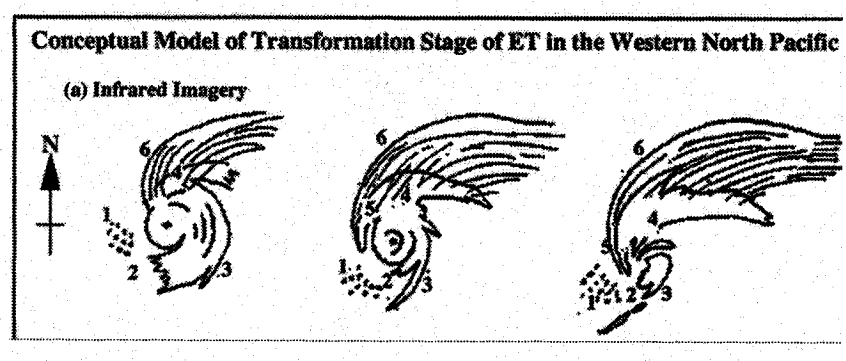

Figure 2.3: From Klein et al. (2000): A conceptual model of the transformation stage of ET.

(2000) created a conceptual model of the transformation stage, as seen in Fig. 2.3. In addition, the three main steps of the transformation stage can be applicable to all cases of ET, as is laid out by Klein et al. (2000):

1. The tropical cyclone moves over cooler sea surface temperatures (SSTs) and starts to interact with a pre-existing baroclinic zone in the mid-latitudes; in addition, further interaction with any existing mid-latitude jet will increase vertical shear.

2. As the tropical cyclone interacts with the baroclinic zone, a temperature advection dipole forms around the storm, with cold air advection (CAA) to the west and warm air advection (WAA) to the east, with the CAA often creating a dry slot in the southwestern quadrant of the storm.

3. The transformation process concludes as the center of the storm is now fully located within the baroclinic zone, and the storm is nearly completely asymmetric in appearance.

The re-intensification stage mentioned by Klein et al. (2000) is defined as the now transformed and asymmetric extratropical cyclone further intensifying, which Hart and Evans (2001) found for 51% of ET storms in the Atlantic Basin. The nature of the strengthening of the transitioned (or transformed) cyclone is similar to what would be seen in an intensifying extratropical cyclone, where cyclonic vorticity advection (CVA) increases with height above the cyclone, creating a large area of divergence at the tropopause and therefore, by mass continuity principles, convergence and rising motion at the storm center. All of the above processes are given by the vorticity advection term in the quasi-geostrophic omega equation (Equation 2.1) for rising

motion, where f_0 is the constant Coriolis parameter (s^{-1}), σ is the static stability parameter ($m^2 s^{-2} kPa^{-2}$), ω is vertical velocity ($hPa s^{-1}$), η_g is the geostrophic relative vorticity (s^{-1}), f is the latitude-dependent Coriolis parameter (s^{-1}), p is pressure, R is the universal gas constant (287 $Jkg^{-1}K^{-1}$), $\mathbf{v_g}$ is the geostrophic wind vector (ms^{-1}), T is temperature (K), and both diabatic and frictional processes are ignored,

$$\left(\nabla_p^2 + \frac{f_0^2}{\sigma}\frac{\partial^2}{\partial p^2}\right)\omega = -\frac{f_0}{\sigma}\frac{\partial}{\partial p}\left(-\mathbf{v_g}\cdot\nabla_\mathbf{p}\left(\zeta_\mathbf{g}+\mathbf{f}\right)\right) + \frac{R}{\sigma p}\nabla_p^2\left(-\mathbf{v_g}\cdot\nabla_\mathbf{p}\mathbf{T}\right). \qquad (2.1)$$

The re-intensification stage concept of Klein et al. (2000) is a sophisticated way of saying what has been known for decades: A baroclinic extratropical cyclone intensifies when there is CVA and/or WAA above it, as seen in the quasi-geostrophic omega equation. Nearly two decades prior to the Klein et al. (2000) study, DiMego and Bosart (1982a) found similar results in an analysis of the redevelopment of Tropical Storm Agnes (1972). In addition to increasing CVA with height, DiMego and Bosart (1982a,b) point to the large amount of low-level vorticity associated with the fading tropical vortex as a positive contributor to surface convergence seen in the redevelopment of Agnes. This can be an important factor for all storms undergoing ET as a method of enhancing precipitation.

Evans and Hart (2003) performed a similar analysis to Klein et al. (2000), but for the western North Atlantic Basin. Evans and Hart (2003) use different nomenclature to categorize the "transformation" and "re-intensification" stages (Klein et al. 2000), referring to the beginning of the "transformation" stage as the "onset of ET" and to the end of the "re-intensification" stage as the "completion of ET." Evans and Hart (2003) also went further than Klein et al. (2000), in using objective indicators in their methodology as opposed to "eye-balling" features using satellite imagery. The objective factors were based on two main concepts: storm symmetry (or lack thereof), and thermal wind profiles. The most important indicators are (Evans and Hart 2003):

1. "Onset" of ET is defined by a significant period of 900-600 hPa thickness asymmetry greater than 10 meters.

2. "Completion" of ET occurs when the storm can be identified as a purely cold-core vortex (i.e. a positive vertical shear).

3. Both the changes in symmetry and the thermal wind structure are measured using a 500 km radius centered on the storm so as to avoid errors that might be caused by vertical tilting of the storm system.

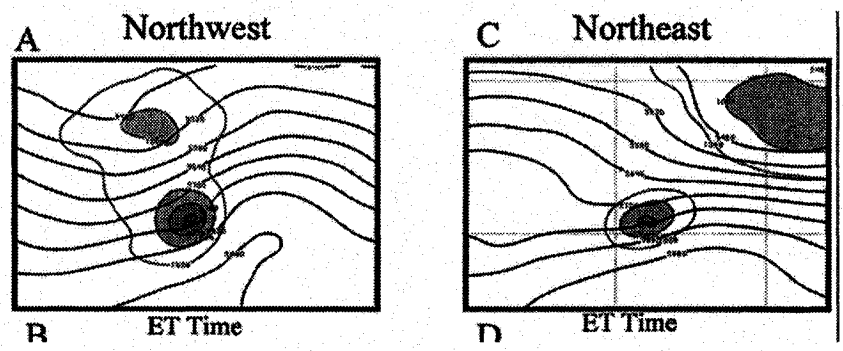

Figure 2.4: From Harr et al. (2000): A composite image of the "northwest" and "northeast" patterns, with 500 hPa height contoured in black and sea-level pressure shaded every 4 hPa under 1008 hPa.

While an objective method of defining ET can be quite useful, the forecaster must keep in mind that such sorting methods are limited by the fact that ET is a complicated process made up of many smaller simultaneous processes. For example, the objective thermal wind method of Evans and Hart (2003) may be somewhat flawed in that several intense tropical cyclones that have undergone ET in the Atlantic Basin have remained at least partially warm-core after ET despite closely resembling a purely extratropical cyclone. Therefore, the ambiguity in defining the beginning, middle, and end of ET, is prevalent in any ET analysis.

While Klein et al. (2000), Evans and Hart (2003) and Matano and Sekioka (1971a) all created an ET classification based on the dynamics of the cyclone itself, Harr et al. (2000) took a different approach in focusing on the type of mid-latitude circulation pattern (i.e 500 hPa pattern) the tropical cyclone interacts with. Harr et al. (2000) define two specific synoptic patterns, labelled "northwest" and "northeast". As seen in Fig. 2.4, the "northwest" pattern is dominated by a strong mid-latitude trough located northwest of the approaching tropical cyclone. This position, in turn, creates a vigorous baroclinic zone to interact with the tropical vortex, which subsequently helps to produce a strong extratropical cyclone. In contrast, the "northeast" pattern consists of a much weaker trough (and baroclinic zone) northwest of the approaching tropical cyclone and a dominant pre-existing extratropical cyclone downstream (northeast) of the tropical vortex. The pre-existing system helps to reduce the interaction between the trough and the tropical cyclone, thereby allowing for only a weak extratropical transition.

Foley and Hanstrum (1994) performed a similar study to those of Klein et al. (2000), Harr et al. (2000) and Evans and Hart (2003), but for the Indian Ocean off

the west coast of Australia. Using a sample size of 39 events (similar to the other studies), Foley and Hanstrum (1994) separated their storms into two synoptic classes:

1. "Cradled" cyclones, where the cyclone is "cradled" by easterly flow toward the pole and travels poleward with a slow average speed of movement.

2. "Captured" cyclones, which are more common and occur when a tropical cyclone moves poleward and becomes embedded in the westerly flow associated with a strong baroclinic zone (or cold front).

"Captured" storms are similar to the transforming, northwest, and warm-to-cold core classes in Klein et al. (2000), Harr et al. (2000), and Evans and Hart (2003), respectively.

It is clear that the position and characteristics of the mid-latitude trough relative to the approaching tropical cyclone are crucial factors in the ET process. Ritchie and Elsberry (2003) put this in perspective by pointing out that "the final intensity of the extratropical cyclone is not only related to the strength of the upper-level trough but must also be related to the structure of the basic midlatitude environment." In addition, Ritchie and Elsberry (2003) concur with DiMego and Bosart (1982a), in arguing that the tropical cyclone itself plays a significant role in the ET process, both through proper alignment with the mid-level trough and high in situ low-level vorticity and moisture values that would not be attained in an ordinary extratropical cyclone. In conclusion, it is crucial to view the ET transformation and re-intensifcation process as a sum of three parts: the strength of the upper-level trough, the positioning of the tropical cyclone with respect to the trough, and the existence of the low-level, warm-core tropical cyclone itself.

2.2b. The tropical cyclone-trough interaction from a potential vorticity perspective

The use of potential vorticity (PV) and dynamic tropopause maps in meteorological analysis was brought to light two decades ago in the seminal paper by Hoskins et al. (1985). The authors point out that the use of Isentropic Potential Vorticity (IPV or, simply PV) is "the key to a very powerful and succinct view of the dynamics" and that "IPV maps...are a natural diagnostic tool well suited to making dynamical processes directly visible to the human eye and to making meaningful comparisons between atmospheric models and reality." In particular, analyses using PV maps are useful because (Hoskins et al. 1985):

1. PV is conserved for adiabatic, frictionless motion.

2. PV is dependent only on isentropic absolute vorticity $f + \zeta_\theta$ and static stability $\nabla_p \theta$ (as seen in Equation 2.2).

3. From the PV invertibility principle, which states that given a particular distribution of PV, one can infer the wind, pressure, and temperature fields.

Equation 2.2 defines PV from Hoskins et al. (1985) where P is potential vorticity (often stated in terms of Potential Vorticity Units (PVU), where 1 PVU $= 10^{-6} m^2 s^{-1} K kg^{-1}$), g is the constant acceleration due to gravity ($9.81 ms^{-2}$), f is the latitude-dependent Coriolis parameter (s^{-1}), ζ_θ is the isentropic relative vorticity (s^{-1}), and θ is potential temperature (K),

$$P = -g(f + \zeta_\theta) \cdot \nabla_p \theta. \tag{2.2}$$

Because PV is conserved for adiabatic, frictionless motion, PV maps allow for a quick and easy identification of areas of large diabatic heating and/or cooling, an important factor in re-intensifying ET systems. Furthermore, Morgan and Nielsen-Gammon (1998) argue that PV analyses are extremely useful, because, unlike most quasi-geostrophic analyses, the researcher or forecaster can view the entire flow regime of the troposphere via an "Eady model view", which consists of only the top (dynamic tropopause) and bottom (near-surface) boundaries. Morgan and Nielsen-Gammon (1998) add that the use of the "Eady" view is "somewhat analogous to the traditional use of 500-hPa and surface maps to diagnose tropospheric development" and that "the traditional method works because...most 500-hPa vorticity extrema are associated with PV variations at the tropopause." It is this "Eady" view which makes PV extremely useful in analyzing ET events, allowing for a clearer view of the tropical cyclone-trough interaction. The use of PV analyses is a major factor in the increase of ET-based studies over the past decade.

Quasi-geostrophic analyses of ET can be both time-consuming and occasionally cumbersome. Utilizing IPV maps at both the dynamic tropopause and near the surface helps to make the mid-tropospheric trough and the tropical cyclone (which by definition of being a warm-core cyclone, has a vorticity maximum at the lower boundary) simultaneously viewable. The piecewise inversion technique briefly mentioned above, where the height and temperature fields, etc. can be deduced from the PV distribution, has been used for almost two decades in analyses of tropical cyclones (e.g. Wu and Emanuel (1995); Hanley et al. (2001),etc.), but only recently has it been used for ET events (Jones et al. 2003).

Morgan and Nielsen-Gammon (1998) indicate that two dynamically equivalent varieties of PV plots are commonly found in the literature: Potential Vorticity on

isentropic surfaces (IPV) and variations of potential temperature on constant PV surfaces (termed "isertelic" analyses). As expressed by Morgan and Nielsen-Gammon (1998), a "warm" potential temperature anomaly at tropopause level on a isertelic analysis is equivalent to a region of low PV at tropopause level on an IPV map, e.g. both representative of an upper-level anticyclone. Accordingly, a "cold" theta anomaly at the tropopause on a isertelic analysis is dynamically equivalent to high values of PV at the same vertical level. As a reference, the PV composite plots in Chapter 3 are of near-tropopause PV (similar to IPV maps), while the dynamic tropopause maps in Chapter 4 of this study are of the isertelic variety. In addition, to complement upper-level IPV or isertelic analyses, warm (cold) potential temperatures at near-surface levels are often used as proxies for high (low) values of low-level PV, as explained by Hoskins et al. (1985) and Morgan and Nielsen-Gammon (1998). A warm (cold) potential temperature anomaly at a near-surface level often is indicative of a cyclonic (anticyclonic) feature, i.e. contrary to the theta-cyclone relationship found at upper levels. Table 2.1 sums up this important distinction.

Level	Potential Vorticity anomaly	Potential Temperature anomaly
Tropopause	high (cyclonic), low (anticyclonic)	cold (cyclonic), warm (anticyclonic)
Near-surface	n/a	warm(cyc.), cold(anticyc.)

Table 2.1: Synoptic importance of PV and potential temperature anomalies at near-surface and near-tropopause levels.

Browning et al. (1998) looked at the ET and subsequent re-intensification of ex-hurricane Lili (1996), an Atlantic Basin tropical cyclone that underwent ET and then moved eastward before affecting the heavily populated British Isles in late October, 1996. The study found that Lili reintensified as an extratropical cyclone after interacting with a stratospheric PV anomaly (mid-tropospheric trough). Furthermore, Browning et al. (2000) found a tropopause fold associated with two mesoscale tropopause depressions, or lowering of the tropopause, to be associated with the intense re-intensification of Lili. The re-intensification of Lili directly contradicts the objective criterion of Evans and Hart (2003), in which a storm is determined to have undergone ET once it can be defined as a cold-core extratropical cyclone. Browning et al. (1998) found that while Lili most certainly looked like an extratropical cyclone on its approach to the British Isles, it maintained an upright warm core up to the 400 hPa level, as seen in Fig. 2.5. This finding illustrates that a) the classification scheme of Evans and Hart (2003) can be at times an oversimplification, and b) PV time series and/or cross sections are extremely useful in diagnosing the thermal profile (warm-

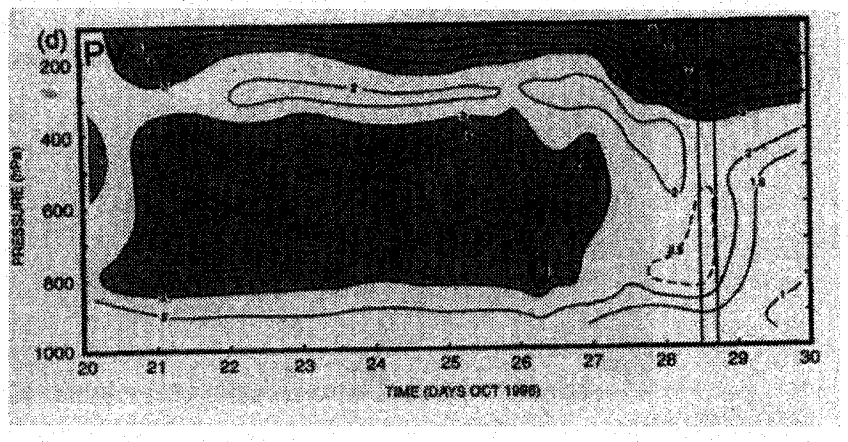

Figure 2.5: From Browning et al. (1998): A time series of PV (PVU) over ex-Hurricane Lili in 1996; notice the high values of PV (shaded) from the surface to 400 hPa, displaying an extensive warm-core system.

or cold-core) of a transitioning system.

Case studies similar to that of Browning et al. (1998) were performed by both Thorncroft and Jones (2000) and Agusti-Panareda et al. (2004) on Hurricanes Felix and Iris (1995) and Hurricane Irene (1999), respectively. In their study of Iris, Thorncroft and Jones (2000) found similar warm-core characteristics to ex-Hurricane Lili (1996) Browning et al. (1998) after ET. Interestingly, while Felix was originally a much stronger tropical cyclone than Iris, Iris ended up being a much stronger extratropical cyclone after transition. Thorncroft and Jones (2000) attribute this to the fact that Felix did not maintain its warm-core structure as it tracked poleward into cooler waters in the North Atlantic. As with Lili (Browning et al. 1998), PV maps were extremely useful in identifying whether or not a particular storm maintained its warm-core post-transition during its trek across the North Atlantic; these PV analyses led Thorncroft and Jones (2000) to conclude that "the contrasting cases of Iris and Felix highlight the problem of defining exactly what is meant by extratropical transition...(since) in the case of Iris the system never developed a cold core, but baroclinic processes played a dominant role in the subsequent extratropical development."

Agusti-Panareda et al. (2004) designed a conceptual model of ET (Fig. 2.6). The model is similar to that designed by Klein et al. (2000), except that it utilizes PV thinking. The model was based on the ET of Hurricane Irene (1999), which produced heavy rains along the east coast of the U.S. before re-intensifying into a very deep extratropical cyclone in the North Atlantic (Agusti-Panareda et al. 2004). The model contains five distinct stages, as seen in Fig. 2.6, and differs from quasi-geostrophic

models of ET in that one is able to get an instantaneous three-dimensional view of the ET process, based on the interaction between the upper and lower systems.

2.3. Precipitation, diabatic effects, and frontogenesis

2.3a. Precipitation distributions associated with ET

Heavy precipitation as a result of tropical or transitioning tropical cyclones is often overlooked by the general public in favor of high winds. However, most of the damage and loss of life related to tropical and transitioning cyclones in recent decades has been directly related to severe flooding events (Marks 1998; Srock et al. 2004a,b; Carr and Bosart 1978; Weese 2003; Atallah and Bosart 2003; Cerveny and Newman 2000). Extratropical transition, in particular, "poses an especially challenging quantitative precipitation forecasting (QPF) problem....Successful QPF requires an accurate prediction of the track, intensity, and structural changes of storms undergoing ET" (Jones et al. 2003). Ordinary rules of thumb for accurate QPF may not necessarily apply to storms undergoing ET, because of the many competing processes that occur at multiple scales within these events. Fortunately, QPF research related specifically to ET has increased over the past five to ten years, although there is much work still to be done.

Elsberry (2002) states that not only is precipitation a crucial part of the ET process, but during the "transformation" stage (Klein et al. 2000), the areal coverage of the precipitation shield often expands from that which is representative of a purely tropical cyclone to that which is often observed in an extratropical cyclone. In addition, it is important that when forecasting precipitation, the forecaster does not just forecast how much rain will fall, but also where it will fall - a variable often expressed relative to the center of the storm. In a mostly symmetric tropical cyclone, heavy precipitation normally occurs on both sides of the storm track (Jones et al. 2003). However, in a storm that has undergone ET in the Northern Hemisphere, the heaviest precipitation is often to the left of the center of the storm track (or to the right in the Southern Hemisphere) (Jones et al. 2003). The change in the precipitation distribution is often due to the interaction of the tropical cyclone with a mid-latitude trough and/or a baroclinic zone (Jones et al. 2003). Precipitation distribution changes are crucial with respect to Eastern Canada, because any heavy precipitation falling to the left of a storm track just along the coast, may affect not only coastal areas, but inland areas as well (Carr and Bosart 1978). Atallah and Bosart (2004) performed a

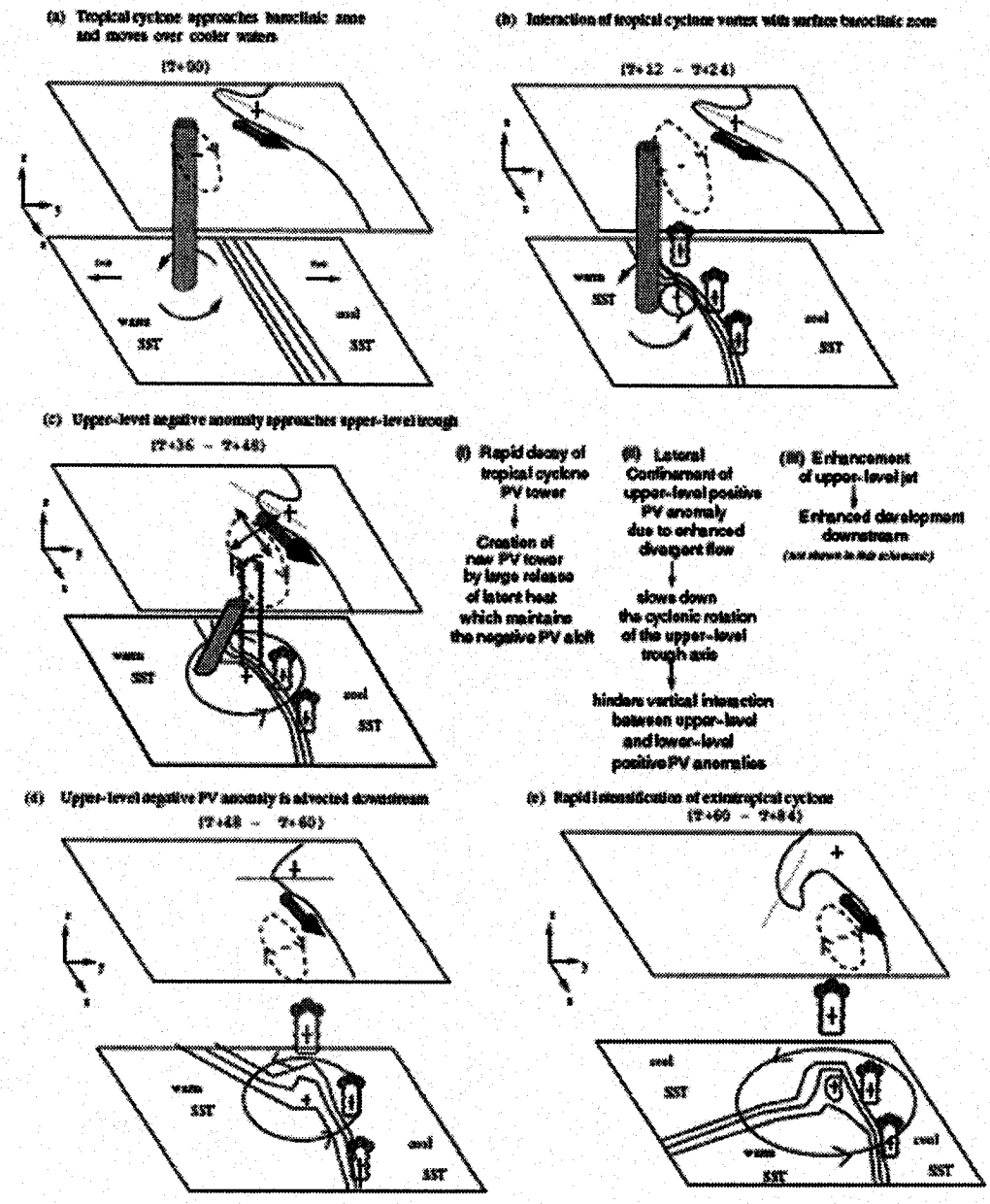

Figure 2.6: From Agusti-Panareda et al. (2004): A conceptual model of ET using PV thinking; helps to display the importance of PV maps in attaining an instantaneous 3-D view of the atmosphere during the ET process.

composite study on precipitation distributions in transitioning tropical cyclones over the Eastern U.S. (Fig. 2.7) and found that during transition, the composite left-of-center (LOC) precipitation distribution (i.e. left of the storm track) showed high values of vertical shear just downstream of the nearby mid-latitude trough and a relatively meridional baroclinic zone, similar to what Harr et al. (2000) found for "northwest" pattern storms. In contrast, storms with a precipitation distribution to the right-of-center (ROC) were characterized by a relatively zonal baroclinic zone, which helped to prevent any significant temperature advections, and thus typically means ROC storms have less precipitation associated with them (Atallah and Bosart 2004). Furthermore, LOC storms seem to be more likely to complete extratropical transition than their ROC counterparts, giving forecasters a signal to look for during an ET event (Atallah and Bosart 2004). To emphasize this point, DeLuca et al. (2004) found that, in the case of Hurricane Connie (1955), the lack of a major interaction with an upstream mid-latitude trough was the main cause behind the failure of the precipitation to shift to the left of the storm track.

2.3b. Diabatic effects during ET

It is often convenient in synoptic meteorology to use the phrase "ignoring diabatic and frictional effects...," so as to make equations easier to use and interactions simpler to analyze. In terms of ET, however, an interaction takes place that is essentially the "juxtaposition of two very different air masses (tropical and baroclinic) resulting in a pronounced temperature gradient...that can lead to copious amounts of precipitation. The diabatic heating resulting from the precipitation then serves as a mechanism for changing the scales and orientations of the upper and lower-level PV anomalies (Atallah and Bosart 2003)." Diabatic heating is an important process in re-intensifying systems that are undergoing or have undergone ET, since it can affect the storm in multiple ways, from intensity and track of the cyclone to copious precipitation amounts and intense frontogenesis.

The study of DiMego and Bosart (1982a) on the transition of Tropical Storm Agnes (1972) was one of the first to illustrate the importance of diabatic processes to the re-intensification of the storm and the positive diabatic feedback caused by heavy precipitation (i.e. heavy precipitation releases latent heat which, in turn, helps to amplify the vertical motion and contributes to more heavy rainfall). Initial ascent associated with Agnes (1972) was forced by warm air advection (WAA), as predicted by Equation 2.1. However, latent heat release associated with heavy rainfall along the spine of the Appalachian mountains, at least partially enhanced by orographic lifting of warm

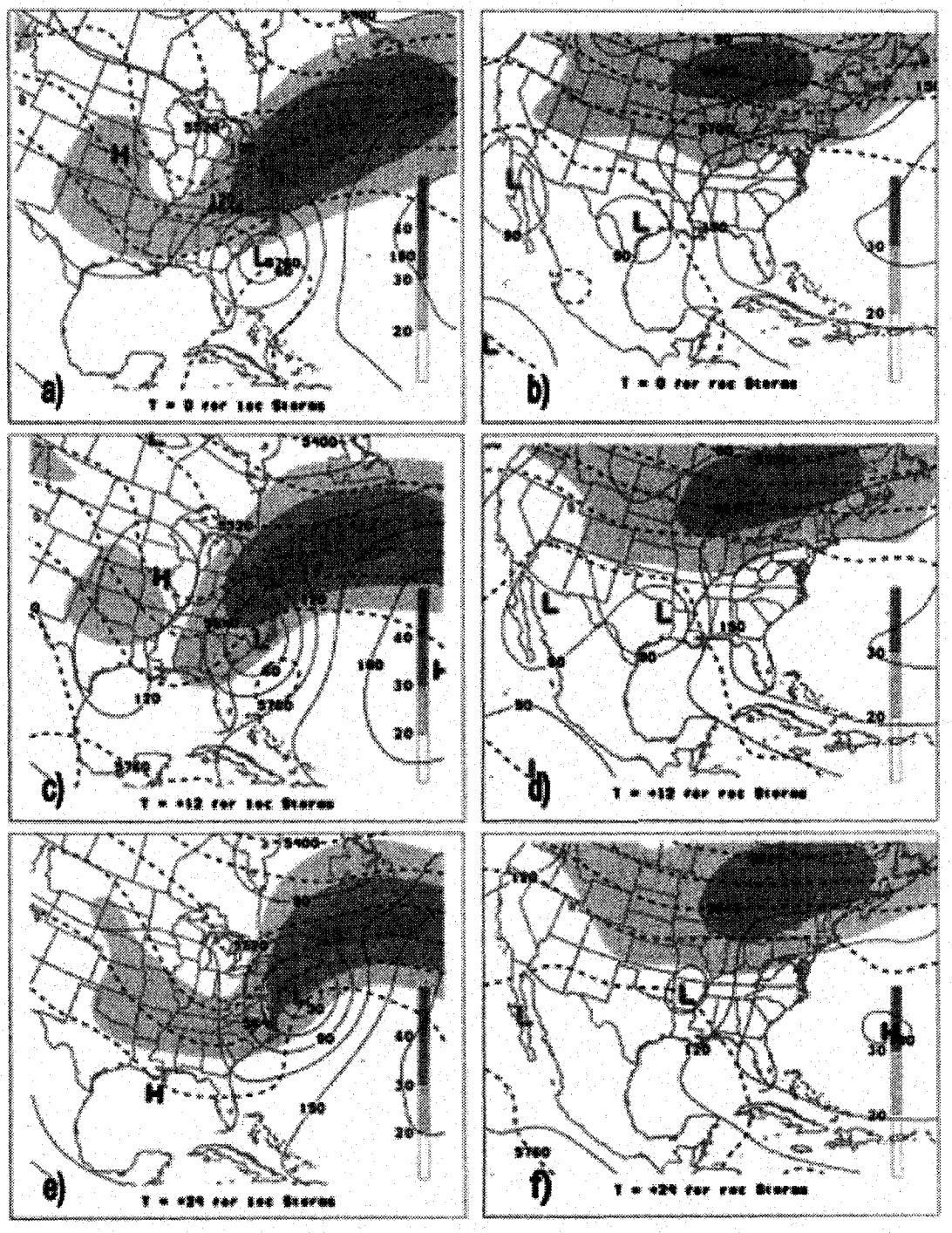

Figure 2.7: Composite synoptic structures of LOC vs. ROC precipitation distributions, from Atallah and Bosart (2004): 1000-500 hPa thickness contours (dashed), 1000 hPa geopotential height contours (solid), and 850-200 hPa shear (shaded) for a) LOC composite at t=0, b) ROC composite at t=0, c) LOC at t=12, d) ROC at t=12, e) LOC at t=24, and f) ROC at t=24).

air from the Atlantic ocean (DiMego and Bosart 1982a), helped create a net result in which the temperature advection and diabatic processes worked in concert to create a large swath of heavy precipitation to the north of Agnes. This positive feedback between the diabatic and temperature advection terms in the quasi-geostrophic omega equation can help explain both catastrophic flooding and storm re-intensification in cases of ET. In the case of Agnes, the re-intensification of the storm as an extratropical cyclone over the mid-Atlantic and northeast U.S. was due to vorticity generation by processes associated with massive surface convergence, including a diabatic component, which, next to CVA, was estimated to be the largest contributor to voriticity generation during the ET of Agnes (DiMego and Bosart 1982b).

Recently, the effects of diabatic processes on ET have been increasingly examined using "Potential Vorticity (PV) Thinking", which can be advantageous, given that PV is conserved for frictionless, adiabatic motion (Hoskins et al. 1985). In other words, areas of non-conservation on a PV map during ET are a clear signal of significant diabatic heating or cooling. Dickinson et al. (2004) used PV maps in the study of Hurricanes Andrew and Lester (1992) to illustrate that diabatic outflow from Hurricane Andrew during its transition along the east coast of the U.S. caused an intensification of an upper-air ridge in the Western Atlantic. Similarly, Atallah and Bosart (2003) found that, in the case of Hurricane Floyd (1999), diabatic heating released by heavy precipitation along the U.S. east coast acted to enhance the downstream ridge over the Western Atlantic; this subsequently changed the orientation of the trough associated with the ET of Floyd from positive to negative, making it more potent. Moreover, because the ridge essentially "bends back" to the NW of the storm center, one often finds a tropopause fold associated with potent intensifications such as the one achieved by Floyd (Atallah and Bosart 2003). Colle (2003) agrees, stating that high resolution modelling of Floyd clearly shows that, when diabatic effects are removed, the storm is approximately 25 hPa weaker at sea-level than when diabatic effects are included.

In summary, the positive feedback associated with diabatic heating consists of three steps: 1) latent heat release from heavy precipitation associated with the cyclone, 2) associated diabatic outflow acting to enhance the downstream ridge and 3) the enhancement of the downstream ridge, causing the trough directly involved in the ET to become negatively tilted and increasing its potency. Several of the more intense ET cases in this study were greatly affected by this diabatic feedback, including Luis (1995), as examined in Chapter 4.

2.3c. Mesoscale processes

The ET process is essentially a combination of systems that are initially on two different scales. Therefore, it is naive to assume that all of the processes occurring during and after ET are on the synoptic scale. In reality, several important mesoscale and microscale processes take place during ET, all of which can have a profound effect on the transitioning storm.

One of the primary mesoscale mechanisms during ET is frontogenesis; Jones et al. (2003) point out that nearly all of the significant precipitation during ET is co-located with areas of warm frontogenesis. This is predominantly due to a mostly nonlinear combination of adiabatic and diabatic dynamics, in which the majority of latent heat release takes place in an area of low symmetric stability. Consequently, there is a stronger ascent-descent vertical motion couplet, which increases the rate of low-level frontogenesis. The increased frontogenesis results in a strengthening of the secondary adiabatic vertical circulation, which causes further latent heat release, and completes the positive feedback cycle (Jones et al. 2003).

Colle (2003) used a high resolution Mesoscale Model Version 5 (MM5) simulation to show that precipitation maxima just inland of the New Jersey coastline were not due to topography, but instead were attributed to intense frontogenesis during the ET of Floyd (1999). In addition, the intense nature of the mesoscale precipitation band that was aligned parallel to the low-level front suggests the possibility of the release of Conditional Symmetric Instability (CSI) (Colle 2003). Bosart and Dean (1991) found a similar result with Tropical Storm Agnes (1972); however, in the case of Agnes, the heavy precipitation band was a combination of intense low-level frontogenesis and topographic lifting along the eastern slope of the Appalachian Mountains.

While low-level frontogenesis has been cited as a cause of intense mesoscale precipitation bands during ET (Bosart and Dean 1991; Colle 2003), the importance of frontogenesis with regard to storm dynamics during ET must also be noted. Harr and Elsberry (2000) found that increased warm frontogenesis on the eastern flank of the transitioning tropical cyclone can be used as a clear signal of ET. However, there is an important caveat to this claim: While low-level warm frontogenesis values can represent the time evolution of the ET process (i.e. time of transition), they cannot account for the implicit details associated with the ET dynamics (Harr and Elsberry 2000). Moreover, Liu and Chen (2003) found that the transition of Typhoon Winnie (1997), marked by a rare rapid intensification over land, was primarily due to the interaction of Winnie with a baroclinic zone, leading to mid-level frontogenesis, which amplified an initially weak upper trough-ridge couplet.

In summary, frontogenesis is an important variable in both synoptic-scale and mesoscale analyses of ET. While low-level frontogenesis can enhance precipitation on the mesoscale (Colle 2003; Bosart and Dean 1991), low- and mid-level frontogenesis can be used as indicators of ET dynamics on the synoptic scale (Harr and Elsberry 2000). Frontogenesis is an important similarity between cyclones undergoing ET and their purely extratropical counterparts.

2.4. ET and explosive extratropical cyclogenesis

Tropical cyclone season in the Atlantic Basin officially runs from June 1st to November 30th, peaking in late August or early September. Thus, tropical cyclones, and therefore ET, are primarily summertime phenomena. In contrast, explosive extratropical cyclogenesis, or "bombogenesis" (Sanders and Gyakum 1980; Sanders 1986; Klein et al. 2000, 2002; Kuo et al. 1991; DiMego and Bosart 1982a; Macdonald and Reiter 1988; Elsberry and Kirchoffer 1988; Manobianco 1989; Sanders and Davis 1988; Lackmann et al. 1996; Sinclair and Revell 2000; Wang and Rogers 2001; Kuo and Low-Nam 1990; Schultz et al. 1998; Lemaitre et al. 1999a; Hart 2003; DiMego and Bosart 1982b; Young et al. 1987; Uccellini and Kocin 1987; Lemaitre et al. 1999b; Uccellini et al. 1985; Uccellini 1986) as it has come to be known, is predominantly a cold-season event in the western Atlantic (Sanders and Gyakum 1980). Therefore, it may seem a contradiction of sorts to attempt a comparison between systems of different seasons. However, in many case and composite studies alike, similarities in synoptic structure and behavior between storms undergoing re-intensification during ET and wintertime extratropical "bombs" are difficult to ignore.

In comparing ET re-intensifications to explosive extratropical cyclogenesis, two predominant characteristics of rapidly intensifying cyclones need to be considered: rate of intensification and storm structure. Sanders and Gyakum (1980) defined a "bomb" as a rapidly intensifying low in which the central sea level pressure value falls at the rate of at least 1 hPa per hour for at least 24 hours. In their ET climatology of the western North Pacific, Klein et al. (2000) found six cases of rapid deepening during re-intensification that met or exceeded a 1 hPa per hour pressure fall for at least 12 hours. Several cases in this study also experience a deepening rate that matches or exceeds the Sanders and Gyakum (1980) "bomb" criterion.

Perhaps the most important characteristic in a comparison of two cyclone types is the structure of each type. A plethora of studies have been done with regard to the structural characteristics of Atlantic Basin "bombs", some of which are as follows

(and almost all of which have been found in at least one ET study, including the cases included in this paper):

- A deepening upper-air short wave trough is often found upstream of the storm development region 12 hours prior to rapid development (Uccellini 1986).
- The presence of an upper-level (tropopause) jet maximum, or jet streak (Elsberry and Kirchoffer 1988).
- Rapid development is essentially caused by strong upper-level forcing enhanced by a very destabilized low-level troposphere (Manobianco 1989).
- Intense latent heat release and subsequently positive diabatic feedbacks, often ignorable in ordinary cyclogenesis (Kuo et al. 1991).
- An interaction between the associated vertical circulations of the left exit region of the subtropical jet and the right entrance region of the polar jet (Uccellini and Kocin 1987).
- A tropopause fold bringing down high values of stratospheric PV 12-24 hours prior to explosive development (Uccellini et al. 1985).
- Satellite imagery of a "bomb" shows that an interaction between an intrusion of dry, stratospheric air (high PV) and the "baroclinic leaf cloud" (essentially a cloud representation of the warm conveyor belt) occurs just prior to explosive development (Young et al. 1987).
- Strong slantwise ascent in an area of intense warm frontogenesis during the time of rapid intensification (Kuo and Low-Nam 1990).

In addition, several studies on ET (Klein et al. 2002; DiMego and Bosart 1982a,b; Liu and Chen 2003) have compared post-ET re-intensifications to what is known as the Petterssen "Type B" cyclone (Petterssen and Smebye 1971), whose characteristics are as follows:

- Storm development occurs when a pre-existing upper trough, with strong CVA ahead of it, expands over a low-level region of WAA, with or without a frontal zone.
- The spacing between the upper-air trough and the surface cyclone rapidly narrows as the storm strengthens.

- The CVA aloft decreases with time, while the low-level temperature advection couplet strengthens with time.
- The amount of low-level baroclinicity increases as the storm intensifies.
- The final storm resembles a classical occluded cyclone.

It is important to note that while not every single case of ET re-intensification and/or explosive extratropical cyclogenesis exactly fit all the criteria, there are enough shared similarities between the two to warrant a comparison. Klein et al. (2002) objectively defined a region which would be favorable to Type B development, based on specific threshold values of upper-level CVA and the low-level temperature advection couplet. It was then determined how many cases in the ET climatology fit the objective criteria. The hypothesis of Klein et al. (2002) is that the occurrence of the re-intensification stage of ET depends on the mid-latitude circulation pattern (the upper trough) providing upper- and mid-level support. Moreover, the alignment of the transforming tropical cyclone relative to the mid-latitude baroclinic zone must be one favorable for development, as in Type B cyclones (Petterssen and Smebye 1971). The results for several cases in the western Pacifc climatology found that proper phasing of the transitioning tropical cyclone with the mid-latitude trough results in a storm re-intensification process very similar to that of Type B (Klein et al. 2002). DiMego and Bosart (1982a,b) found a comparable result in the case of the transitioning Tropical Storm Agnes (1972), albeit in the case of Agnes, the Type B process was significantly enhanced by an area of warm moist air and low-level in-situ vorticity associated with the original tropical cyclone.

Clearly, the classification scheme of Petterssen and Smebye (1971) is applicable to both rapidly developing extratropical cyclones and rapidly re-intensifying cases of ET. In addition, many characteristics of explosively intensifying extratropical cyclones have also been found in strong ET re-intensifications. Consequently, the forecaster should be able to utilize knowledge of explosive cool-season (wintertime) cyclogenesis in order to enhance their forecasting skill of warm-season explosive ET.

Chapter 3

Compositing Methodology and Results

3.1. Dynamical partitioning methodology

The primary objective of large-scale composite synoptic analyses is to examine the similarities and differences in synoptic structure between "intensifying" and "decaying" storms. Before defining a partitioning methodology, it is important to note the difference between the transition of the storm and the subsequent intensification or decay. The quasi-geostrophic (QG) omega equation (Equation 2.1) and the Sutcliffe approximation to the QG omega equation (Equation 3.4) are diagnostic equations that are used to identify when a storm is undergoing or has completed extratropical transition. In other words, a symmetric and relatively small (in horizontal extent) vertical motion field will typically expand (in horizontal extent) and become more asymmetrical as the storm becomes extratropical. These equations are used in Section 3.2 for analysis purposes. In this section, however, a partitioning methodology is outlined specifically to differentiate between "intensifying" and "decaying" storms, based on the rates of change of vorticity, as defined by the quasi-geostrophic vorticity equation (Bluestein 1992).

$$\frac{\partial \eta}{\partial t} = -f_0 \delta. \tag{3.1}$$

Thus, using this prognostic equation, storm cases can be dynamically partitioned into "intensifying" and "decaying" classes. In contrast, the QG omega equation (Equation 2.1) and the dynamically equivalent Sutcliffe approximation (Equation 3.4) should only be used as a diagnostic tool to analyze, among other features, precipitation, vertical motion, and storm characteristics (i.e. extratropical vs. tropical). It is of note that the vertical motion associated with the forcing terms in the QG omega

equation can be implicitly related to the vorticity tendency term in Equation 3.1 by utilizing the mass continuity equation (Equation 3.2), where the pressure derivative of omega is equal to the negative of the divergence.

$$\frac{\partial \omega}{\partial p} = -\delta. \tag{3.2}$$

The four weakest vortices in the study (Alberto (1988), Chris (1988), Unnamed (1991) and Dennis (1999)) have minimum Sea Level Pressure values (SLP) more than one standard deviation above the average minimum SLP value; therefore, these storms are dropped from the composite study. This is done so that a very weak vortex will not be classified in the intensifying category, even if it does undergo a slight intensification. The remaining 28 storms are partitioned into two groups, "intensifying" and "decaying," based on the rate of change of the low-level (700-850 hPa) absolute vorticity. An intensifying case is defined by minimum low-level absolute vorticity increase of $5 \times 10^{-5} s^{-1}$ over a time period of twelve hours, with a decreasing absolute vorticity of similar magnitude as the criterion for a decaying case. For example, Fig. 3.1 displays the strongly positive slopes (vorticity increases) at both the mid- and low-levels for the most rapidly intensifying case in the study, Luis (1995). In contrast, Fig. 3.2 displays strongly negative slopes (vorticity decreases) at both the mid- and low-levels for the most rapidly decaying case in the study, Isabel (2003). Utilizing this methodology, eleven storms are found to fit the "intensifying" criterion, while eleven cases are categorized as "decaying" (Table 3.1). Five cases have vorticity slopes too small (positive or negative) to fit in either bin, and Juan (2003) is also not classified in either group due to the NARR's poor representation of the storm (Section 5.3).

All composites are completed using a storm-relative compositing method (Atallah and Bosart 2004). This process involves compositing the storm cases relative to a specific latitude-longitude point based on a reference storm track. In this study, the reference storm track chosen for each group is an average position of the cases in the group. For example, all the grids in the "intensifying" composite at time t=0 are shifted so that each storm center is located at the same latitude-longitude coordinate, as specified by the reference storm track. Therefore, all motion of the composite storm is relative to the reference track and not to the apparent geography on the map. The geography is retained on the plots, however, for the purpose of discussion of relevant features, and as a reminder that the study is based in the Western North Atlantic basin. Storm positions at each time are in general within five degrees latitude of each other, therefore minimizing curvature problems (Atallah and Bosart 2004).

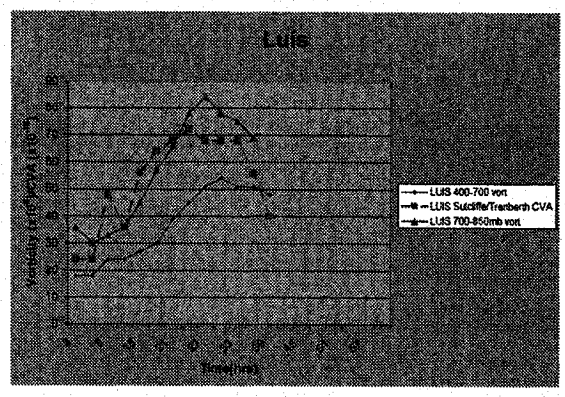

Figure 3.1: For Luis (1995): NARR 400-700 hPa absolute vorticity $\times 10^{-5} s^{-1}$ (blue), NARR 700-850 absolute vorticity $\times 10^{-5} s^{-1}$ (green), NARR CVA by the Sutcliffe method $\times 10^{-10} s^{-2}$ (pink); t=0 represents the time the storm was judged to have begun to affect Canada.

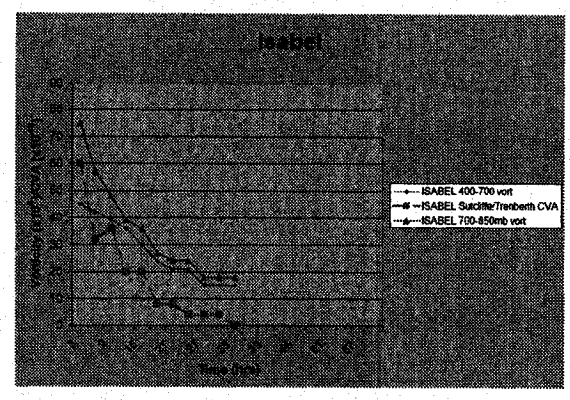

Figure 3.2: For Isabel (2003): NARR 400-700 hPa absolute vorticity $\times 10^{5} s^{-1}$ (blue), NARR 700-850 absolute vorticity $\times 10^{-5} s^{-1}$ (green), NARR CVA by the Sutcliffe method $\times 10^{-10} s^{-2}$ (pink); t=0 represents the time the storm was judged to have begun to affect Canada.

Year	Intensifying	Decaying	Neither
1979	none	David, Frederic	none
1985	Gloria	none	none
1989	none	Hugo	Dean
1990	Bertha	none	Lili
1991	none	Bob	none
1995	Allison, Barry, Luis	Opal	none
1996	none	Bertha, Fran, Hortense	Josephine
1998	Earl	none	none
1999	none	Floyd	none
2000	Leslie, Michael	Gordon	none
2001	Erin	none	Karen
2002	Arthur, Gustav	none	none
2003	none	Isabel	Juan
2004	none	none	Frances

Table 3.1: Intensifying, Decaying, and Neither, by year.

3.2. Quasi-geostrophic composites

Firstly, the ambiguity in the quasi-geostrophic omega equation (Equation 3.3), where f_0 is the constant Coriolis parameter (s^{-1}), $\sigma(m^2s^{-2}kPa^{-2})$ is the static stability parameter, ω is vertical velocity (hPa/s) , ζ_g is the geostrophic relative vorticity (s^{-1}), f is the latitude-dependent Coriolis parameter (s^{-1}), p is pressure (hPa), R is the universal gas constant ($Jkg^{-1}K^{-1}$), $\mathbf{v_g}$ is the geostrophic wind vector (ms^{-1}), T is temperature (K), and both diabatic and frictional processes are ignored), must be removed (Trenberth 1978). This ambiguity refers to the potential cancellation of terms between the main vertical motion-forcing terms, vorticity and temperature advection.

$$\left(\nabla_p^2 + \frac{f_0^2}{\sigma}\frac{\partial^2}{\partial p^2}\right)\omega = -\frac{f_0}{\sigma}\frac{\partial}{\partial p}\left(-\mathbf{v_g}\cdot\nabla_\mathbf{p}\left(\zeta_\mathbf{g}+\mathbf{f}\right)\right) + \frac{R}{\sigma p}\nabla_p^2\left(-\mathbf{v_g}\cdot\nabla_\mathbf{p}\mathbf{T}\right) \qquad (3.3)$$

Using principles of development originally derived by Sutcliffe (1947); Sutcliffe and Forsdyke (1950) and later expanded by Petterssen (1955), Trenberth (1978) derived an approximate expression (Equation 3.4), the Trenberth approximation to the QG omega equation (sometimes called the Sutcliffe or Sutcliffe/Trenberth approximation or method). This approximation combines the vorticity and temperature advection terms in Equation 3.3 into a single term, whereby upward motion is present where there is cyclonic vorticity advection (CVA) by the thermal wind. There are several advantages and caveats to using this form of the quasi-geostrophic omega equation:

- Vertical motions can be evaluated using only one synoptic map that should feature vorticity and thickness contours, since the thermal wind is parallel to lines of constant thickness (Trenberth 1978).
- The use of this formulation works best in the mid-troposphere, where cancellation of the vorticity and temperature advection terms in Equation 3.3 is most problematic (Trenberth 1978).
- Both 1000-500 hPa (Trenberth 1978) and 1000-200 hPa (Atallah and Bosart 2003) thickness contours have been used with the Trenberth approximation and seem to be adequate.

This study follows the method of Atallah and Bosart (2003) and utilizes 1000-200 hPa thickness values with 400-700 hPa layer-averaged absolute vorticity. Absolute vorticity and relative vorticity are qualitatively interchangeable in the mid-latitudes inside the Trenberth approximation, since the advection of planetary vorticity can

be ignored where the thermal wind shear tends to be westerly and the Coriolis parameter varies only meridionally (Bluestein 1992). The Trenberth approximation, Equation 5.7.42 on page 349 of Bluestein (1992), where f_0 is the Coriolis parameter (s^{-1}), $\sigma(m^2 s^{-2} kPa^{-2})$ is the static stability parameter, ω is the vertical velocity in pressure coordinates ($hPa s^{-1}$), $\mathbf{v_g}$ is the geostrophic wind vector (ms^{-1}), and ζ_g is the geostrophic relative vorticity (s^{-1}), is as follows:

$$\left(\nabla_p^2 + \frac{f_0^2}{\sigma}\frac{\partial^2}{\partial p^2}\right)\omega = \frac{f_0}{\sigma} 2 \left(\frac{\partial \mathbf{v_g}}{\partial p} \cdot \nabla_\mathbf{p} \zeta_\mathbf{g}\right) \tag{3.4}$$

Areas of large values of cyclonic vorticity advection by the thermal wind coincide with large values of upward motion, as dictated by Equation 3.4. Thus, one can stipulate that in an intensifying storm in which the vorticity is increasing over time by Equation 3.1, the cyclonic vorticity will increase for a given baroclinic zone, and thus the upward vertical motion and resulting precipitation will also increase (Equation 3.4)

Composite images are displayed for t=-12 h, t=0 h, and t=12 h, where t=0 h is defined as the initial time that the low-level absolute vorticity begins to change significantly, as defined in the compositing methodology. Important similarities and difference in the dynamical structures of the intensifying and decaying composites (as determined by the methodology in Section 3.1) include:

- At t=-12 h, the precursor trough seen on the map near the Great Lakes in intensifying cases (Fig. 3.3) is stronger than that found in the decaying composite(Fig. 3.4).

- The tilt of the precursor trough and its geographical proximity to the tropical cyclone are crucial. In particular, the trough has a noticeable positive tilt in the intensifying composite, as well as being physically closer to the tropical cyclone than in the decaying cases. This suggests that the "tilt" and proximity of the trough to the cyclone are just as important as the intensity.

- The baroclinic zone that sets up between the tropical cyclone and upstream trough is much more meridional in the intensifying composite (Fig. 3.5) and more zonal in the decaying composite (Fig. 3.6).

- The magnitude of the scale increase of the tropical cyclone at t=+12 h is much larger in the intensifying composite (Fig. 3.7) than in the decaying storms (Fig. 3.8).

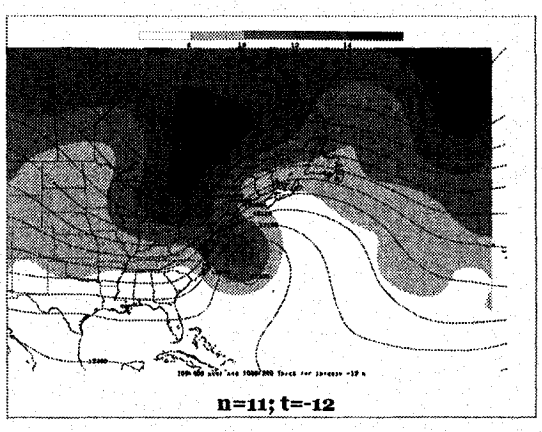

Figure 3.3: Intensifying quasi-geostrophic grid-centered composite at t=-12 h, with 400-700 hPa layer-averaged relative vorticity ($\times 10^5 s^{-1}$, shaded) and 200-1000 hPa thickness (meters, contoured).

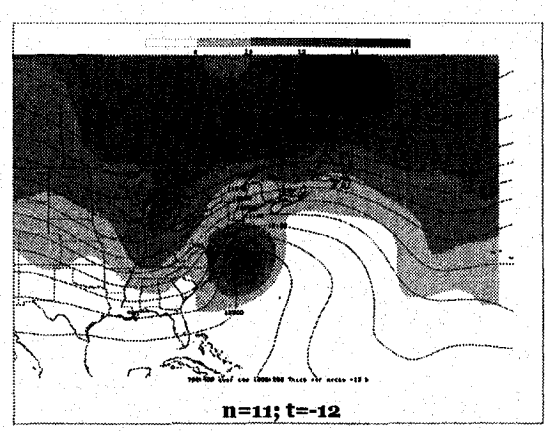

Figure 3.4: Decaying quasi-geostrophic grid-centered composite at t=-12 h, with 400-700 hPa layer-averaged relative vorticity ($\times 10^5 s^{-1}$, shaded) and 200-1000 hPa thickness (meters, contoured).

- The downstream ridge is more amplified in the intensifying cases following the interaction of the upstream trough and the tropical cyclone. This is primarily due to latent heat release as a result of heavy precipitation and is more easily observed in potential vorticity composites (Section 3.3).

3.3. Potential vorticity composites

Potential vorticity (PV) composites are very useful in ET studies because of the conservative property of PV in an adiabatic frictionless environment (Hoskins et al. 1985; Morgan and Nielsen-Gammon 1998). In other words, areas of intense diabatic heating and due to latent heat release from heavy precipitation are easily identifiable on a PV map, represented as areas of non-conservative PV. In addition, the PV composites in the study (following the logic of Atallah and Bosart (2004)) allow observation of the interaction between the low-level (tropical) and mid-level (trough) systems on one map. Thus, all PV composite maps are comprised of 200-300 hPa PV (warm colors) and 850-700 hPa relative vorticity (cool colors) with winds at both the upper (white) and lower (black) levels overlaid. As discussed in Section 2.2b, high values of PV at a near-tropopause level (200-300 hPa) represent cyclonic (trough) features, while low values of PV suggest an anticyclonic (ridge) feature. Important conclusions about dynamic structures in the PV composites include:

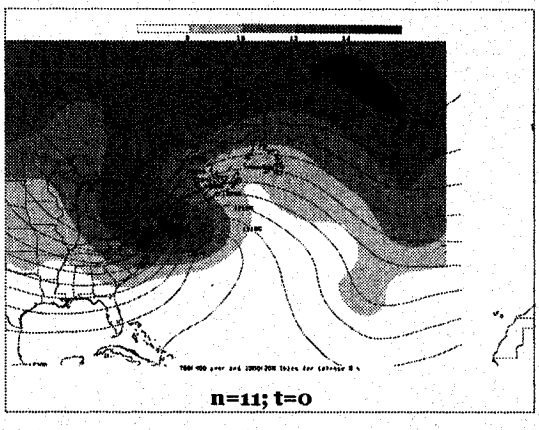

Figure 3.5: Intensifying quasi-geostrophic composite at t=0 h, with parameters as in Fig. 3.3.

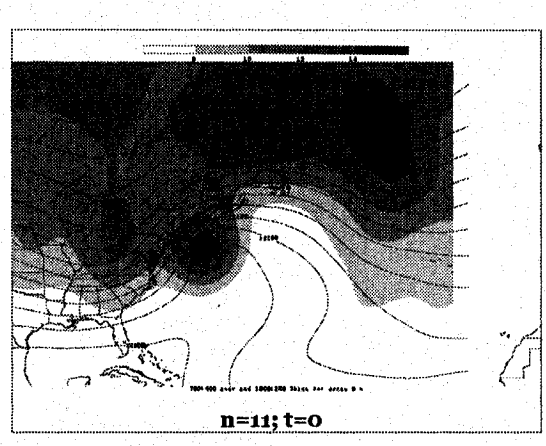

Figure 3.6: Decaying quasi-geostrophic composite at t=0 h, with parameters as in Fig. 3.4.

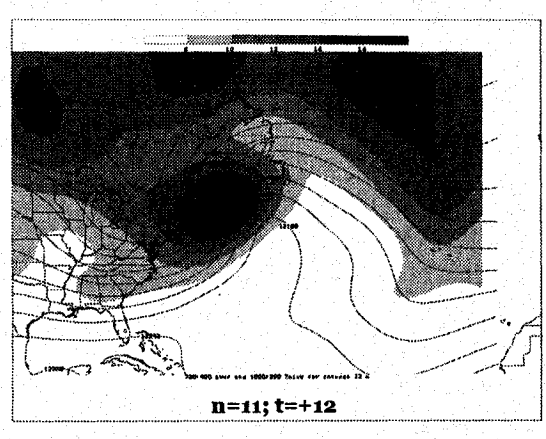

Figure 3.7: Intensifying quasi-geostrophic composite at t=+12 h, with parameters as in Fig. 3.3.

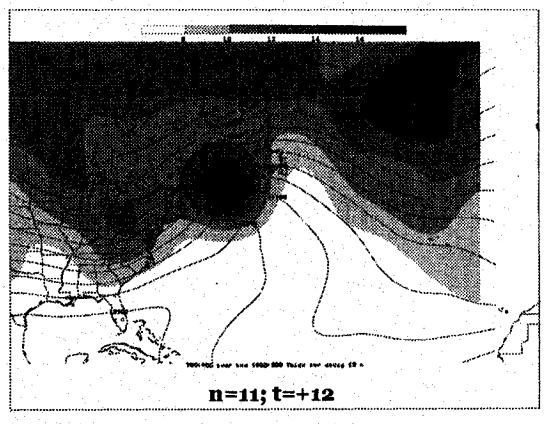

Figure 3.8: Decaying quasi-geostrophic composite at t=+12 h, with parameters as in Fig. 3.4.

- As seen in the quasi-geostrophic composites, the upstream trough is stronger, more positively tilted, and closer to the tropical cyclone in the intensifying composite (Fig. 3.9) than in the decaying composite (Fig. 3.10) at t=-12 h.

- Prior to interaction and transition (at t=-12 h), the tropical cyclone is actually more intense in the decaying composite (Fig. 3.10) than in the intensifying composite (Fig. 3.9). This result is similar to that found by Atallah (personal communication) and is possibly due to the storm's position, which is directly underneath a large-scale ridge; this is a prime condition for strengthening of purely tropical cyclones. However, as the storm becomes extratropical, its position underneath the large-scale ridge is no longer favorable for intensification (i.e. the proper dynamics are not in place to prevent the storm from weakening rapidly due to frictional effects).

- At t=0 h, while the decaying storms (Fig. 3.12) do interact with the baroclinic zone, the intensifying composite (Fig. 3.11) shows the additional interaction of the tropical cyclone with the upstream trough, within the baroclinic zone. This suggests that it is the proximity and tilt of the trough, not the strength of the mid-latitude baroclinic zone, that is the primary difference between the intensifying and decaying cases.

- The downstream ridge becomes progressively more amplified from t=-12 h to t=+12 h in the intensifying cases, unlike in the decaying composite. At t=+12 h, the intensifying composite (Fig. 3.13) shows an impingement of the ridge on the upstream trough to the northwest of the transitioning cyclone. The enhancement of the ridge (and thus non-conservation of PV) is due to latent heat release from heavy precipitation associated with the intensifying system. No similar westward ridge impingement is seen in the decaying composite (Fig. 3.14).

3.4. Precipitation distributions

Precipitation distributions are important consequences of and factors in the dynamics of a storm undergoing ET. For many of the rapidly intensifying cases, the NARR 3-hourly accumulated precipitation field shows evidence of a cyclonic rotation around the cyclone as it transitions and explosively re-intensifies at a high latitude. In contrast, many of the decaying cases exhibit an anti-cyclonic rotation around the low pressure center as a storm continued to weaken.

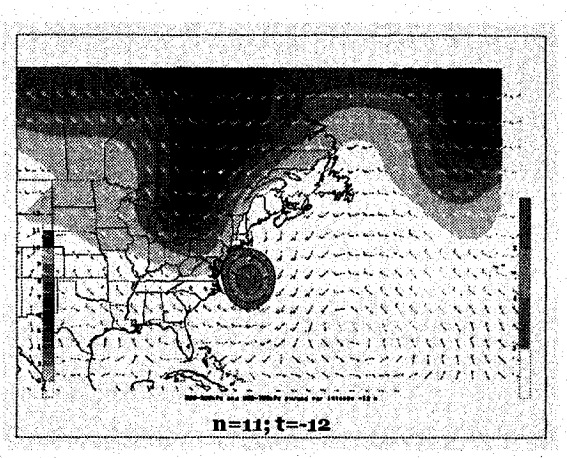

Figure 3.9: Intensifying PV composite at t=-12 h, with 200-300 hPa PV shaded (warm colors), 700-850 hPa relative vorticity shaded (cool colors), and low-level (upper-level) winds overlaid in black (white).

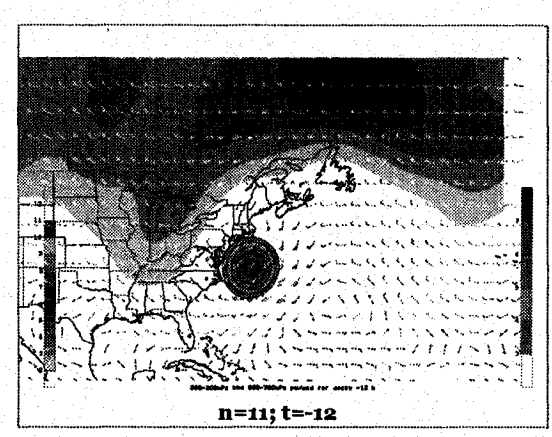

Figure 3.10: Decaying PV composite at t=-12 h, with 200-300 hPa PV shaded (warm colors), 700-850 hPa relative vorticity shaded (cool colors), and low-level (upper-level) winds overlaid in black (white).

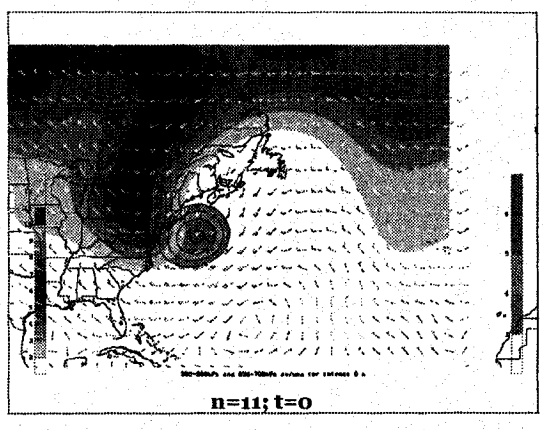

Figure 3.11: Intensifying PV composite at t=0 h, with parameters as in Fig. 3.9.

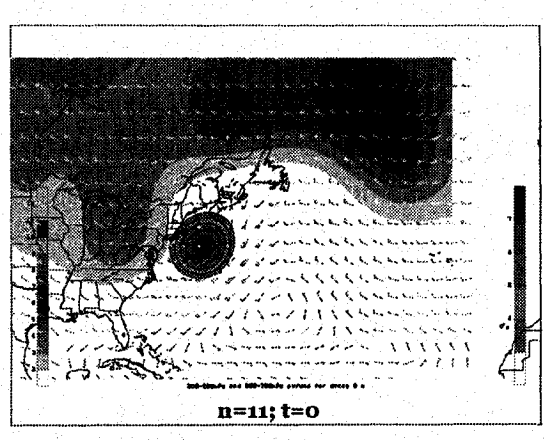

Figure 3.12: Decaying PV composite at t=0 h, with parameters as in Fig. 3.10.

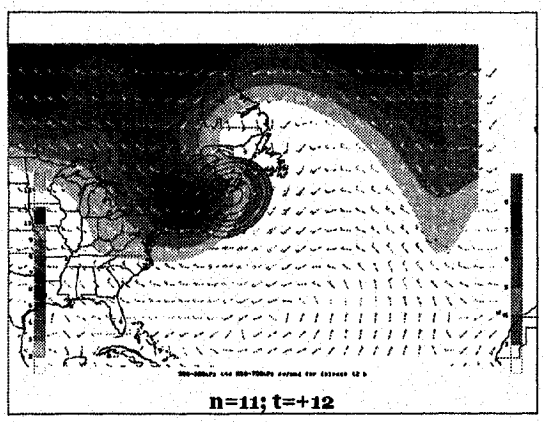

Figure 3.13: Intensifying PV composite at t=+12 h, with parameters as in Fig. 3.9.

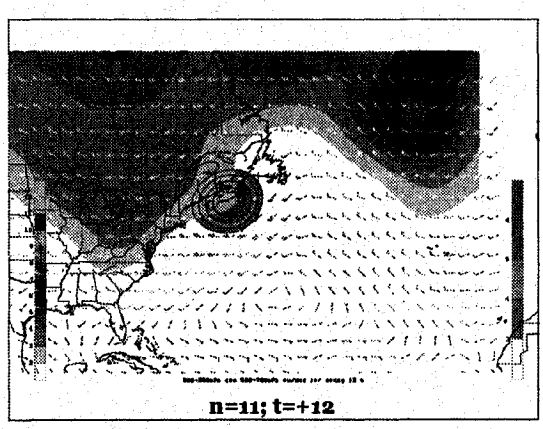

Figure 3.14: Decaying PV composite at t=+12 h, with parameters as in Fig. 3.10.

Figure 3.15 illustrates the NARR 3-hourly precipitation distributions of the eleven intensifying storms, just prior to explosive intensification. Note that prior to intensification, the majority of the precipitation regions are to the east or northeast of the surface low pressure center (labelled "L"), with the exception of Bertha (1990), in which the main area of rainfall is located to the north of the surface low center. Consequently, Fig. 3.16 shows that at a time 12-24 hours later, the main regions of precipitation have rotated cyclonically around the surface low-pressure center, following the interaction of the storm with a nearby mid-level trough. Thus, the subsequent location of the main area of rainfall tends to be in the northwestern quadrant, particularly for the more rapidly deepening cases such as Luis (1995) and Earl (1998). These findings support the assertion of DiMego and Bosart (1982a), who state that as the storm intensifies, regions of WAA and intense diabatic heating (and thus, the regions of precipitation) rotate cyclonically around the storm. The results found for the intensifying cases are in direct contrast with those found in the decaying cases. As seen in Fig. 3.17, there are few consistent precipitation structures between cases prior to storm decay. However, consistency is found in looking at Fig. 3.18, where 12-24 hours after decay has begun, many of the cases in the decaying class have experienced an anti-cyclonic rotation of the main precipitation area around the surface low-pressure center. In many cases, the areal extent of the precipitation region gets smaller over time, as do accumulated precipitation amounts. In general, the region of precipitation is located to the east of the storm following cyclone decay. This precipitation is most likely still in the region of the associated warm front, albeit as the storm weakens, the warm front is located farther away from the surface low-pressure center (note the

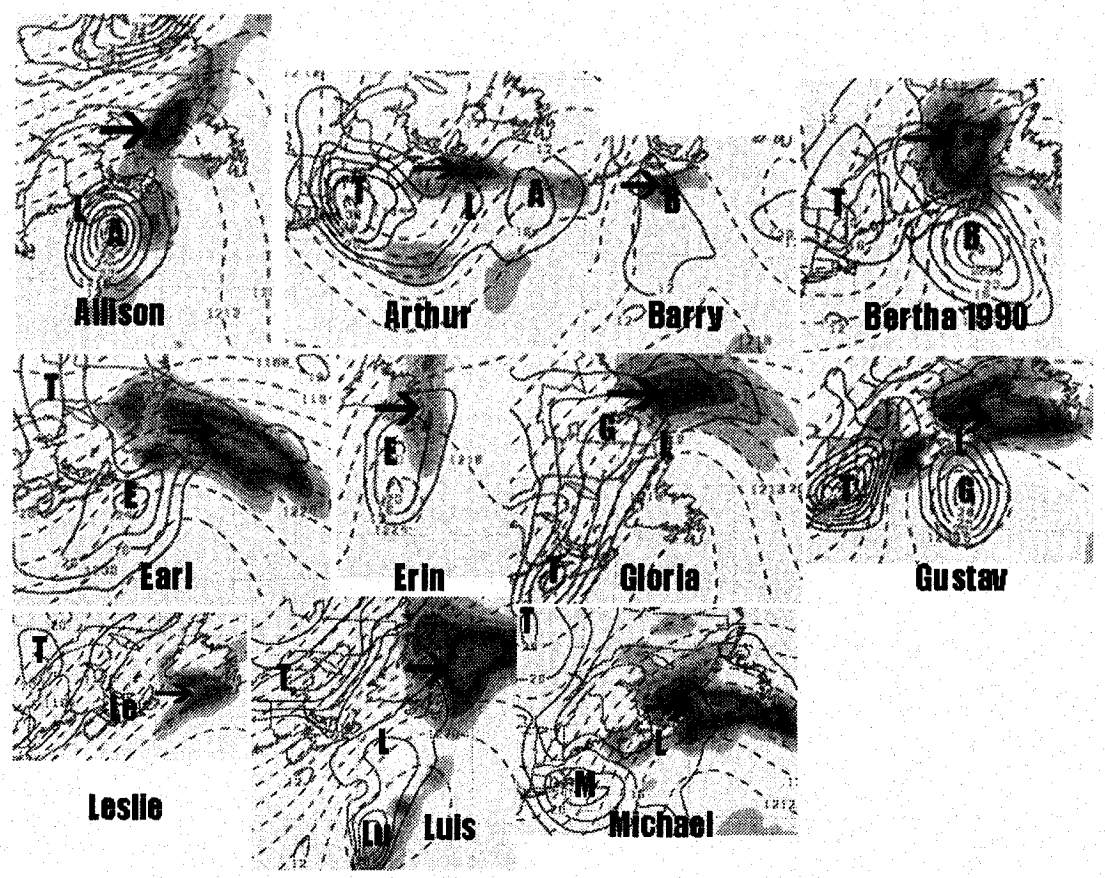

Figure 3.15: Eleven Intensifying Storms and their precipitation distributions just prior to explosive intensification; NARR 3-hourly precipitation (mm, shaded), NARR 400-700 hPa absolute vorticity ($\times 10^{-5} s^{-1}$, solid contours), NARR 200-1000 hPa thickness contours (m, dashed contours).

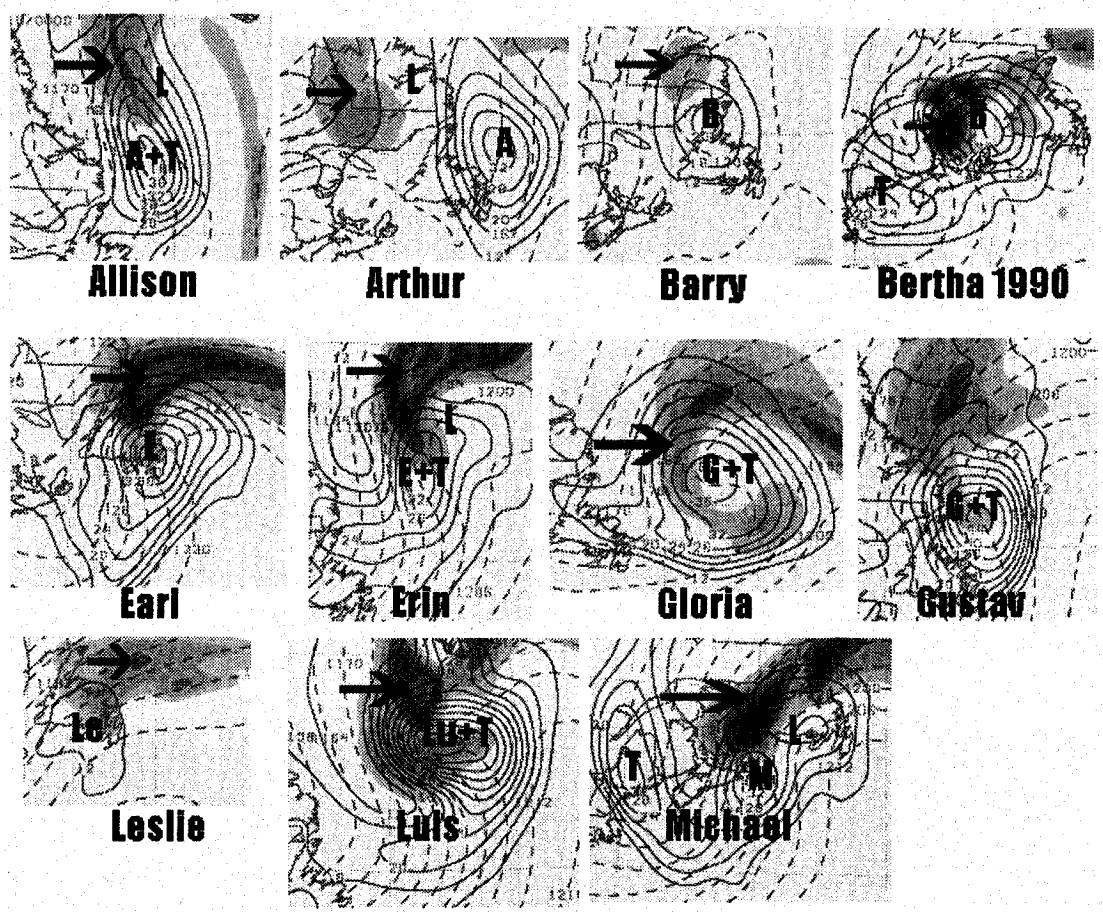

Figure 3.16: Eleven Intensifying Storms and their precipitation distributions just after explosive intensification; parameters are as for Fig. 3.15.

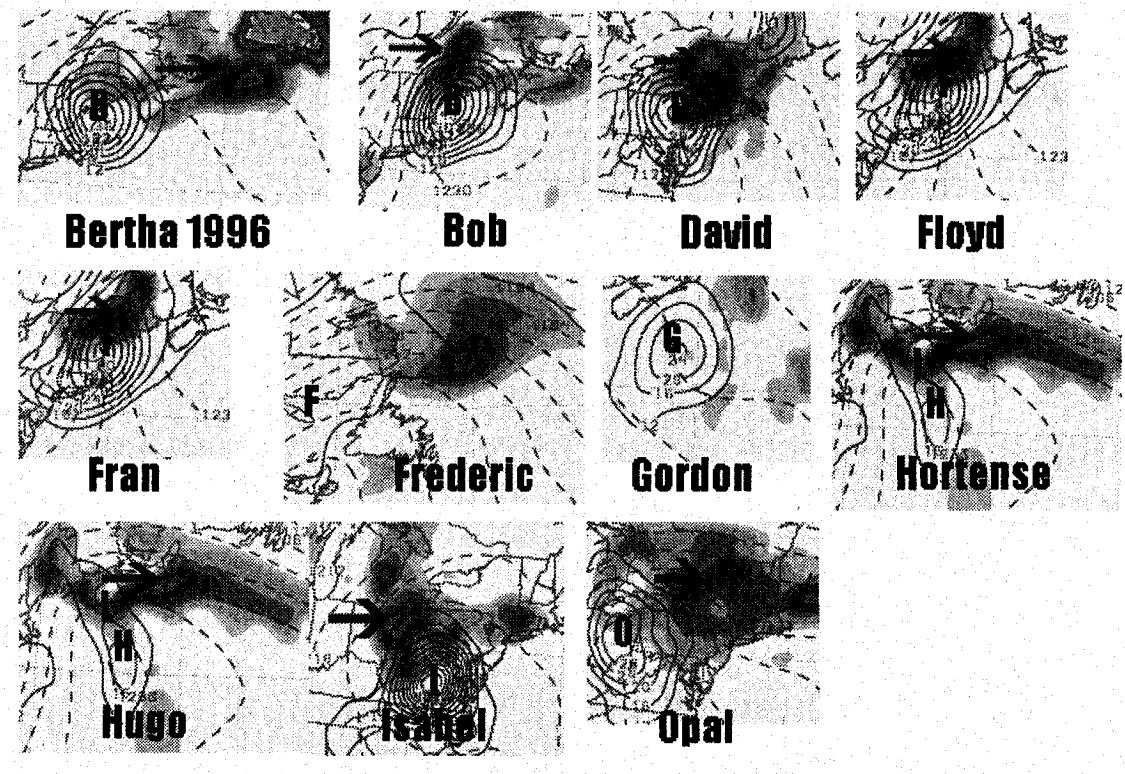

Figure 3.17: Eleven Decaying Storms and their precipitation distributions just prior to decay; parameters are as in Fig. 3.15.

increasing distance over time of the precipitation region from the low pressure center in many of the decaying cases).

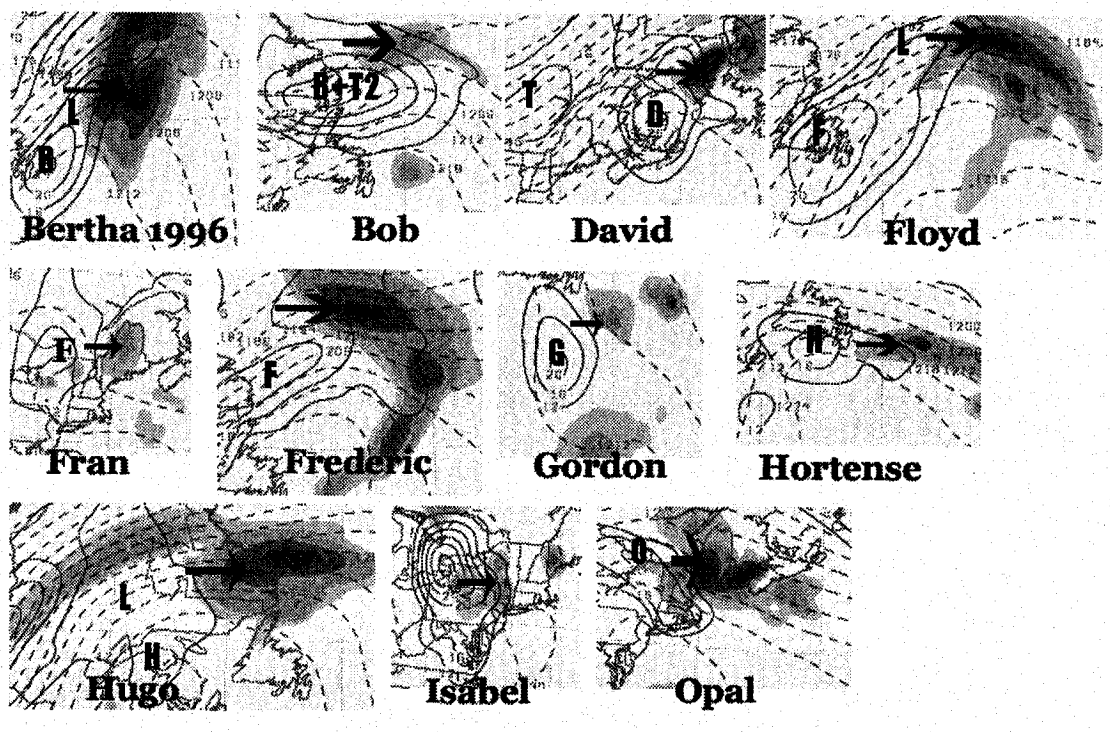

Figure 3.18: Eleven Decaying Storms and their precipitation distributions just after rapid decay; parameters are as in Fig. 3.15.

Chapter 4

Case Analysis: Luis (1995) and Isabel (2003)

4.1. Overview

The composite analyses in Chapter 3 explore the basic synoptic structures and precipitation distributions associated with two distinct classes of systems undergoing ET, "intensifying" and "decaying". The criterion utilized to partition the storms into distinct groups of intensity change is based on the change of vorticity over time (as seen in Figures 4.2 and 4.13, for Luis and Isabel, respectively). In this chapter, Luis (1995) and Isabel (2003), the largest positive and negative vorticity changes over time, respectively, are examined and contrasted in-depth.

4.2. Intensifying case: Luis (1995)

Luis is a classic Cape Verde tropical cyclone that moved across the Atlantic and menaced the northern Leeward Islands as a category 4 storm before curving northwestward and moving toward Atlantic Canada (Fig. 4.1). By September 10th, 1995, Luis was on a path to make landfall in Newfoundland when it started to undergo ET (Fig. 4.2). The storm moved over Newfoundland rapidly as a transitioning system on September 11th; winds of 50-70 knots were reported, along with extremely heavy rainfall. The transition and subsequent rapid intensification of Luis is the most intense case in this study.

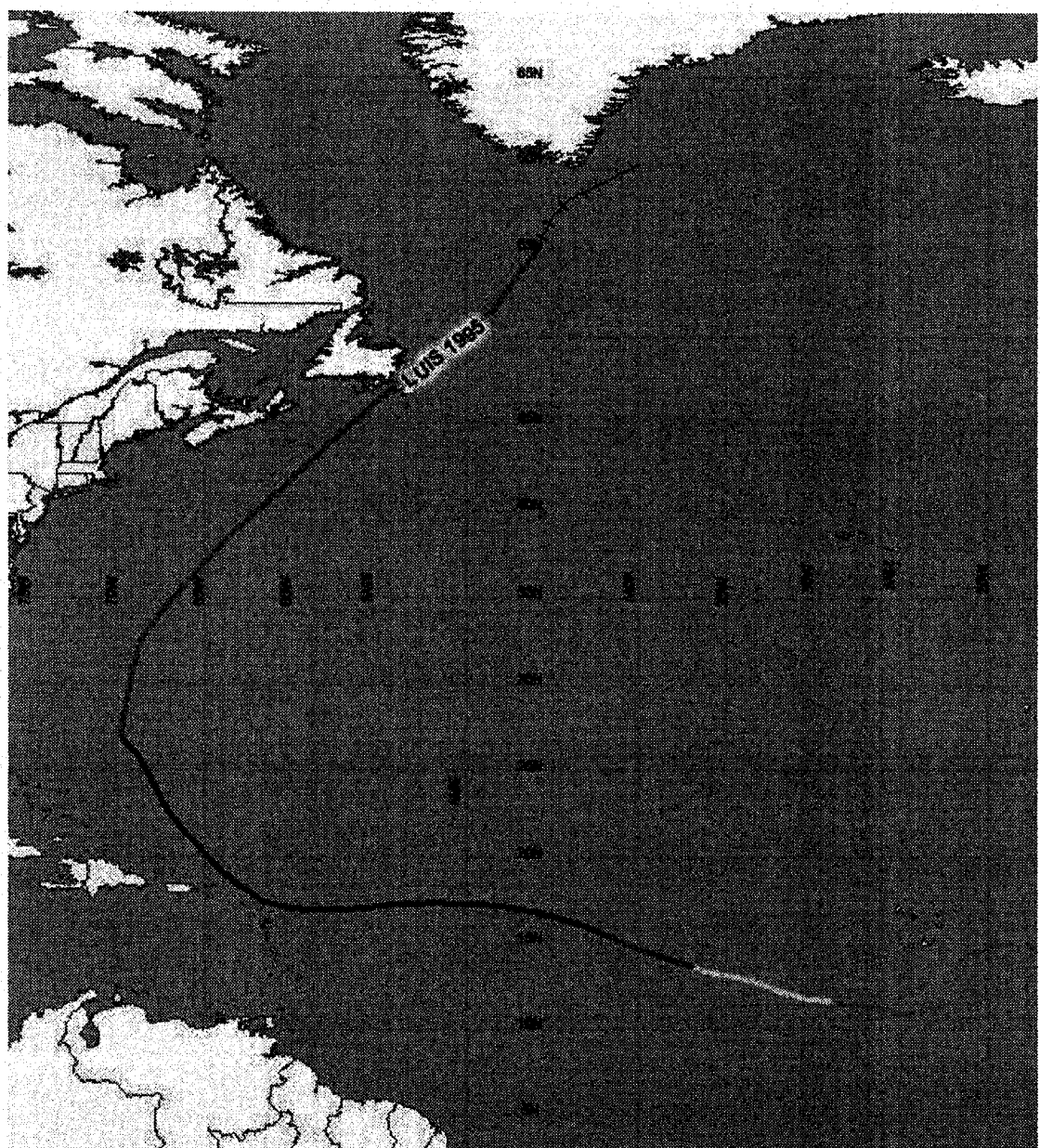

Figure 4.1: Track of Luis (1995).

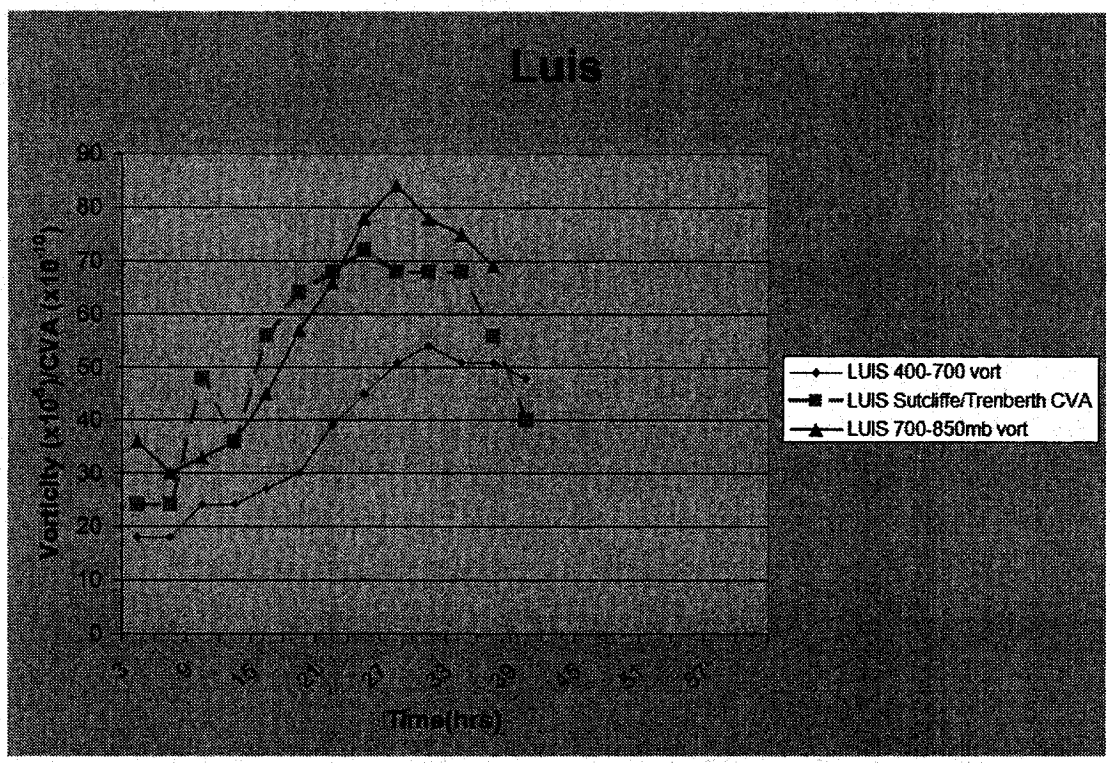

Figure 4.2: For Hurricane Luis (1995): NARR 400-700 hPa absolute vorticity $\times 10^{-5} s^{-1}$ (blue), NARR 700-850 absolute vorticity $\times 10^{-5} s^{-1}$ (green), NARR CVA by the Sutcliffe method $\times 10^{-10} s^{-2}$ (pink); t=0 represents the time the storm was judged to have started to affect Canada.

4.2a. Quasi-geostrophic structures and precipitation

Figure 4.3 depicts a warm-core Luis (labelled "Lu") well southwest of Newfoundland at 0000 UTC/11. Two important features are present on the mid-level vorticity map (Figure 4.3): An extremely strong baroclinic zone and an intense mid-level shortwave trough to the west in the Gulf of St. Lawrence. In the composite plots, it is evident that an interaction of the tropical cyclone with a mid-level trough, embedded in a mid-latitude baroclinic zone, is a signal of rapid intensification. In the case of Luis, however, both the shortwave trough and the baroclinic zone are much more vigorous than in other re-intensification cases. This scenario of rapid re-intensification begins to play out by 1200 UTC/11 (Fig. 4.4), as ET has begun and the mid-level vortices of Luis and the trough have begun to merge (labelled "L+T"). Note that as the mid-level vortex is embedded in the heart of an extremely narrow and intense thickness gradient, rapid intensification is likely. At 0000 UTC/12, the mid-level vortex has rapidly intensified to $54 \times 10^{-5} s^{-1}$), the largest value found in this study. Moreover, the S-shaped thickness pattern often seen in rapid intense extratropical cyclogenesis is quite well-defined in the case of Luis. The aforementioned strongest winds (70 knots) over Newfoundland were reported to be out of the northwest, indicating that the storm's most rapid intensification occurs offshore of Newfoundland as Luis translates northward toward Greenland.

Precipitation over Newfoundland was quite heavy in association with the ET of Luis. Reported values ranged anywhere from 60 to 120 mm (CHC, 2005), in a rather short time span considering the high forward speed of the system. The cyclonic rotations of the precipitation is quite evident in the time series of plots. Moreover, at 0000 UTC/11 (Fig. 4.3), just prior to intensification, the main precipitation area is in the northeastern quadrant of the cyclone. By 1200 UTC/11 (Fig. 4.4), as the cyclone begins to intensify rapidly, the precipitation has rotated cyclonically to the north of the storm's center. Finally, at 0000 UTC/12 (Fig. 4.5), the bulk of the precipitation is located in the northwestern quadrant of the cyclone, evidence of a remarkable 24 hours in which the surface low-pressure center underwent a deepening of 40 hPa.

Luis is a perfect example of the awesome qualities and power that a storm undergoing a vigorous ET can exhibit. Had Luis undergone such a transition just a few hundred kilometers to the south, undoubtedly much more damage and loss of life would have occurred. As it is, the storm will go down as one of the most intense Atlantic Basin extratropical transitions in recent history.

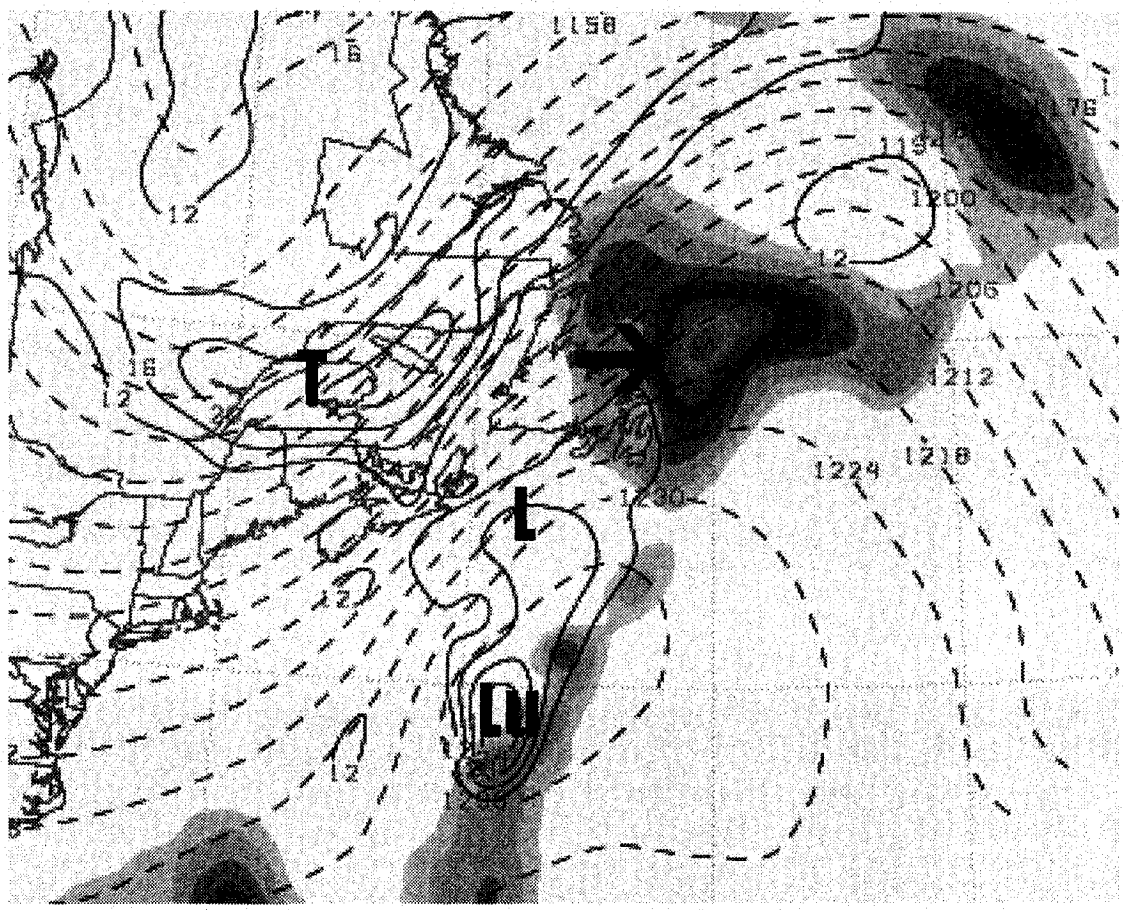

Figure 4.3: Luis at 0000 UTC/11 September; NARR 3-hourly accumulated precipitation (mm, shaded), NARR 400-700 hPa layer-averaged absolute vorticity ($\times 10^{-5} s^{-1}$, solid contours), NARR 200-1000 hPa thickness (m, dashed contours).

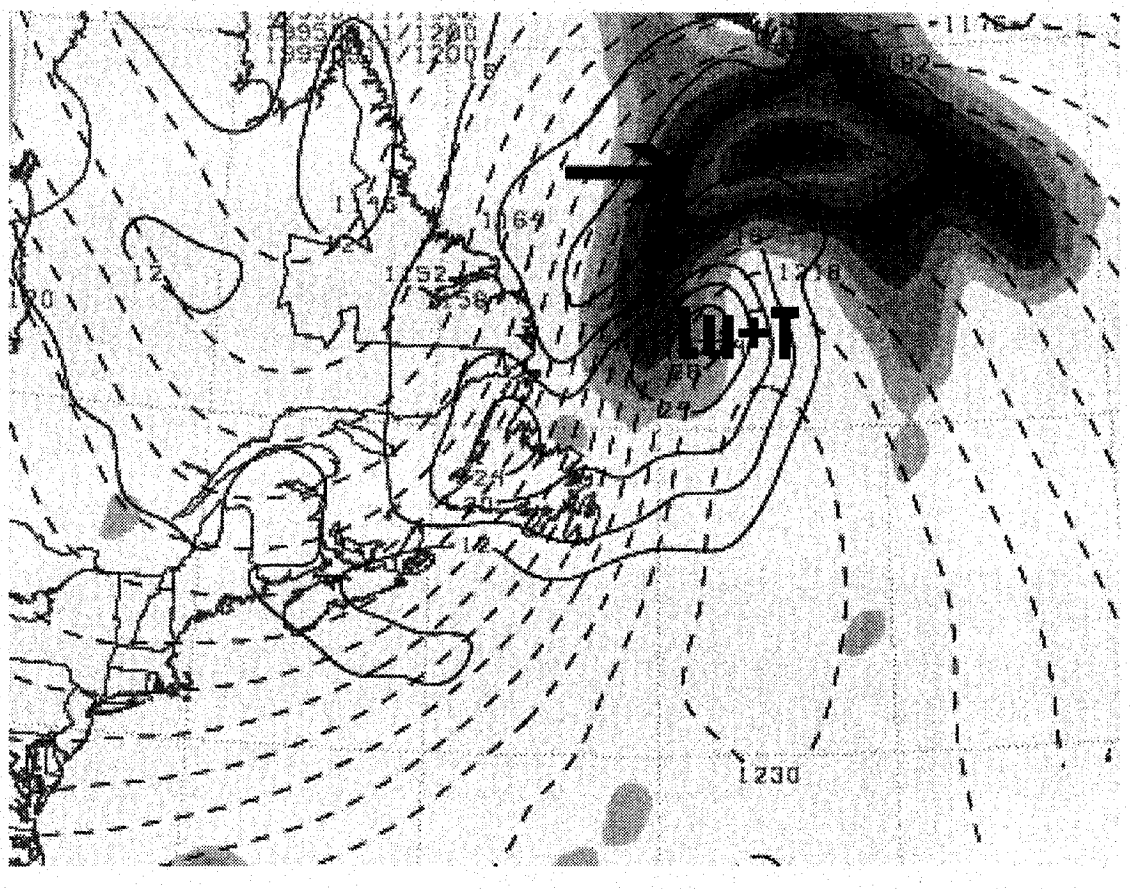

Figure 4.4: Luis at 1200 UTC/11 September; parameters are as in Fig. 4.3.

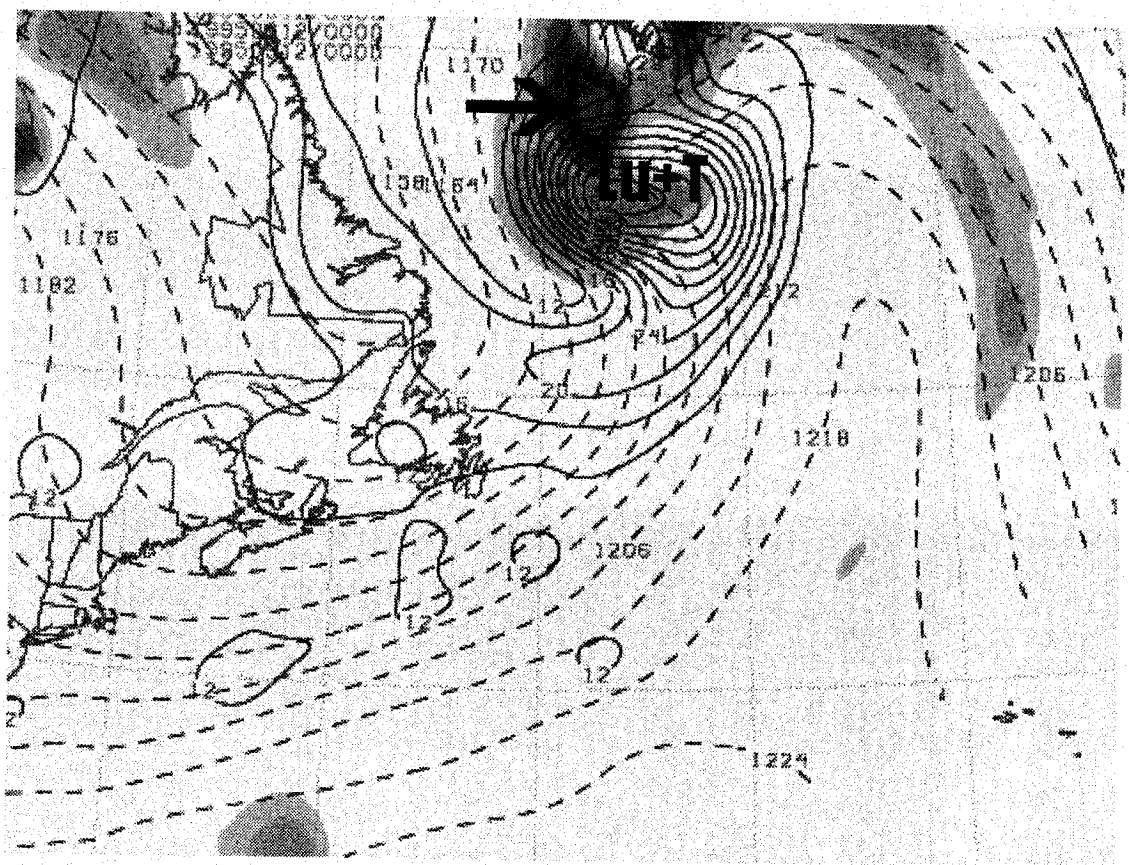

Figure 4.5: Luis at 0000 UTC/12 September; parameters are as in Fig. 4.3.

4.2b. Potential vorticity and diabatic heating

Fig. 4.6 depicts Luis (labelled "Lu") just east of the Newfoundland coast with a (lowest closed contour) SLP of 996 hPa, just prior to rapid intensification. The cool shaded colors in Fig. 4.6 are indicative of the upper-level cold theta anomaly (i.e. mid-level trough) poised to interact with Luis and aid in rapid intensification of the cyclone. As Luis interacts with the positive PV anomaly at 1200 UTC/11 (Fig. 4.7) and 0000 UTC/12 (Fig. 4.8), enormous structural changes are seen in the newly intensifying cyclone. Firstly, Luis' SLP falls from 996 hPa at 0000 UTC/11 to 976 hPa at 1200 UTC/11 to 956 hPa at 0000 UTC/12, a 40 hPa intensification that greatly exceeds the "bomb" criterion of Sanders and Gyakum (1980). Secondly, the circulation at the dynamic tropopause above Luis goes from a warm theta anomaly to a cold theta anomaly, in association with the mid-latitude trough interaction. The intrusion of stratospheric (cold theta) air (first in the southwestern quadrant of the storm, then towards the cyclone center), is very evident at 0000 UTC/12. This intrusion is in accordance with that found by Browning et al. (1998) and Agusti-Panareda et al. (2004).

In addition, the non-conservation property of PV (Hoskins et al. 1985) is quite evident in the case of Luis. This is clear in the cyclonic rotation (i.e. westward impingement) of warm potential temperatures (i.e. low IPV on the dynamic tropopause, as discussed in Section 2.2b) on the dynamic tropopause as Luis rapidly intensifies to the northwest of Newfoundland. At 1200 UTC/11, the downstream PV ridge extends further westward than it does at 0000 UTC/11. Similarly, at 0000 UTC/12, while cold theta air fills the center of the cyclone, the westward impingement of the ridge has progressed into the northwestern quadrant of the surface cyclone. The westward impingement of the ridge (warm theta air) is indicative of diabatic warming resulting in large amounts of latent heat release, in association with heavy precipitation from Luis. Subsequently, the newly displaced ridge helps to "push" more cold theta air into the surface cyclone, which in turn further intensifies the cyclone and enhances the rainfall. This positive feedback is described in detail in Section 2.3b, and Luis serves as a prominent example of diabatic processes that occur during an explosive extratropical transition.

4.2c. Frontogenesis and moisture

As discussed in section 2.3c, mesoscale processes are an important part of extratropical transition. Jones et al. (2003) documented that almost all the heavy pre-

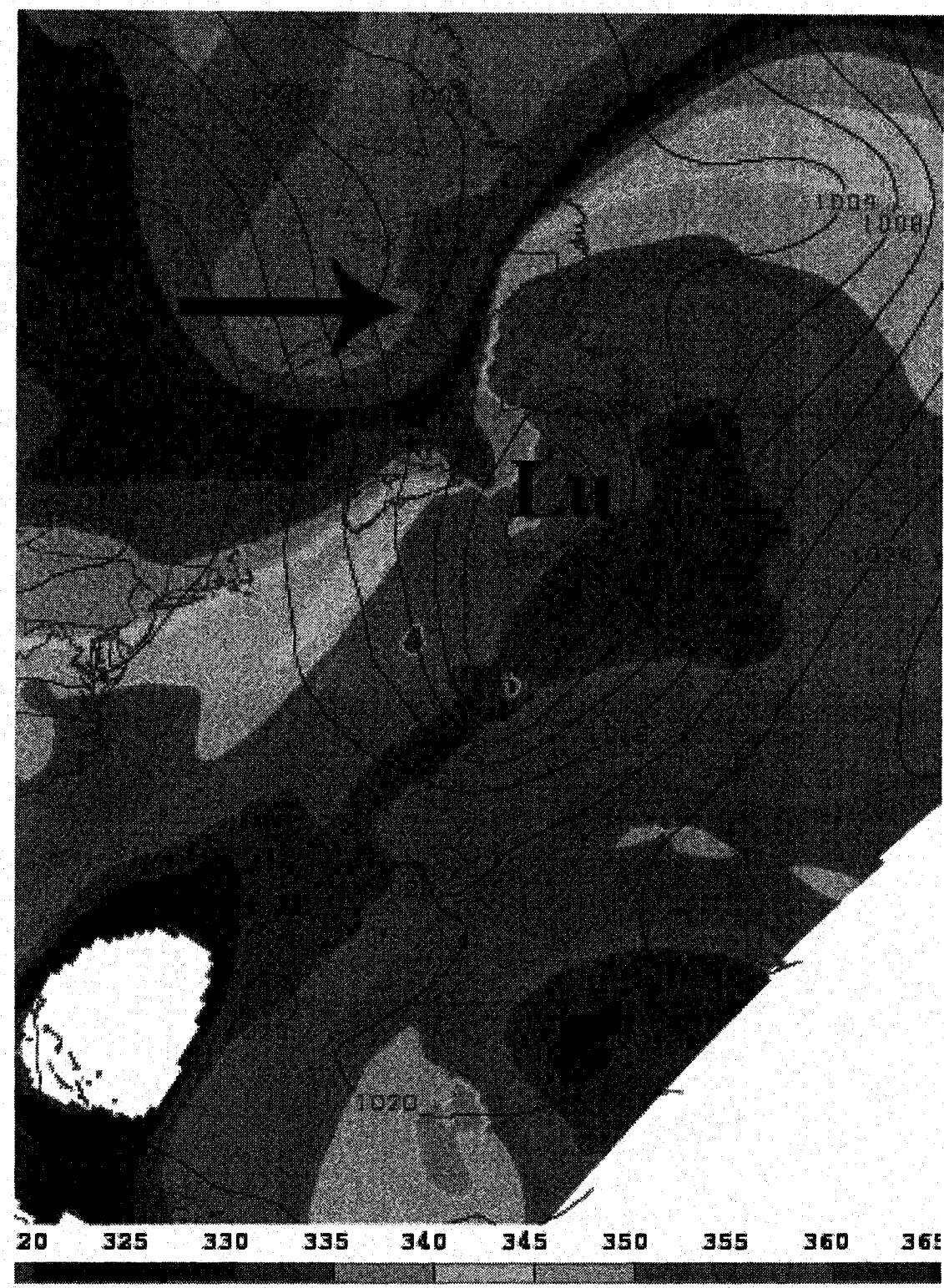

Figure 4.6: Luis at 0000 UTC/11 September; NARR potential temperature on the dynamic tropopause (K, shaded), NARR SLP (hPa, solid contours).

Figure 4.7: Luis at 1200 UTC/11 September; parameters are as in Fig. 4.6.

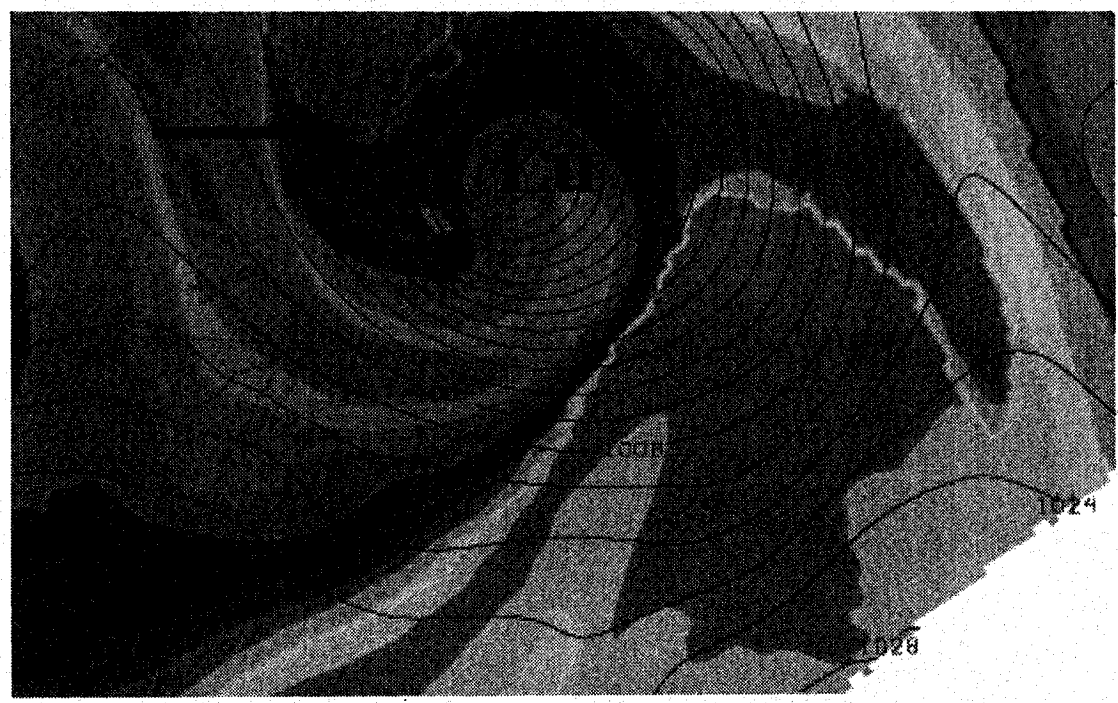

Figure 4.8: Luis at 0000 UTC/12 September; parameters are as in Fig. 4.6.

cipitation in a transition event is co-located with areas of warm frontogenesis. In addition, Bosart and Dean (1991) found that the most intense precipitation in the case of the transitioning Tropical Storm Agnes (1972) is found in the vicinity of a strengthening and cyclonically rotating warm front. These observations hold true for the explosive ET of Luis (1995). Moisture transport convergence (MTC) is used as a proxy for precipitation is this section and is defined in Equation 4.1, where MTC is moisture transport convergence (kgs^{-1}), q is specific humidity ($kg_{water}kg_{air}^{-1}$) and **v** is the wind vector (ms^{-1}).

$$MTC = -\nabla \cdot q\mathbf{v} \tag{4.1}$$

Figure 4.9 shows that at 0000 UTC/11, only a weak area of frontogenesis is evident just north of the cyclone center, but is co-located with an area of moisture transport convergence, indicating rising motion and a high probability of precipitation. Twelve hours later, at 1200 UTC/11, the area of frontogenesis remains to the north of the cyclone center, but has grown in both intensity and areal extent (Fig. 4.10). The new larger area of warm frontogenesis continues to be co-located with a now stronger and larger area of moisture convergence. This observation is in accordance with the larger area of precipitation observed with Luis as it rapidly intensifies (Fig. 4.4). Toward the conclusion of the rapid intensification period (0000 UTC/12, Fig. 4.5), the main area of frontogenesis has both increased in strength and rotated cyclonically around the low pressure system, in agreement with the rotation observed in the precipitation distribution (Fig. 4.5). The increased intensity in frontogenesis is similar to that found by Bosart and Dean (1991), since arguably the heaviest precipitation during Luis' transition is observed at 0000 UTC/12.

4.3. Decaying case: Isabel (2003)

Hurricane Isabel, a Cape Verde tropical cyclone that crossed the North Atlantic Basin in September 2003, made landfall in eastern North Carolina as a strong Category Two hurricane on September 18th. As Isabel tracked inland over the Mid-Atlantic region of the U.S., numerous forecasts in Ontario were calling for a repeat of Hazel, in which Isabel would interact with a mid-latitude trough over Southern Ontario and cause massive amounts of flooding. The storm does track into Ontario on September 19th (Fig. 4.12), but forecasts of a re-intensification as an extratropical cyclone turned out to be grossly incorrect. Moderate amounts of precipitation were recorded over Southern Ontario, but observed amounts were almost an order of magnitude below what was forecasted.

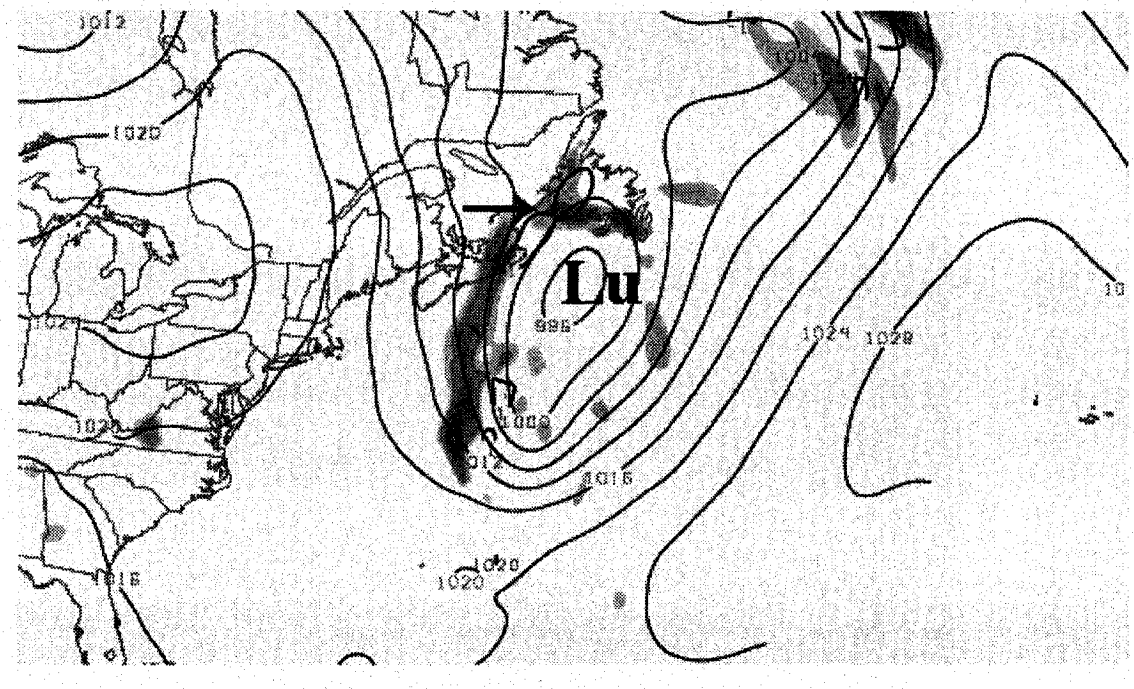

Figure 4.9: Luis at 0000 UTC/11 September; NARR moisture transport divergence ($\times 10^7 kgs^{-1}$, shaded warm colors)/convergence ($\times 10^7 kgs^{-1}$, shaded cool colors), NARR frontogenesis ($Km^{-1}s^{-1}$, bold solid contours)/frontolysis ($Km^{-1}s^{-1}$, bold dashed contours), NARR SLP (hPa, light solid contours).

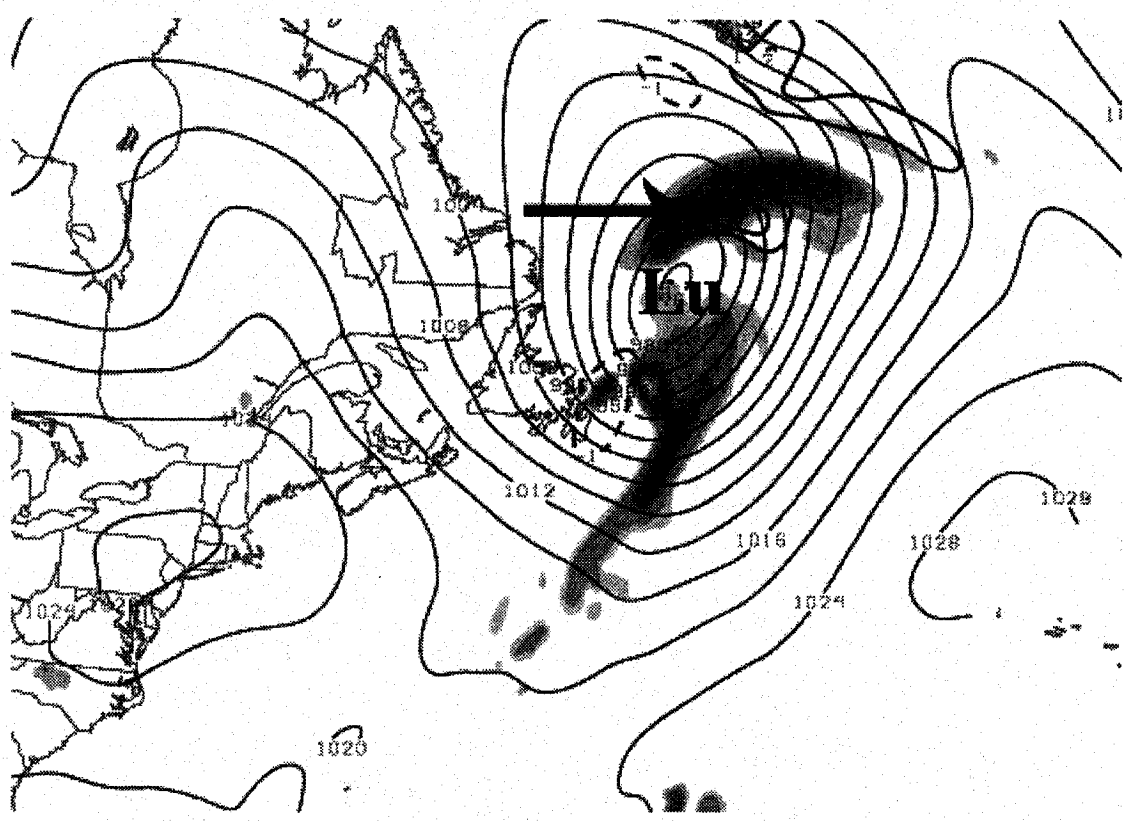

Figure 4.10: Luis at 1200 UTC/11 September; parameters are as in Fig. 4.9.

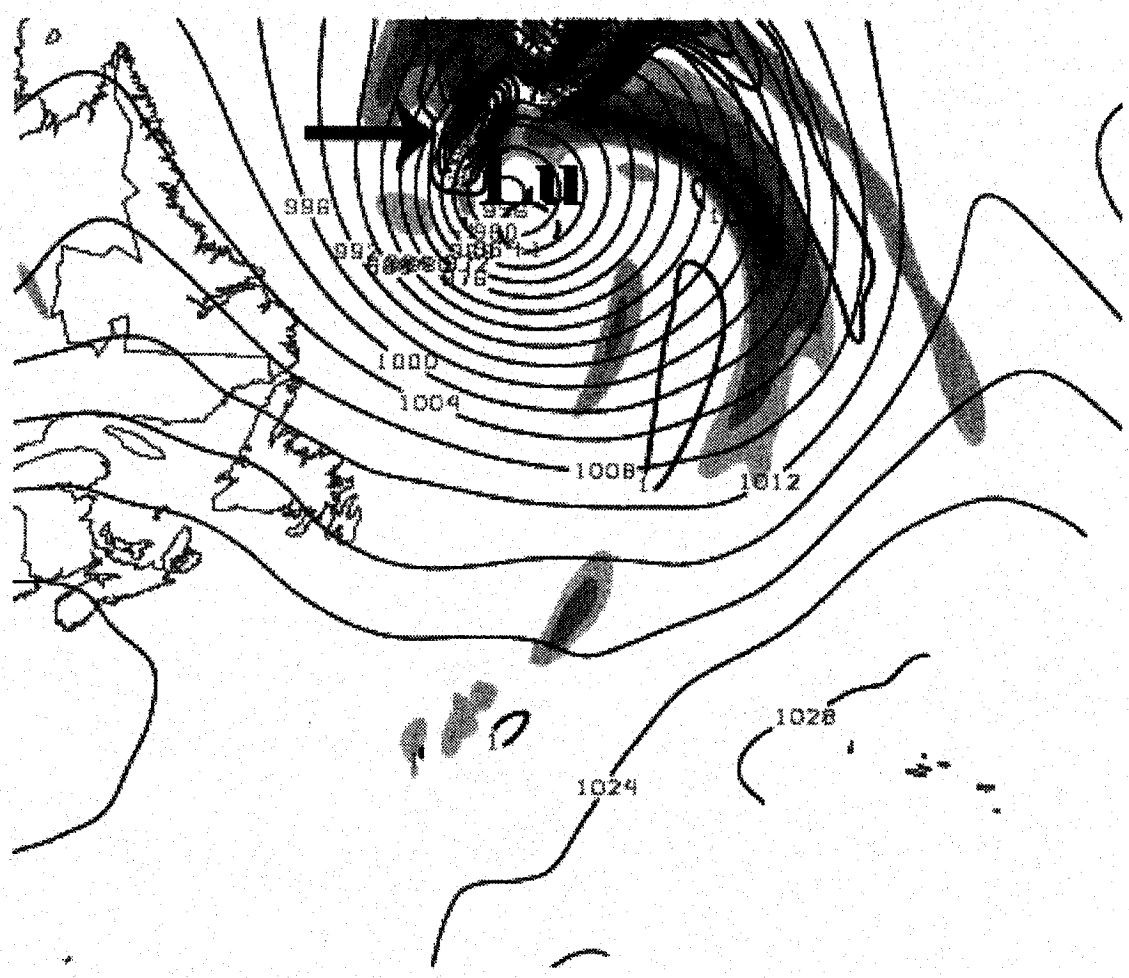

Figure 4.11: Luis at 0000 UTC/12 September; parameters are as in Fig. 4.9.

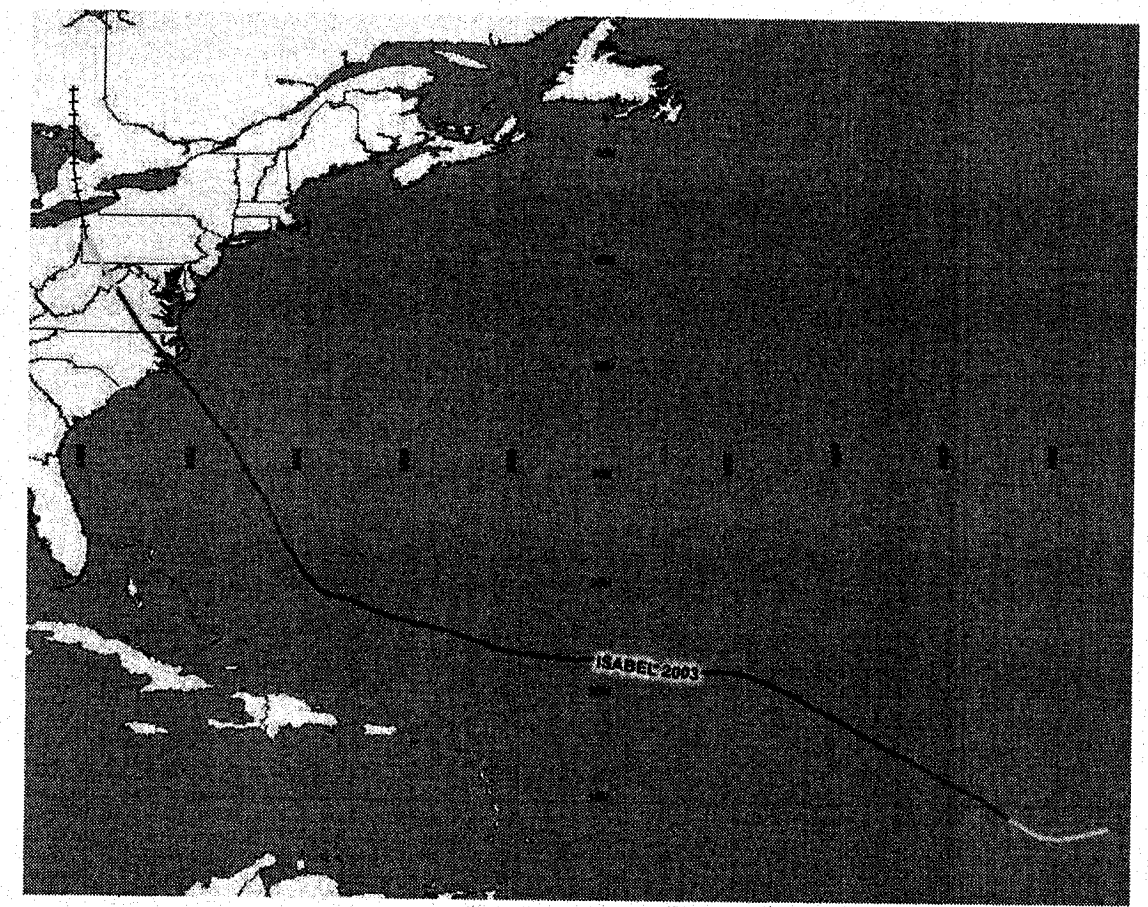

Figure 4.12: Track of Isabel (2003)

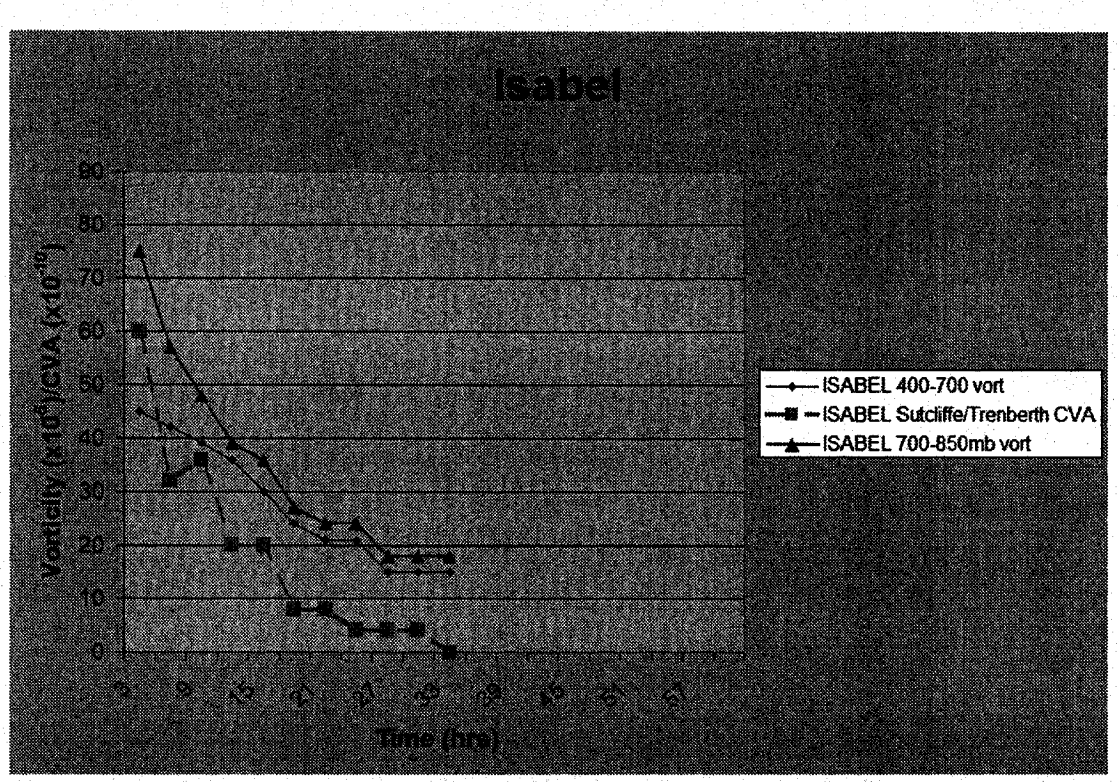

Figure 4.13: For Hurricane Isabel (2003): NARR 400-700 hPa absolute vorticity $\times 10^{-5} 5 s^{-1}$ (blue), NARR 700-850 absolute vorticity $\times 10^{-5} s^{-1}$ (green), NARR CVA by the Sutcliffe method $\times 10^{-10} s^{-2}$ (pink); t=0 represents the time the storm was judged to have begun to affect Canada.

4.3a. Quasi-geostrophic structures and precipitation

As seen in Fig. 4.14, Isabel (labelled "I") is still a potent hurricane inland over Virginia at 0600 UTC/19. At the same time, a mid-level trough is located over southern Minnesota and moving eastward. Many forecasts at the time called for the trough to interact with Isabel near Lake Erie and subsequently re-intensify to form a powerful extratropical cyclone. Despite these predictions, the trough does not advance towards the east quickly enough to interact with the remnants of Isabel, as seen at 1800 UTC/19 (Fig. 4.15) and 0600 UTC/20 (Fig. 4.16). Instead, Isabel remains underneath a large thickness ridge and slowly weakens due to friction over land without any reinforcing mid-latitude feature to interact with. It is plausible that the model forecast error might be due to problematic prediction of latent heat release from heavy precipitation that fell over the mid-Atlantic states. The diabatic heating caused by the precipitation may have acted to strengthen the ridge, thereby slowing the forward progress of the upstream trough just long enough to prevent an interaction with Isabel. Clearly, further research is needed on the failure of the forecast models to accurately represent the non-interaction of Isabel with the trough. By 1800 UTC/20 (not shown), Isabel essentially dissipates and is absorbed by the frontal system ahead of the aforementioned trough.

Maximum observed values of precipitation over Southern Ontario in association with Isabel are in the 30 to 50 mm range. The precipitation distribution is consistent with what one would expect from a rapidly weakening storm. At 0600 UTC/19, most of the precipation is located in the northwest quadrant of the surface cyclone. As Isabel weakens rapidly toward the Canadian border, the main area of precipitation lessens in intensity and areal extent. Moreover, it rotates anticyclonically around the surface low pressure center, as seen at 1800 UTC/19. Isabel was a forecast bust in Canada and is the opposite of a case such as Luis, whose precipitation distribution rotates cyclonically as it intensified during ET.

4.3b. Potential vorticity and diabatic heating

The quasi-geostrophic analyses in the previous section show that Isabel (2003, labelled "I") remains under a large ridge during its post-landfall lifetime and never interacts with a mid-level trough moving eastward from the Northern Plains of the U.S.. The PV plots clearly depict this scenario, with a large area of cold potential temperature (or high PV, as explained in Section 2.2b) air dominating the eastern third of North America at 0600 UTC/19 (Fig. 4.17), just after Isabel makes landfall.

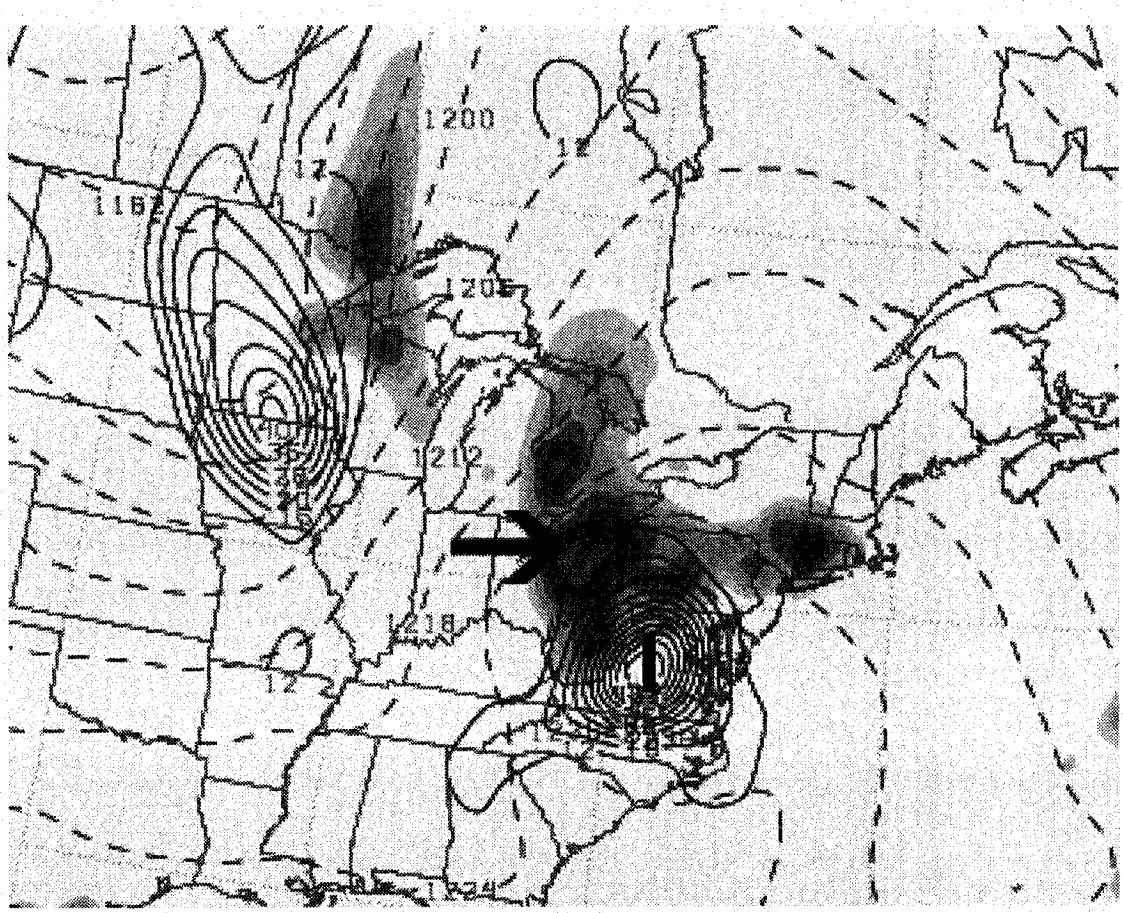

Figure 4.14: Isabel at 0600 UTC/19 September; parameters are as in Fig. 4.3.

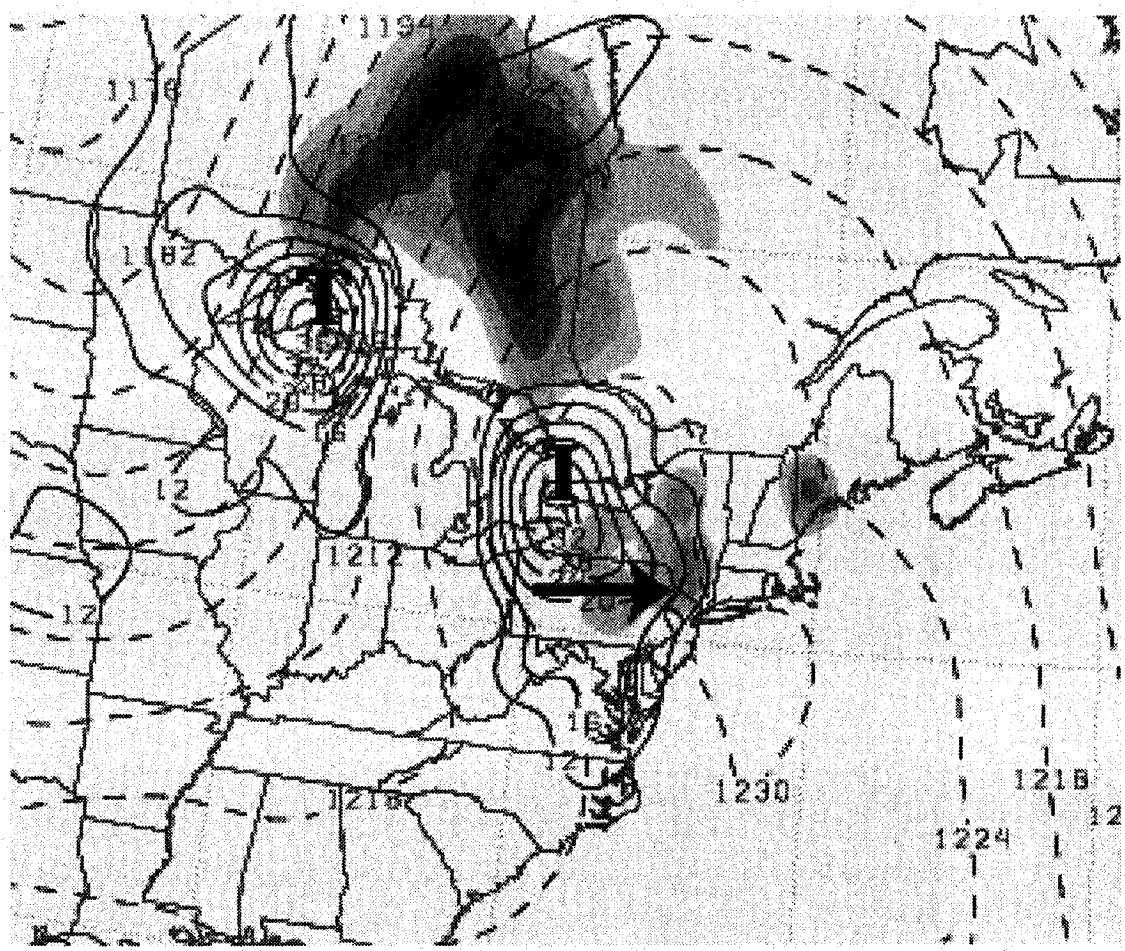

Figure 4.15: Isabel at 1800 UTC/19 September; parameters are as in Fig. 4.3.

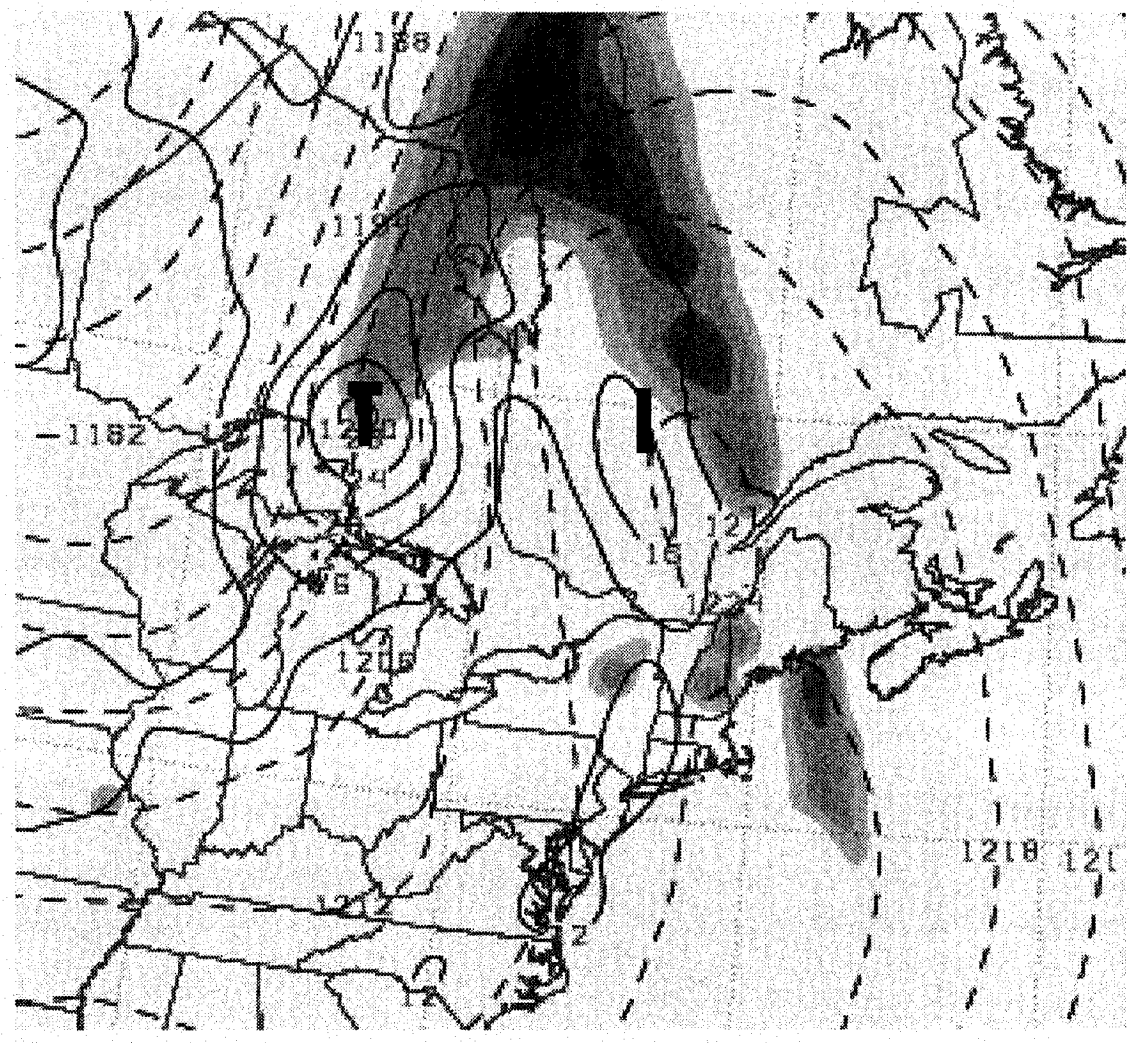

Figure 4.16: Isabel at 0600 UTC/20 September; parameters are as in Fig. 4.3.

By 1800 UTC/19 (Fig. 4.18), Isabel weakens significantly (996 hPa to 1004 hPa) as it moves into the Great Lakes region. The cold theta anomaly (labelled "T") is located near Lake Superior. Isabel remains under a large-scale warm theta region, which, in accordance with the quasi-geostrophic analyses, is not conducive to intensification. Finally, at 0600 UTC/20 (Fig. 4.19), Isabel is no longer identifiable as a unique theta anomaly. The storm is absorbed by the larger mid-latitude cyclone to the west, and fails to interact with the cold theta air formerly over Lake Superior.

In contrast to Luis (1995), there is a lack of a stratospheric PV intrusion (cold theta air) in association with Isabel. Moreover, while heavy precipitation is observed during the early post-landfall stages over the Mid-Atlantic region of the U.S. (Fig. 4.14, the diabatic heating is not nearly enough to compensate for the lack of dynamical support for intensification. Thus, precipitation gradually weakens and more sparse as friction diminishes the cyclone. This suggests that diabatic heating alone is not enough to spur a strong re-intensification of an ET system and needs to be working in concert with favorable synoptic conditions, as emphasized by Bosart and Dean (1991) and Jones et al. (2003).

4.3c. Frontogenesis and moisture

The heavy rain associated with Isabel that fell over Pennsylvania and Ohio is in accordance with the area of moisture convergence (Equation 4.1) in the northwestern quadrant of Isabel seen in Fig. 4.20. However, unlike in the case of Luis, no prominent area of frontogenesis exists at 0600 UTC/19. As Isabel continues to weaken at 1800 UTC/19 (Fig. 4.21) and essentially dissipates by 0600 UTC/20 (Fig. 4.22), there is a continued lack of frontogenesis in the region around the cyclone. Moreover, by 1800 UTC/19, no areas of moisture convergence are observed near Isabel, in accordance with the rapidly dissipating precipitation seen in Fig. 4.15.

As implied by Bosart and Dean (1991), areas of frontogenesis are important signals for heavy rainfall during extratropical transition, particularly in cases of re-intensification, such as Luis (1995). For Isabel, however, frontogenesis is essentially a non-factor. Future investigation is required to determine whether frontogenesis is a non-factor for all decaying cases.

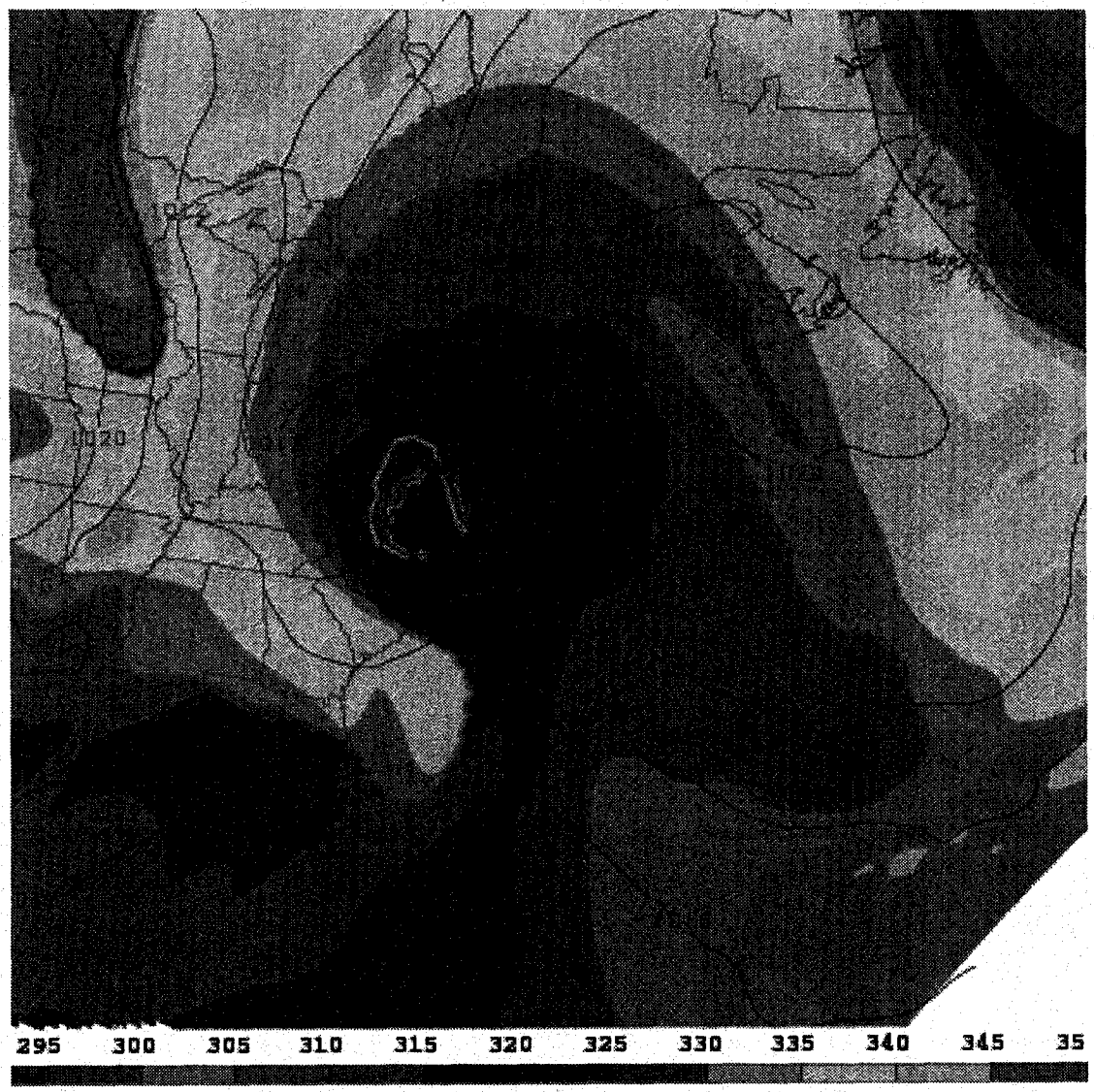

Figure 4.17: Isabel at 0600 UTC/19 September; parameters are as in Fig. 4.6.

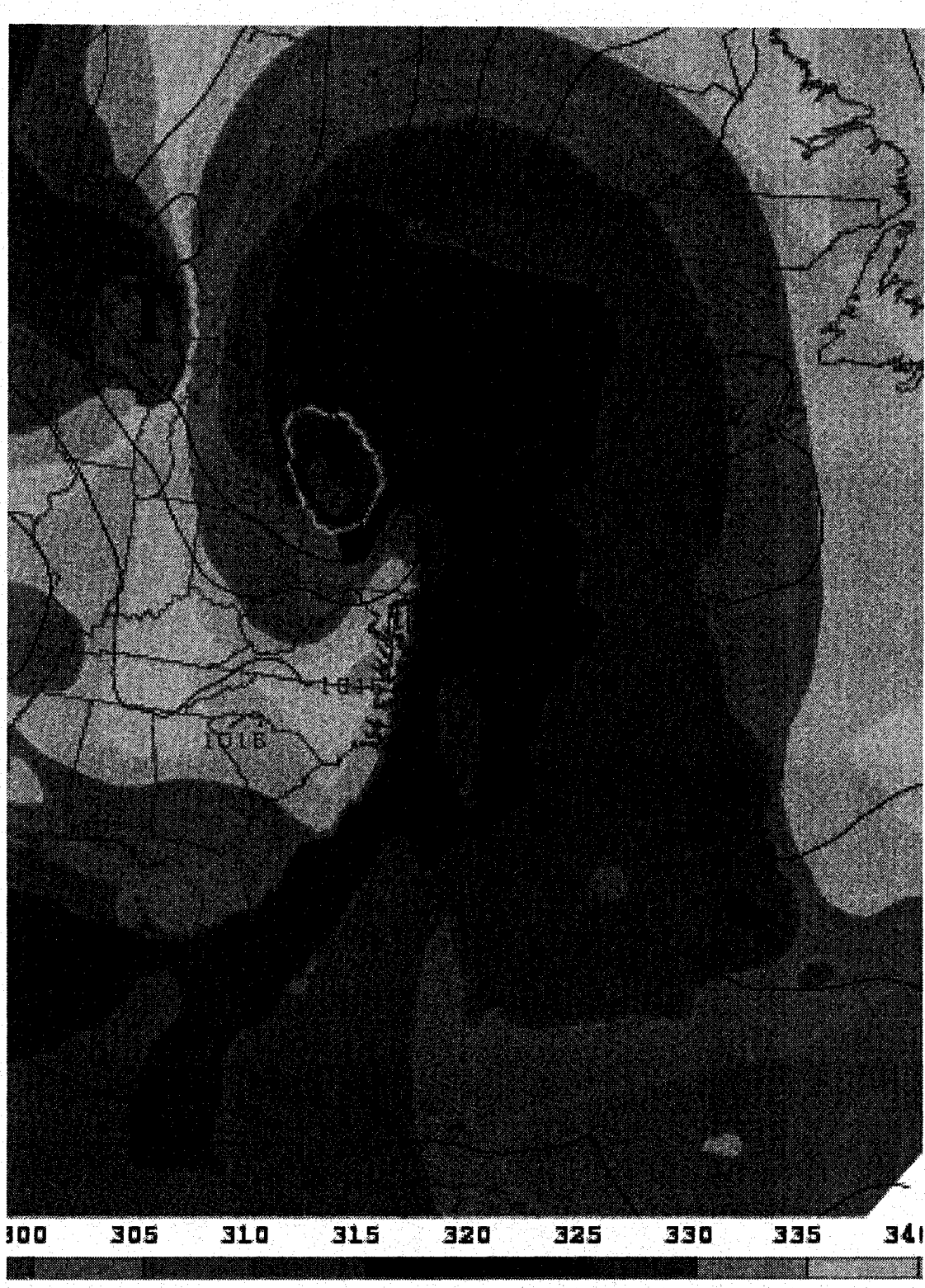

Figure 4.18: Isabel at 1800 UTC/19 September; parameters are as in Fig. 4.6.

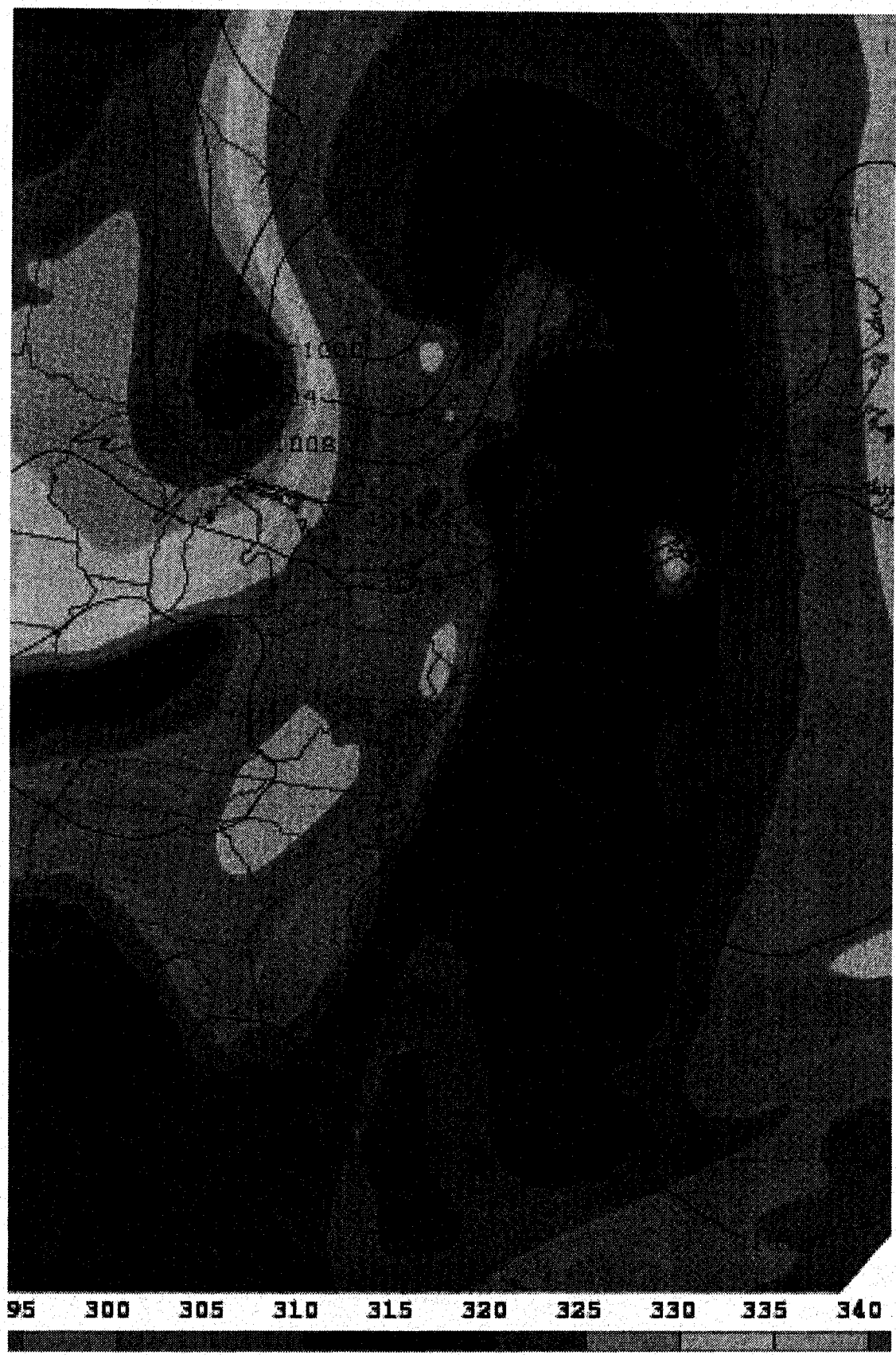

Figure 4.19: Isabel at 0600 UTC/20 September; parameters are as in Fig. 4.6.

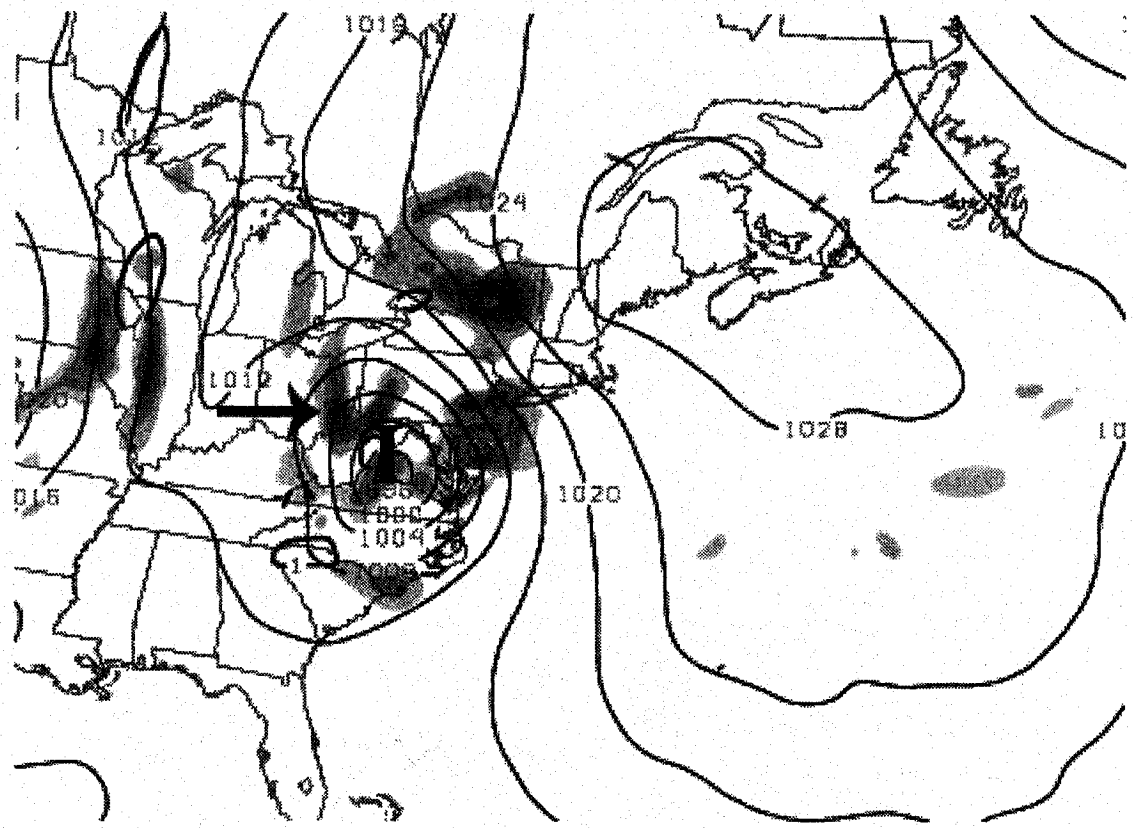

Figure 4.20: Isabel at 0600 UTC/19 September; parameters are as in Fig. 4.9.

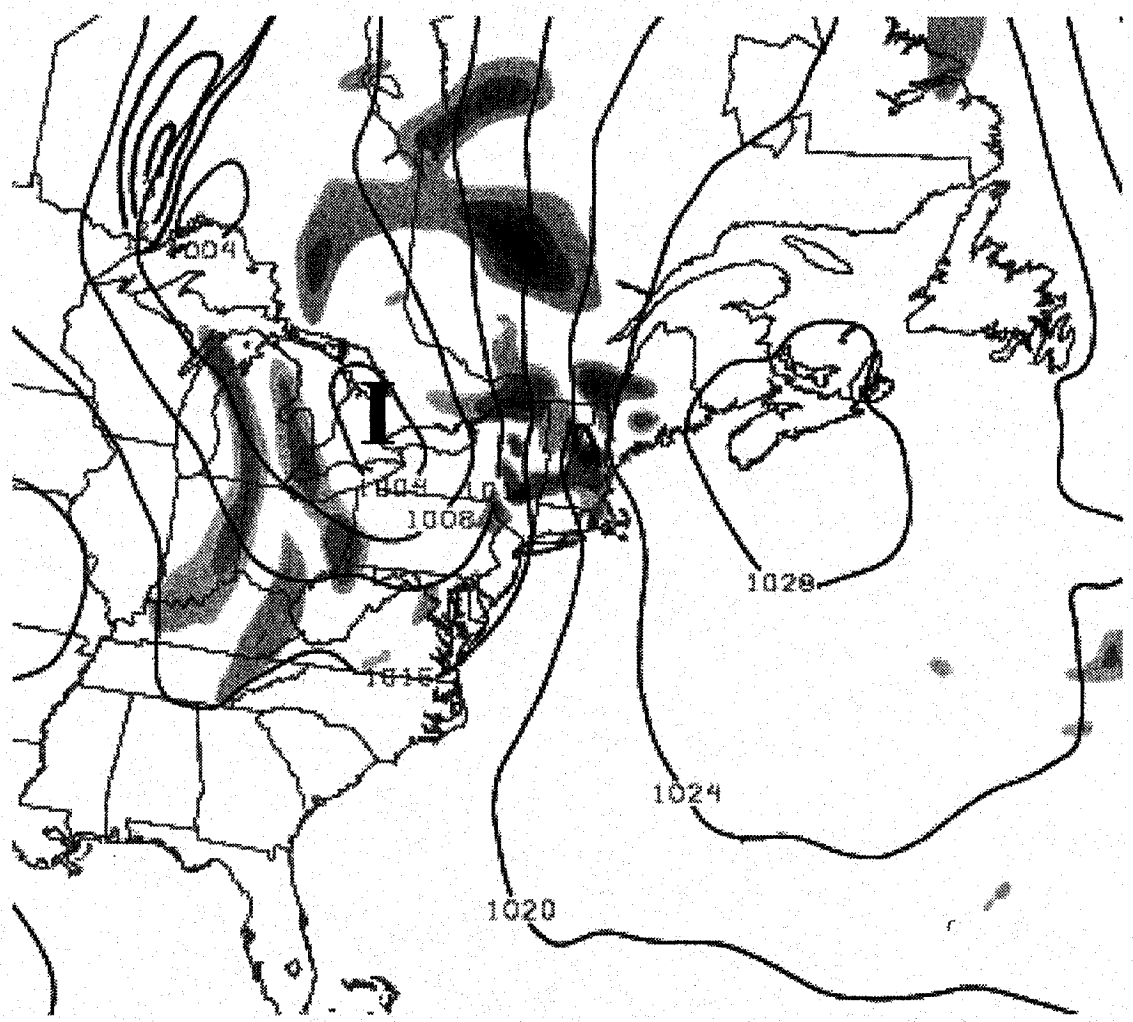

Figure 4.21: Isabel at 1800 UTC/19 September; parameters are as in Fig. 4.9.

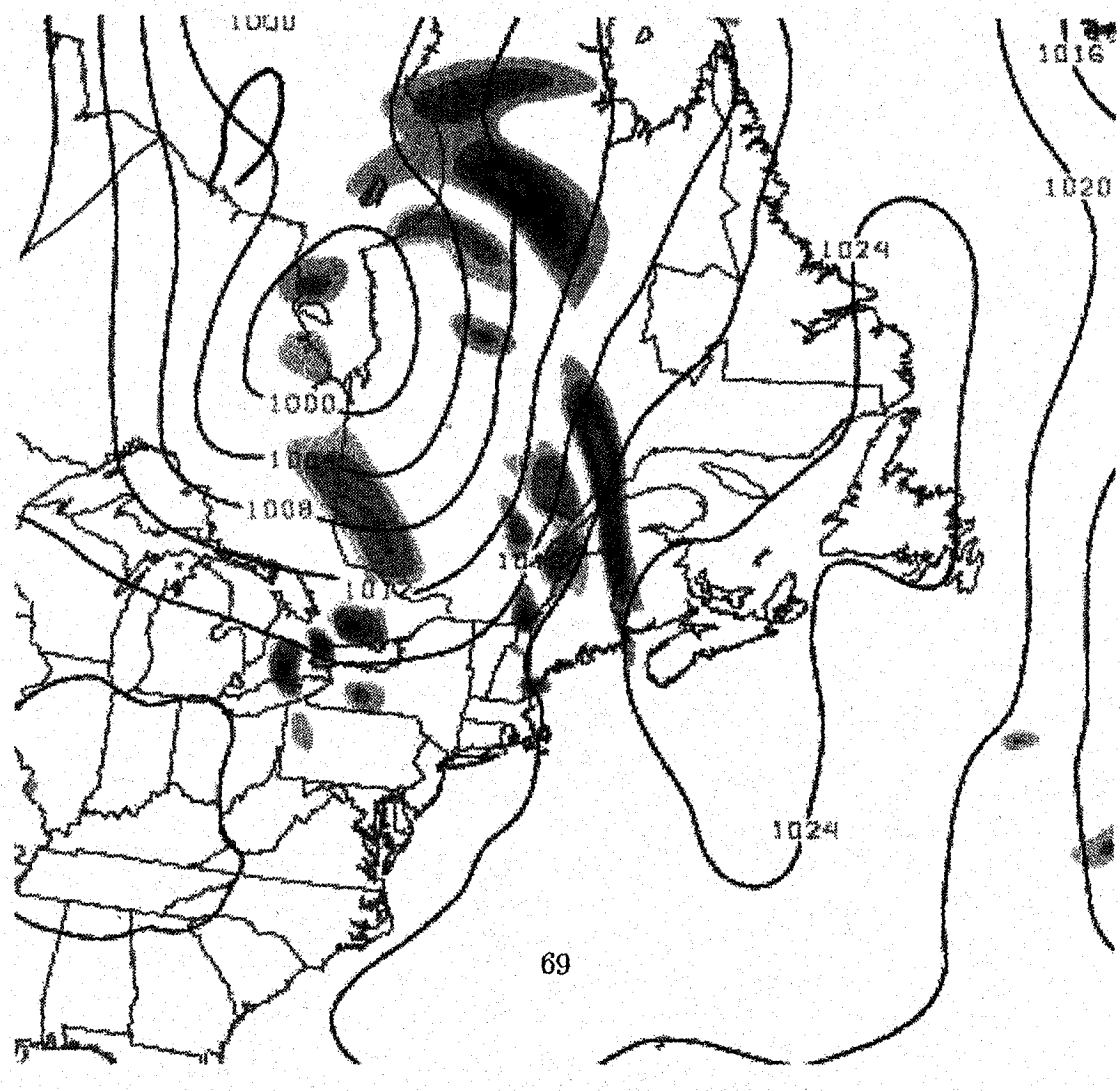

Figure 4.22: Isabel at 0600 UTC/20 September; parameters are as in Fig. 4.9.

Chapter 5

The Good, the Bad, and the Ugly of the North American Regional Reanalysis

5.1. The good NARR: Improved resolution, etc.

The NARR 3-hourly precipitation accumulation field allows for an analysis of preciptation over Canada, similar to that produced by Atallah and Bosart (2004) utilizing the NCEP Unified Precipitation Dataset (UPD). In addition, the increased horizontal resolution of the NARR, as compared to that of the NCEP Global Reanalysis, serves as a major asset. Two storms, Alberto (1988) and Chris (1988), were not identified as stand-alone vorticity maxima in the NCEP Global Reanalysis. As is shown in the case of Alberto (Fig. 5.1), the NARR is able to resolve the mid-level vorticity maximum associated with the storm, while the NCEP Global Reanalysis is too coarse to do so. The issue of resolution is an important one, especially for tropical systems travelling and/or making landfall at high latitude, which tend to be much smaller than typical extratropical cyclones. Utilizing the NARR, cases that would be missed by the NCEP Global Reanalysis, are able to be analyzed.

5.2. The bad NARR: Canadian precipitation prior to 2003

The 3-hourly accumulated precipitation field was initially assimilated for the NARR using mostly gauge data over land and entirely model data over water (Mesinger et al. 2004). Precipitation over the lower 48 states of the U.S. is thus nearly identical to that analyzed by the NCEP Unified Precipitation Dataset (UPD). While no one would claim one-hundred percent accuracy of either the NARR or UPD over the U.S., precip-

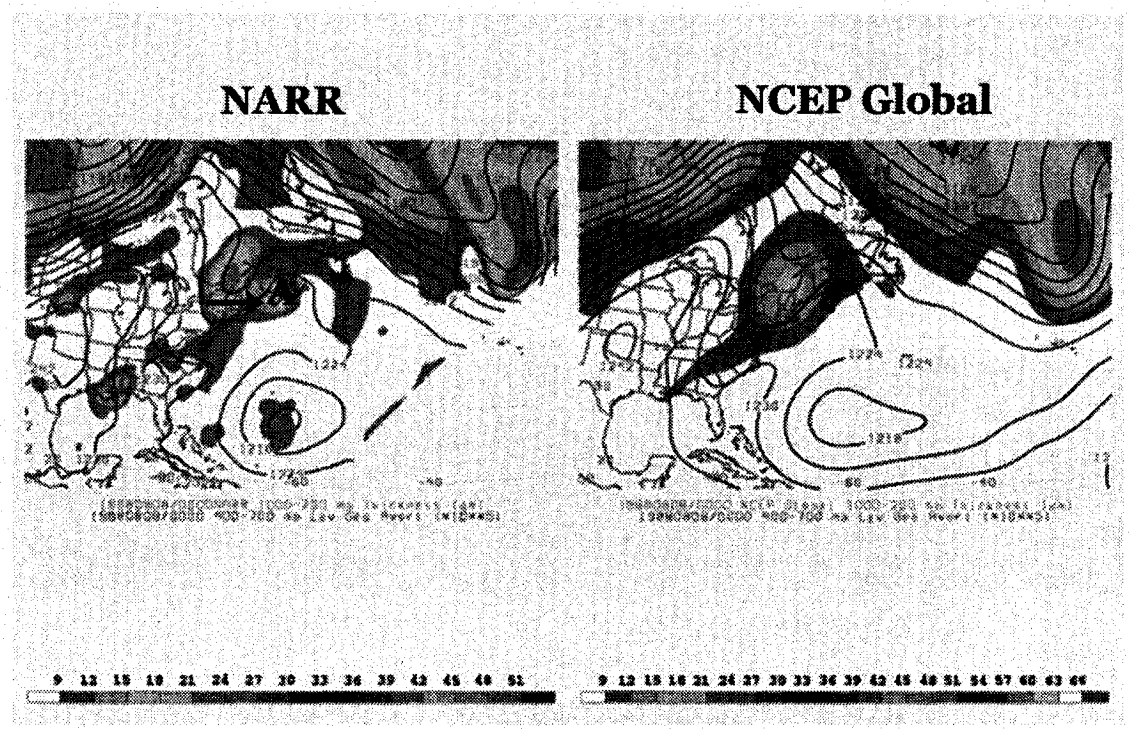

Figure 5.1: 400-700 hPa absolute vorticity ($\times 10^{-5} s^{-1}$, shaded), 200-1000 thickness (m, contoured). Alberto (1988) resolved by the 32 km horizontal resolution of the NARR (left); not resolved by the 2.5 degree NCEP Global Reanalysis (right).

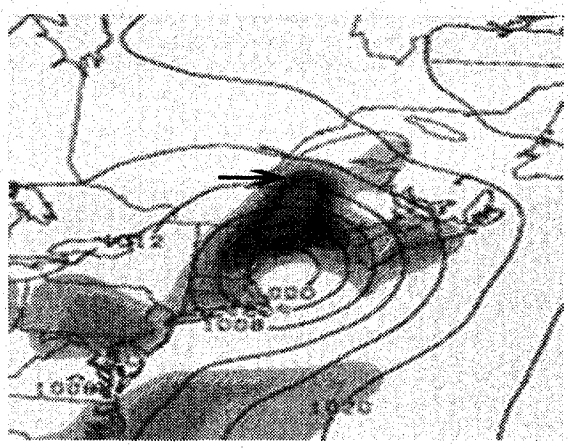

Figure 5.2: NARR 3-hourly precipitation (mm, shaded) with Sea-level Pressure (hPa, contoured) for Hurricane Bob (1991); the precipitation appears to "stop" at the U.S.-Canadian border.

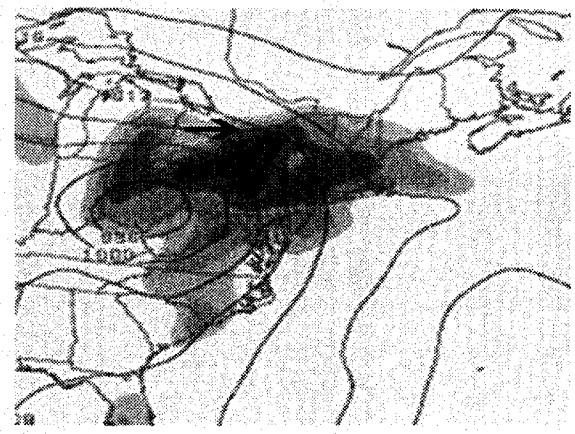

Figure 5.3: As in Fig. 5.2, but for Hurricane Opal (1995); the precipitation appears to "stop" at the U.S.-Canadian border.

itation structures are, in general, well-represented. From 1979-2002, the NARR also attempted to assimilate precipitation over Canada using mostly gauge data. However, the number of rain gauges available for use by the NARR is significantly less in Canada than in the United States. Consequently, precipitation over land in Canada prior to 2003 is often mis- and/or under-represented. After being alerted to this deficiency in the NARR, NCEP changed their methodology for 2003 and beyond so that all precipitation over Canada would be model-based only.

Figure 5.2 displays a common problem in the NARR precipitation field prior to 2003. The precipitation associated with transitioning Hurricane Bob (1991) appears to follow the U.S.-Canada political border, despite the proximity of the surface low center to Canada. Over the subsequent six hours (not shown), the NARR precipitation does not cross the political border at any point. A similar result is found during the ET of Hurricane Opal (1995) in the Great Lakes region (Fig. 5.3). Again, the precipitation appears to follow the political border of the United States and Canada. Cases entirely over Canada have also exhibited mis-representations in the NARR precipitation field, often in the form of either a vast under-representation of the actual precipitation or as a random bulls-eye, where a region with one or two gauges displays precipitation just near the gauge(s) to be much heavier than in reality.

While this problem is clearly not ideal for the purposes of this study, a large majority of the cases in this research are Atlantic Canada cases, where at least portions of the precipitation associated with the storm are located over water. Thus, a large num-

ber of cases are largely unaffected by the errors in the assimilation scheme. However, southern Ontario/Great Lakes storms such as Opal are affected and the reliability of the NARR precipitation over Canada in these cases is deemed questionable at best.

An example of the NARR Canadian precipitation problem is presented for the case of Hurricane Gustav (2002), which affected Atlantic Canada in mid-September, 2002. Figure 5.4 shows the NARR 3-hourly precipitation associated (i.e precipitation accumulated from 0600 UTC to 0900 UTC) with Gustav at 0600 UTC/12 September near Newfoundland and the Gulf of St. Lawrence. Note that while a large area of precipitation is resolved over the Gulf of St. Lawrence, no precipitation is analyzed by the NARR over Newfoundland. This image is now compared to Environment Canada radar data taken from the Marble Mountain (XME) radar in western Newfoundland (Fig. 5.5). Figures 5.6, 5.7, and 5.8 display radar images from the XME radar at 0630 UTC, 0730 UTC, and 0830 UTC, respectively, coinciding with the accumulated precipitation in the NARR as seen in Fig. 5.4. Rather surprisingly, the NARR analysis appears to do relatively well, at least in terms of distribution, if not precipitation amounts. There appears to be some underestimation of precipitation over southern Newfoundland, but the overall structure is relatively coherent. Whether or not this relatively accurate representation of the precipitation is unique to this case is difficult to discern. Similar radar images are examined for the case of Hurricane Michael in 2000 (not shown), which affected southeastern Newfoundland, and the NARR distribution is not totally unreasonable, albeit there is some lag time in the crossover of the precipitation from ocean to land.

The switch to the use of model-based precipitation only in 2003, while not perfect, results in a vast improvement of the NARR representation of precipitation over land in Canada. In general, precipitation distributions are more coherent and continuous across political boundaries. Figure 5.9 shows the NARR precipitation and sea-level pressure field during the time of Hurricane Juan (labelled "J") on September 29th, 2003 (Juan is discussed in-depth in the next section); the key feature on the plot is a relatively innocuous synoptic-scale low pressure system in northeastern Quebec. The NARR precipitation distribution in association with this storm is smooth in Canada (i.e. no random maxima) and continuous across the U.S.-Canada border, signifying the improvement in the use of model precipitation only.

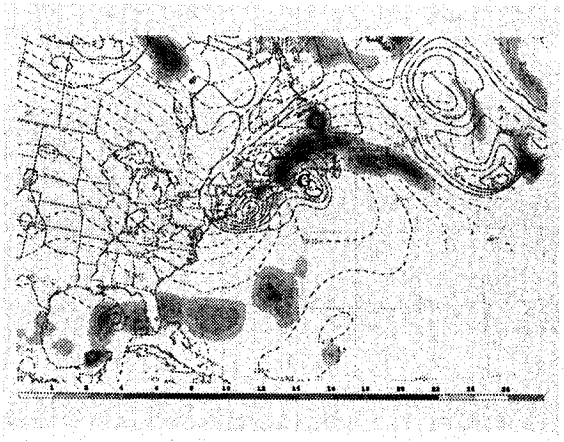

Figure 5.4: NARR 3-hourly precipitation (mm, shaded) with Sea-level Pressure (hPa, contoured) at 0600 UTC, September 12th, 2002; Hurricane Gustav is labelled "G".

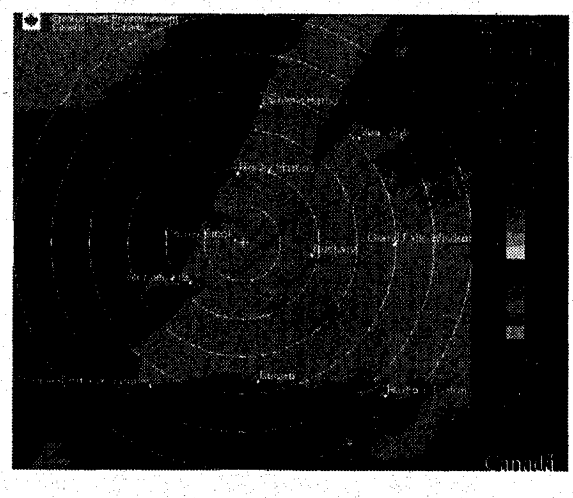

Figure 5.5: Marble Mountain, Newfoundland radar areal coverage, as used for Hurricane Gustav radar imagery.

Figure 5.6: XME Radar during Hurricane Gustav; Sept. 12th, 2002 at 0630 UTC.

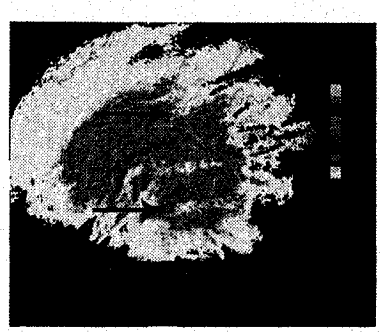

Figure 5.7: XME Radar during Hurricane Gustav; Sept. 12th, 2002 at 0730 UTC.

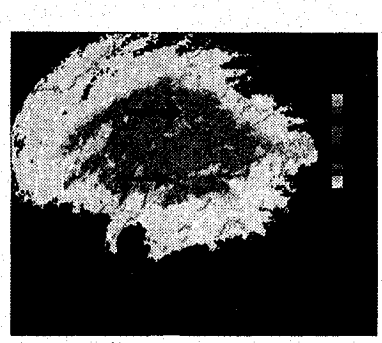

Figure 5.8: XME Radar during Hurricane Gustav; Sept. 12th, 2002 at 0830 UTC.

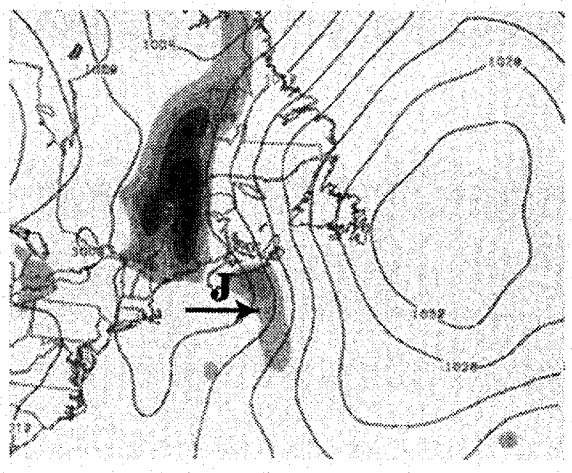

Figure 5.9: As in Fig. 5.2, but at 0000 UTC, September 29th, 2003; Hurricane Juan is marked with a J.

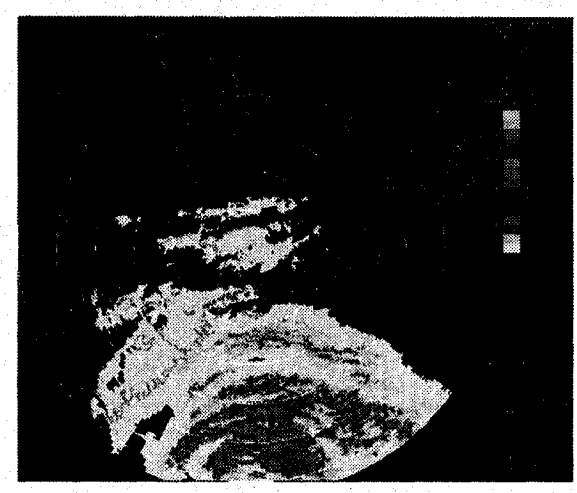

Figure 5.10: XGO (Halifax) radar image from 2350 UTC/28 September as Juan approached the Nova Scotia coast.

5.3. The ugly NARR: Hurricane Juan (2003)

Hurricane Juan was the most destructive tropical system to hit Atlantic Canada in over a century when it made landfall near Halifax in September, 2003. However, despite its good representation of the other thirty-one storms in this study, the NARR (and thus the ETA model) does not accurately represent the intensity and/or destructive power associated with Juan. At the time of landfall just west of Halifax, the minimum observed SLP was 973 hPa, as Juan roared ashore as a Category 2 hurricane on the Saffir-Simpson scale. In contrast, the NARR SLP plot (Fig. 5.9) at 0300 UTC/29 September, depicts Juan as a 1008 hPa low (with no closed isobar). While the strength of tropical systems are often underestimated in numerical models, an error of 35 hPa in a reanalysis makes Juan a major failure for the NARR. Moreover, while the NARR did analyze a mid-level vortex associated with Juan (labelled "J", Figures 5.14, 5.15, and 5.16) on its approach to Nova Scotia, the analyzed intensity of the vortex is questionable at best, especially in comparison to similar storms in this study.

McTaggart-Cowan et al. (2005b) ran a simulation on Juan using the Princeton University GFDL hurricane model, and the results are shown in Figs. 5.11, 5.12, and 5.13. As depicted in the GFDL forecast for 1200 UTC/28 (Fig. 5.11), Juan is a strong hurricane north of Bermuda, tracking almost directly northward. Juan is located under a large thickness ridge, indicative of a pattern favorable for the strengthening of a tropical cyclone (small vertical shear), but unfavorable for an extratropical

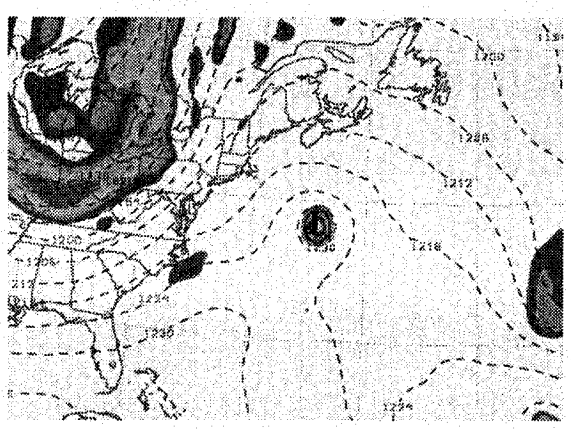

Figure 5.11: Juan at 1200 UTC/28 September; GFDL 400-700 hPa absolute vorticity ($\times 10^{-5} s^{-1}$, shaded), GFDL 200-1000 hPa thickness (m, dashed contours)

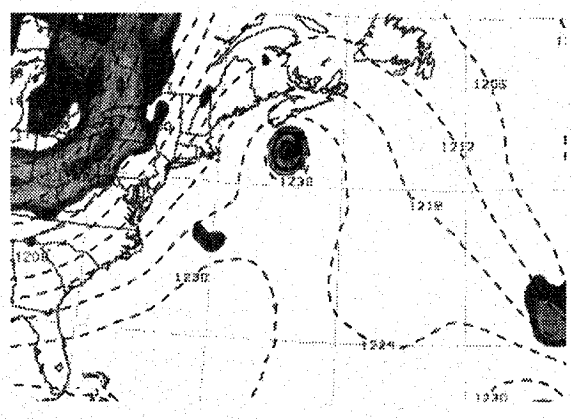

Figure 5.12: As in Fig. 5.11, but at 0000 UTC/29 September.

cyclone. Juan, however, remains quite tropical into high latitudes, as evidenced by its extremely small size at 0000 UTC/29 (Fig. 5.12). The mid-latitude trough well to the west of Juan does not play a part in Juan's progression northward. Due to its positioning directly under the ridge, Juan begins to weaken substantially by 1200 UTC/29 (and becomes slightly larger in size) once it starts to undergo ET, after making landfall as a hurricane in Nova Scotia (Fig. 5.13). At no point does Juan undergo an explosive intensification during or after ET, and it weakens rapidly after moving into colder waters in the Gulf of St. Lawrence. Clearly, the GFDL simulation outperforms the NARR in the representation of Hurricane Juan.

McTaggart-Cowan et al. (2005a,b) provide more in-depth analysis and documentation of Juan and the associated numerical model performance, but potential reasons for the NARR's lack of skill with regard to Juan include:

- The NARR does have problems with cyclones that are very tropical in nature, and although Juan moved into relatively high latitudes, it did remain quite tropical.
- Juan's small size and compact structure.
- The ETA model analysis and forecasts, which were not very accurate in the case of Juan, were simply never corrected by the NARR assimilation scheme.

Finally, the NARR 3-hourly precipitation analysis greatly underestimates the precipitation from Juan. Figure 5.9 shows the NARR model-based 3-hourly precipitation

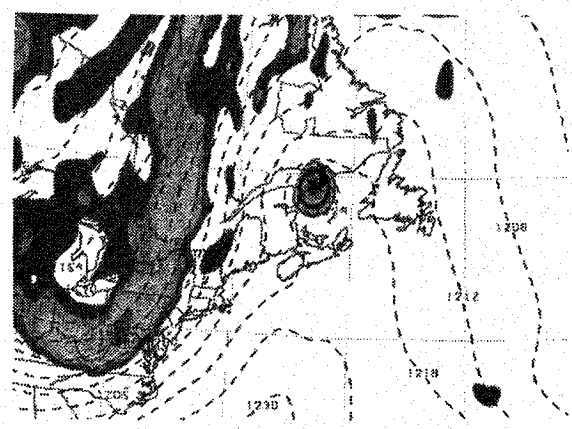

Figure 5.13: As in Fig. 5.11, but at 1200 UTC/29 September.

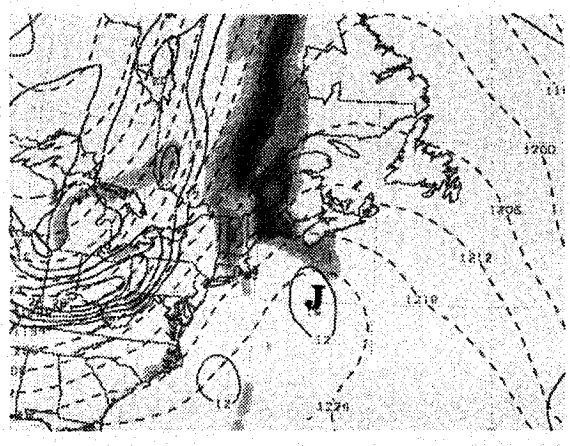

Figure 5.14: As in Fig. 3.15, but for Juan at 1800 UTC/28 September.

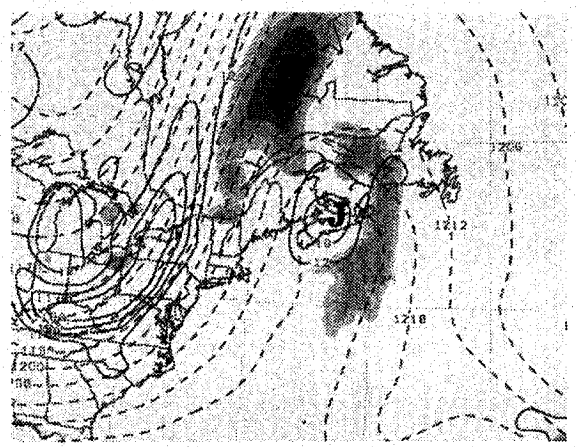

Figure 5.15: As in Fig. 3.15, but for Juan at 0600 UTC/29 September.

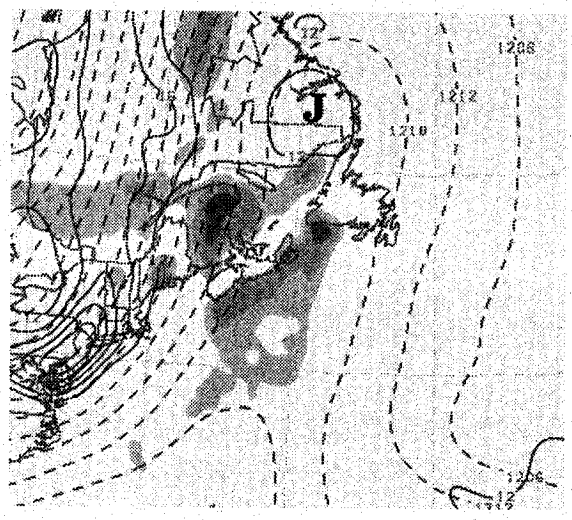

Figure 5.16: As in Fig. 3.15, but for Juan at 1800 UTC/29 September.

field, while Fig. 5.10 displays the Halifax (XGO) radar imagery as Juan approaches Halifax. Note that the radar shows intense precipitation associated with even the outer bands of Juan just before 0000 UTC/29 September, while the NARR precipitation field shows only very light accumulation between 0000 and 0300 UTC/29 September. The precipitation analysis confirms the poor representation of Juan by the NARR that is found in the dynamical analyses.

Chapter 6

Summary and Conclusions

The extratropical transition (ET) of tropical cyclones is a complex and multi-faceted process in which two initially separate features (one tropical and one extra-tropical) combine to produce a potentially powerful extratropical cyclone that can have a wide impact on human interests (McTaggart-Cowan et al. 2004b). The complexity of ET is represented by the fact that the process itself is essentially the merging of two systems (a tropical cyclone and a mid-latitude trough) that individually are on two separate length scales (i.e. a tropical cyclone is at the high end of the mesoscale and a mid-latitude trough/ridge couplet is at the high end of the synoptic scale). In other words, as the tropical cyclone moves northward and interacts with a mid-latitude trough to the west or northwest, storm undergoes a shift from a predominantly "warm-core" tropical cyclone to a larger, often "cold-core" extratropical cyclone. This shift from warm-core to cold-core occurs as the storm moves into colder waters (or onto land), thereby decreasing its dependency on warm sea-surface temperatures. Furthermore, in a purely tropical cyclone (warm-core), the effect of diabatic heating in the core of the system overwhelms that of adiabatic cooling due to ascent. However, as the storm moves into cooler waters and becomes extratropical, adiabatic cooling due to large values of ascent begins to dominate diabatic effects. This process subsequently reduces the thickness in the core of the storm, therefore completing the storm's transition from a warm-core to cold-(or at least colder)core system. It is important to note, however, that while intense extratropical cyclones are often thought of as purely cold-core systems, those that remain over relatively warm waters at higher latitudes (e.g. over the Gulf Stream) often retain at least a portion of their original warm-core signature (Thorncroft and Jones 2000).

This study examines this phenomenon as it relates to Canada. The synoptic and dynamic characteristics of ET are presented, followed by a comparison of ET to

explosively intensifying wintertime cold-season extratropical cyclones.

Thirty-two tropical cyclones that have affected Canada, most of which undergo extratropical transition, are included in this study. The storms are analyzed from a dynamical perspective, and divided into different groups based on the rate of change in their vorticity, utilizing the Sutcliffe/Trenberth approximation to the quasi-geostrophic omega equation (Equation 3.4). Subsequently, the time-evolving precipitation distribution for each "intensifying" or "decaying" storm is documented. The use of the NCEP North American Regional Reanalysis (NARR) is advantageous in precipitation analysis as it provides a 3-hourly accumulated precipitation field that is not available in the NCEP Global Reanalysis.

Atallah and Bosart (2004) looked at ET in the United States by first inspecting the associated precipitation distributions and subsequently examining the corresponding storm dynamics. This study takes a different approach to ET analysis by looking at the dynamics first (using the Sutcliffe approximation) and applying it to the precipitation analysis. The methodology involves partitioning the storms in the study based on the intensity of the change in low-level vorticity. Firstly, the four weakest vortices in the study (those with minimum SLP values more than one standard deviation above the average minimum SLP value) are removed from compositing consideration. Secondly, the rate of change of the NARR layer-averaged low-level (700-850 hPa) vorticity is evaluated for each storm. Each case is then categorized into one of the following groups: "intensifying", "decaying", and "neither". Eleven storms are classified as "intensifying", with positive rates of change in vorticity of greater than or equal to $5\times10^{-5}s^{-1}$ per twelve hours. Similarly, eleven storms fit the "decaying" profile, with negative rates of change in vorticity of at least $5\times10^{-5}s^{-1}$ per twelve hours. Six storms, including the poorly analyzed Hurricane Juan, are placed in the "neither" category, as the associated rates of change fail to meet either the "intensifying" or "decaying" qualifications.

Composite plots are presented from both a quasi-geostrophic and potential vorticity perspective, to help compare and contrast the synoptic characteristics of the intensifying storms versus those of the decaying cases. Key features in the composites include, but are not limited to:

- A stronger precursor upper air trough exists over the midwestern U.S. in the intensifying composite, as well as a stronger positive tilt to the trough.
- A more meridional flow is observed in the intensifying composite as compared to more zonal in the decaying group.

- A stronger downstream ridge is found in the intensifying group, due, at least it part, to latent heat release from heavy precipitation.
- A lack of interaction between the tropical cyclone and a mid-latitude trough is seen in the decaying cases, regardless of whether the tropical cyclone moves into an area of high baroclinicity.

An analysis of precipitation distributions from both the "intensifying" and "decaying" groups shows that intensifying cases tend to have areas of precipitation that rotate cyclonically around the storm as the storm intensifies. In contrast, storms that are decaying often have precipitation distributions that rotate anticyclonically around the cyclone, while simultaneously decreasing in areal extent. The cyclonic rotation of the precipitation in the "intensifying" cases often mirrors the path of the temperature advection couplet. Moreover, an extreme cyclonic rotation, where the main area of precipitation shifts from the northeastern to northern or northwestern sector of the cyclone, is seen in many of the most rapidly intensifying cases. Canada is impacted when tropical cyclones undergoing a strong re-intensification after ET cause heavy precipitation on land in Atlantic Canada, even if the center of the transitioning cyclone is well offshore.

Several dynamical aspects are outlined in the analysis of two representative cases of the respective composite groups, Luis (1995, intensifying) and Isabel (2003, decaying). An examination of the quasi-geostrophic, potential vorticity and frontogenetical analyses of these two cases leads to the conclusion that, in general, the composite structures outlined in Chapter 3 are applicable to even the most extreme of "intensifying" and "decaying" cases.

Use of the NARR has several advantages, including relatively high resolution to capture smaller, more tropical cases, and the 3-hourly precipitation field. However, there are a few problems with the NARR. Firstly, the NARR precipitation field in Canada prior to 2003 is not nearly as accurate as it is over the United States and Mexico. NCEP found that the lack of available rain gauge data over Canada significantly hindered precipitation assimilation. In 2003, NCEP switched started using model-based precipitation only, in Canada, which, while not perfect, greatly reduces the "stopped-at-the-border" and random maxima errors. In all, this assimilation scheme error greatly inhibits the use of the NARR over inland Canada, and does affect several storms in this study, in particular those that affect the Great Lakes region. However, since most of the cases in this study are in Atlantic Canada, and NARR precipitation over the oceans is completely model-based, the problem does not

have a tremendous impact on this study. Finally, Hurricane Juan is the only storm in this study to be poorly represented in the NARR. Several potential reasons for the NARR's mis-representation of Juan are suggested, including the shoddy performance of the ETA model.

Much has been learned in the past decade about the extratropical transition of tropical cyclones. This study attempts to further advance understanding of ET structures and effects on Eastern Canada. More work, however, remains to be done. This includes but is not limited to:

- Analyses of mesoscale precipitation features at high latitudes in association with ET events.
- A compilation of western North Pacific ET events that impact western Canada following re-curvature and their precipitation impacts.
- An assessment of forecast model performance during ET events (both intensifying and decaying events).

The extratropical transition of tropical cyclones is an important atmospheric phenomenon that can have a large impact on Canadian interests and thus requires more attention and study than it has been previously given.

Bibliography

Abraham, J., C. Fogarty, and W. Strapp, 2002: Extratropical transition of Hurricanes Michael and Karen: Storm reconnaissance with the Canadian Convair 580 aircraft. Preprints, 25th Conference on Hurricanes and Tropical Meteorology, American Meteorological Society, San Diego, CA.

Agusti-Panareda, A., C. Thorncroft, G. Craig, and S. Gray, 2004: The extratropical transition of Hurricane Irene (1999): A potential-vorticity perspective. Quarterly Journal of the Royal Meteorological Society, 130, 1047–1074.

Anthes, R., 1990: Advances in the understanding and prediction of cyclone development with limited-area fine-mesh models. The Erik Palmen Memorial Volume, 221–253.

Atallah, E. H. and L. F. Bosart, 2003: The extratropical transition and precipitation distribution of Hurricane Floyd (1999). Monthly Weather Review, 131, 1063–1081.

— 2004: An evaluation of the precipitation distribution in landfalling tropical cyclones. Preprints, 20th Conference on Weather Analysis and Forecasting, American Meteorological Society, Seattle, WA.

Bluestein, H. B., 1992: Synoptic-dynamic meteorology in midlatitudes: Volume I. Oxford University Press.

Bosart, L. F. and D. B. Dean, 1991: The Agnes rainstorm of June 1972: Surface feature evolution culminating in inland storm redevelopment. Weather and Forecasting, 6, 515–536.

Browning, K., A. Thorpe, A. Montani, D. Parsons, M. Griffiths, P. Panagi, and E. Dicks, 2000: Interactions of tropopause depressions with an ex-tropical cyclone and sensitivity of forecasts to analysis errors. Monthly Weather Review, 128, 2734–2755.

Browning, K., G. Vaughan, and P. Panagi, 1998: Analysis of an ex-tropical cyclone after its reintensification as a warm-core extratropical cyclone. Quarterly Journal of the Royal Meteorological Society, 124, 2329–2356.

Carr, F. H. and L. F. Bosart, 1978: A diagnostic evaluation of rainfall predictability for Tropical Storm Agnes, June 1972. Monthly Weather Review, 106, 363–374.

Cerveny, R. S. and L. E. Newman, 2000: Climatological relationships between tropical cyclones and rainfall. Monthly Weather Review, 128, 3329–3336.

Colle, B. A., 2003: Numerical simulations of the extratropical transition of Floyd (1999): Structural evolution and responsible mechanisms for the heavy rainfall over the northeast United States. Monthly Weather Review, 131, 2905–2926.

Darr, J. K., 2002: Quantitative measurements of extratropical transition in the Atlantic basin. Preprints, 25th Conference on Hurricanes and Tropical Meteorology, American Meteorological Society, San Diego, CA.

DeLuca, D. P., L. F. Bosart, and D. Keyser, 2004: The distribution of precipitation over the Northeast accompanying landfalling and transitioning tropical cyclones. Preprints, 20th Conference on Weather Analysis and Forecasting, American Meteorological Society, Seattle, WA.

Dickinson, M., L. Bosart, K. Corbosiero, S. Hopsch, K. Lombardo, M. Novak, B. Smith, and A. Wasula, 2004: The extratropical transitions of eastern Pacific Hurricane Lester (1992) and Atlantic Hurricane Andrew (1992): A comparison. Preprints, 26th Conference on Hurricanes and Tropical Meteorology, American Meteorological Society, Miami, FL.

DiMego, G. J. and L. F. Bosart, 1982a: The transformation of Tropical Storm Agnes into an extratropical cyclone. Part I: The observed fields and vertical motion computations. Monthly Weather Review, 110, 385–411.

— 1982b: The transformation of Tropical Storm Agnes into an extratropical cyclone. Part II: Moisture, vorticity and kinetic energy budgets. Monthly Weather Review, 110, 412–433.

Elsberry, R. L., 2002: Predicting hurricane landfall precipitation: Optimistic and pessimistic views from the symposium on precipitation extremes. Bulletin of the American Meteorological Society, 83, 1333–1339.

— 2004: Comments on "The influence of the downstream state on extratropical transition: Hurricane Earl (1998) case study" and "A study of the extratropical reintensification of former Hurricane Earl using Canadian Meteorological Centre regional analyses and ensemble forecasts". Monthly Weather Review, 132, 2511–2513.

Elsberry, R. L. and P. J. Kirchoffer, 1988: Upper-level forcing of explosive cyclogenesis over the ocean based on operationally analyzed fields. Weather and Forecasting, 3, 205–216.

Evans, J. L. and R. E. Hart, 2003: Objective indicators of the life cyclone evolution of extratropical transition for Atlantic tropical cyclones. Monthly Weather Review, 131, 909–925.

Fogarty, C., 2002: Operational forecasting of extratropical transition. Preprints, 25th Conference on Hurricanes and Tropical Meteorology, American Meteorological Society, San Diego, CA.

Fogarty, C. T., 2000: Hurricane Michael, 17-20 October 2000 Part I: Summary report and storm impact on Canada.

Fogarty, C. T. and J. R. Gyakum, 2005: A study of extratropical transition in the western North Atlantic Ocean, 1963-1996. Atmosphere-Ocean, 43, 173–191.

Foley, G. and B. Hanstrum, 1994: The capture of tropical cyclones by cold fronts off the west coast of Australia. Weather and Forecasting, 9, 577–590.

Gyakum, J. R., 2003: The extratropical transformation: A scientific challenge. Atmosphere-Ocean Interactions, 47–81.

Hanley, D., J. Molinari, and D. Keyser, 2001: A composite study of the interactions between tropical cyclones and upper-tropospheric troughs. Monthly Weather Review, 129, 2570–2584.

Harr, P. A. and R. L. Elsberry, 2000: Extratropical transition of tropical cyclones over the western North Pacific. Part I: Evolution of structural characteristics during the transition process. Monthly Weather Review, 128, 2613–2633.

Harr, P. A., R. L. Elsberry, and T. F. Hogan, 2000: Extratropical transition of tropical cyclones over the western North Pacific. Part II: The impact of midlatitude circulation characteristics. Monthly Weather Review, 128, 2634–2653.

Hart, R. E., 2003: A cyclone phase space derived from thermal wind and thermal asymmetry. Monthly Weather Review, Volume 131, 585–616.

Hart, R. E. and J. L. Evans, 2001: A climatology of the extratropical transition of Atlantic tropical cyclones. Journal of Climate, 14, 547–564.

Hoskins, B., M. McIntyre, and A. Robertson, 1985: On the use and significance of isentropic potential vorticity maps. Quarterly Journal of the Royal Meteorological Society, 111, 877–946.

Hughes, L., F. Baer, G. Birchfield, and R. Kaylor, 1955: Hurricane Hazel and a long wave outlook. Bulletin of American Meteorological Society, 36, 528–533.

Jones, S. C., P. A. Harr, J. Abraham, L. F. Bosart, P. J. Bowyer, J. L. Evans, D. E. Hanley, B. N. Hanstrum, R. E. Hart, F. Lalaurette, M. R. Sinclair, R. K. Smith, and C. Thorncroft, 2003: The extratropical transition of tropical cyclones: Forecast challenges, current understanding and furture directions. Weather and Forecasting, 18, 1052–1092.

Kalnay, E., M. Kanamitsu, R. Kistler, W. Collins, D. Deaven, L. Gandin, M. Iredell, S. Saha, G. White, J. Woollen, Y. Zhu, M. Chelliah, W. Ebisuzaki, W. Higgins, J. Janowiak, K. Mo, C. Ropelewski, J. Wang, A. Leetmaa, R. Reynolds, R. Jenne, and D. Joseph, 1996: The NCEP/NCAR 40-year reanalysis project. Bulletin of the American Meteorological Society, 77, 437–471.

Klein, P. M., P. A. Harr, and R. L. Elsberry, 2000: Extratropical transition of western North Pacific tropical cyclones: An overview and conceptual model of the transformation stage. Weather and Forecasting, 15, 373–395.

— 2002: Extratropical transition of western North Pacific tropical cyclones: Midlatitude and tropical cyclone contributions to reintensification. Monthly Weather Review, 130, 2240–2259.

Koch, S. E., M. desJardins, and P. J. Kocin, 1983: An interactive Barnes objective map analysis scheme for use with satellite and conventional data. Journal of Applied Meteorology, 22, 1487–1503.

Kuo, Y.-H. and S. Low-Nam, 1990: Prediction of nine explosive cyclones over the western Atlantic ocean with a regional model. Monthly Weather Review, 118, 3–25.

Kuo, Y.-H., M. shapiro, and E. G. Donall, 1991: The interaction between baroclinic and diabatic processes in a numerical simulation of a rapidly intensifying extratropical marine cyclone. Monthly Weather Review, 119, 368–384.

Lackmann, G. M., L. F. Bosart, and D. Keyser, 1996: Planetary- and synoptic-scale characteristics of explosive wintertime cyclogenesis over the western North Atlantic Ocean. Monthly Weather Review, 124, 2672–2702.

Lemaitre, Y., A. Protat, and D. Bouniol, 1999a: Pacific and Atlantic 'bomb-like' deepenings in mature phase: A comparative study. Quarterly Journal of the Royal Meteorological Society, 125, 3513–3534.

Lemaitre, Y., A. Protat, and G. Scialom, 1999b: Dynamics of a "bomb like" deepening secondary cyclone from airborne Doppler radar. Quarterly Journal of the Royal Meteorology Society, 125, 2797–2818.

Liu, C.-S. and G. T.-J. Chen, 2003: The extratropical transition of Typhoon Winnie (1997): Self-amplification after landfall.

Ma, S., H. Ritchie, J. Gyakum, J. Abraham, C. Fogarty, and R. McTaggart-Cowan, 2003: A study of the extratropical reintensification of former Hurricane Earl using Canadian Meteorological Centre regional analyses and ensemble forecasts. Monthly Weather Review, 131, 1342–1359.

Macdonald, B. C. and E. R. Reiter, 1988: Explosive cyclogenesis over the eastern United States. Monthly Weather Review, 116, 1568–1586.

Manobianco, J., 1989: Explosive East Coast cyclogenesis over the west-central North Atlantic Ocean: A composite study derived from ECMWF operational analyses. Monthly Weather Review, 117, 2365–2383.

Marks, F. D., 1998: Precipitation processes in landfalling tropical cyclones. NCAR Advanced Study Program Colloquium: Hurricanes at Landfall, NCAR/ASP, NOAA/HRD.

Matano, H. and M. Sekioka, 1971a: On the synoptic structure of Typhoon Cora, 1969, as the compound system of tropical and extratropical cyclones. Journal of the Meteorological Society of Japan, 49, 282–294.

— 1971b: Some aspects of extratropical transformation of a tropical cyclone. Journal of the Meteorological Society of Japan, 49, 736–743.

Matano, J., 1958: On the synoptic structure of Hurricane Hazel, 1954, over the eastern United States. Journal of the Meteorological Society of Japan, 36, 23–31.

McTaggart-Cowan, R., L. Bosart, E. Atallah, and J. Gyakum, 2005a: Hurricane Juan (2003). Part I: A diagnostic and compositing lifecycle study. Monthly Weather Review (in press).

— 2005b: Hurricane Juan (2003). Part II: Forecasting and numerical simulation. Monthly Weather Review (in press).

McTaggart-Cowan, R., J. Gyakum, and M. Yau, 2001: Sensitivity testing of extratropical transitions using potential vorticity inversions to modify initial conditions: Hurricane Earl case study. Monthly Weather Review, 129, 1617–1636.

— 2003: The influence of the downstream state on extratropical transition: Hurricane Earl (1998) case study. Monthly Weather Review, 131, 1910–1929.

— 2004a: The impact of tropical remnants on extratropical cyclogenesis: Case study of Hurricanes Danielle and Earl (1998). Monthly Weather Review, 132, 1933–1951.

— 2004b: Reply. Monthly Weather Review, 132, 2514–2519.

Mesinger, F., T. L. Black, D. W. Plummer, and J. H. Ward, 1990: Eta model precipitation forecasts for a period including Tropical Storm Allison. Weather and Forecasting, 5, 483–493.

Mesinger, F., G. DiMego, E. Kalnay, P. Shafran, W. Ebisuzaki, D. Jovic, J. Woollen, K. Mitchell, E. Rogers, M. Ek, Y. Fan, R. Grumbine, W. Higgins, H. Li, Y. Lin, G. Manikin, D. Parrish, and W. Shi, 2004: North American Regional Reanalysis.

Morgan, M. C. and J. W. Nielsen-Gammon, 1998: Using tropopause maps to diagnose midlatitude weather systems. Monthly Weather Review, 126, 2555–2579.

Muir-Wood, R., R. Dixon, and A. Boissonnade, 2004: The impact of extratropical transition on hurricane risk in the northeast US. Preprints, 26th Conference on Hurricanes and Tropical Meteorology, American Meteorological Society, Miami, FL.

Palmén, E., 1958: Vertical circulation and release of kinetic energy during the development of Hurricane Hazel into an extratropical storm. Tellus, 10, 1–23.

Petterssen, S., 1955: A general survey of factors influencing development at sea level. Journal of Meteorology, 12, 36–42.

Petterssen, S. and S. Smebye, 1971: On the development of extratropical cyclones. Quarterly Journal of the Royal Meteorological Society, 97.

Richter, D. and E. DiLoreto, 1956: The transformation of Hurricane Flossy into an extratropical cyclone, September 25-29, 1956. Monthly Weather Review, 84, 343–352.

Ritchie, E. A. and R. L. Elsberry, 2003: Simulations of the extratropical transition of tropical cyclones: Contributions by the midlatitude upper-level trough to reintensification. Monthly Weather Review, 131, 2112–2128.

Sanders, F., 1986: Explosive cyclogenesis in the west-central North Atlantic Ocean, 1981-84. Part I: Composite structure and mean behavior. Monthly Weather Review, 114, 1781–1794.

Sanders, F. and C. A. Davis, 1988: Patterns of thickness anomaly for explosive cyclogenesis over the west-central North Atlantic Ocean. Monthly Weather Review, 116, 2725–2730.

Sanders, F. and J. R. Gyakum, 1980: Synoptic-dynamic climatology of the "bomb". Monthly Weather Review, 108, 1589–1606.

Schultz, D. M., D. Keyser, and L. F. Bosart, 1998: The effect of large-scale flow on low-level frontal structure and evolution in midlattitude cyclones. Monthly Weather Review, 126, 1767–1790.

Sinclair, M. R. and M. J. Revell, 2000: Classification and composite diagnosis of extratropical cyclogenesis events in the southwest Pacific. Monthly Weather Review, 128, 1089–1105.

Srock, A. F., L. F. Bosart, and J. Molinari, 2004a: A composite study of precipitation distribution in U.S. landfalling tropical cyclones. Preprints, 20th Conference on Weather Analysis and Forecasting, American Meteorological Society, Seattle, WA.

Srock, A. F., L. F. Bosart, and J. E. Molinari, 2004b: Composite and case studies of precipitation distribution in U.S. landfalling tropical cyclones. Preprints, 26th Conference on Hurricanes and Tropical Meteorology, American Meteorological Society, Miami, Fl.

Sutcliffe, R., 1947: A contribution to the problem of development. Quarterly Journal of the Royal Meteorological Society, 73, 370–383.

Sutcliffe, R. and A. Forsdyke, 1950: The theory and use of upper air thickness patterns in forecasting. Quarterly Journal of the Royal Meteorological Society, 76, 189–217.

Thorncroft, C. and S. C. Jones, 2000: The extratropical transitions of Hurricanes Felix and Iris in 1995. Monthly Weather Review, 128, 947–972.

Trenberth, K. E., 1978: On the interpretation of the diagnostic quasi-geostropic omega equation. Monthly Weather Review, 106, 131–137.

Uccellini, L. W., 1986: The possible influence of upstream upper-level baroclinic processes on the development of the QE II Storm. Monthly Weather Review, 114, 1019–1027.

Uccellini, L. W., D. Keyser, K. F. Brill, and C. H.Wash, 1985: The Presidents' Day cyclone of 18-19 February 1979: Influence of upstream trough amplification and associated tropopause folding on rapid cyclogenesis. Monthly Weather Review, 113, 962–988.

Uccellini, L. W. and P. J. Kocin, 1987: The interaction of jet streak circulations during heavy snow events along the East Coast of the United States. Weather and Forecasting, 2, 289–308.

Wang, C.-C. and J. C. Rogers, 2001: A composite study of explosive cyclogenesis in different sectors of the North Atlantic. Part I: Cyclone structure and evolution. Monthly Weather Review, 129, 1481–1499.

Weese, S. R., 2003: A reanalysis of Hurricane Hazel (1954). Master's thesis, McGill University.

Wu, C.-C. and K. A. Emanuel, 1995: Potential vorticity diagnostics of hurricane movement. Part I: A case study of Hurricane Bob (1991). Monthly Weather Review, 123, 69–92.

Young, M., G. Monk, and K. Browning, 1987: Interpretation and satellite imagery of a rapidly deepening cyclone. Quarterly Journal of the Royal Meteorology Society, 113, 1089–1115.